ABSTRACT

PASCUA CUBIDES, YVETTE THIBAULT. Developing Milk Protein Based Structure for New Dairy Products. (Under the direction of Dr. E A Foegeding).

Abstract. Cheddar cheese has a desirable texture that is described as moderately firm and springy, which forms a cohesive mass of smooth particles during mastication and also has a slow instrumental breakdown pattern. Sensory texture is perceived during oral processing and is related to the physical properties and structure of the food material. In general, properties such as fracture stress and strain are related to sensory firmness and deformability respectively. Percent recoverable energy, Young's Modulus and water holding are related to springiness, stiffness and moisture release respectively. Breakdown patterns are related to crumbliness. The overall goal of this thesis was to develop a high protein, no-fat, soft-solid model gel that has a Cheddar cheese-like texture. The research investigated texture development of model dairy protein gels by monitoring 1) changes in whey protein gel material and sensory properties caused by partial replacement of whey protein with casein micelles or dispersed casein, 2) the influence of embedded crystalline particles on breakdown properties of casein-whey protein gels, and 3) the influence of protein-phospholipid particles, a neutracuetical ingredient, on whey protein gel material properties. Secondarily, relationships among microstructure and material or sensory properties were investigated.

In the first phase, known casein-whey protein interactions were used to alter the material properties of whey protein gels and yield a range of soft-solid sensory textures by combining casein micelles or dispersed caseins with whey proteins in heat set gels. Replacing whey protein with casein drastically reduced fracture stress but minimally altered

recoverable energy. Water holding capacity was decreased by casein addition. Breakdown patterns were shifted from brittle-like to ductile-like for dispersed casein at pH 5.5 or micellar casein at pH 6. Additionally, sensory evaluation showed that whey protein-casein gels broke down more rapidly into a more cohesive mass during mastication than did the whey protein gels without casein. Overall, it was demonstrated that material and sensory properties of whey protein gels can be altered to a more Cheddar cheese-like texture using caseins as a texture modifier while maintaining a high total protein concentration. Shifts in microstructure observed by confocal microscopy could not explain the changes in mechanical or sensory textures.

In the second phase, crystalline particles of starburst-like morphology were embedded in whey protein-dispersed casein gels. The dispersed casein solution was prepared by addition of citrate chelator in a 0.7:1 or 1:1 molar ratio of chelator to calcium in milk protein concentrate solution. Crystalline particles minimally influenced the breakdown pattern, but increased fracture stress and reduced fracture strain. Breakdown patterns were influenced however by chelator to calcium ratio. Breakdown patterns for gels with 0.7:1 chelator to calcium ratio were slow where as those with 1:1 ratios were fast. Overall, the results demonstrate the feasibility of shifting the breakdown pattern of whey protein-dispersed casein gels to one more similar to Cheddar cheese by altering the molar ratio of chelator to calcium in the dispersed casein solution.

Finally, in the third phase, the influence of protein-phospholipid particles on whey protein gel properties and their status as an active or inactive filler particle were investigated. Composite gels showed typical response for an active filler by increasing the gel strength with increasing particle phase volume. However, relative to whey protein gels of equivalent

protein concentration, composite gels had reduced gel stiffness (Young's Modulus), strength (fracture stress), deformability (fracture strain), and broke into numerous pieces upon fracture. These results suggest that this particle may be used to alter gel properties by increasing fracturability but would this would be at the cost of reducing gel firmness and deformability relative to gels of equivalent protein concentration.

© Copyright 2014 Yvette Thibault Pascua Cubides

All Rights Reserved

Developing Milk Protein Based Structure for New Dairy Products

by
Yvette Thibault Pascua Cubides

A thesis submitted to the Graduate Faculty of
North Carolina State University
in partial fulfillment of the
requirements for the degree of
Doctor of Philosophy

Food Science

Raleigh, North Carolina

2014

APPROVED BY:

_____	_____
Dr. A. E. Foegeding Committee Chair	Dr. C. R. Daubert
_____	_____
Dr. M. A. Drake	Dr. J. Genzer
_____	
Dr. Eva Johanes	

DEDICATION

This thesis is dedicated to those who are the most dear in my life; my ever endearing husband Javier and my always supportive parents.

BIOGRAPHY

Yvette Thibault Pascua Cubides was born in St. Augustine, FL on December 31, 1977. She graduated from Johnson & Wales University of Charleston, SC in 1999, with an Applied Science degree in Culinary Arts. After graduation, she joined the Fearrington House Restaurant of Pittsboro, NC as the Executive Pastry Chef. While at the Fearrington House Restaurant, she had the opportunity to design and execute intricate multi-component plated desserts at the four-star, five-diamond venue. In the fall of 2004, she joined the Department of Food, Nutrition and Bioprocessing Sciences at North Carolina State University (NCSU) to pursue a Bachelor of Science degree. After graduating in 2007, she joined the USDA Agriculture Research Services unit as a Biological Science Technician, focusing on sweet potato research, under the supervision of Dr. Van-Den Truong. During her tenure with the USDA, she began a Master of Science degree program in the Department of Food, Nutrition and Biological Science at NCSU working under the advisement of Dr. Josip Simunovic with whom she studied continuous flow microwave processing of diced tomatoes. In 2011, Yvette began her doctorate program under the advisement of Dr. E. A. Foegeding also at NCSU. Her current studies focuse on sensory texture and microstructure development of dairy protein soft-solid gel systems.

ACKNOWLEDGMENTS

First and foremost, I would like to thank my advisor Dr. E. A. Foegeding. Dr. Foegeding, you have been the best role model I could have ever asked for. Thank you for your patience, encouragement, and the little pokes that you provided along the way to steer me back on course. You have a gift for seeing the bigger picture and a fantastic ability to explain complicated matters easily and with clarity. These traits, among many others, have made you a successful advisor and I am so grateful to have had the opportunity to work under you in your lab.

I greatly appreciate the advisement of my committee Dr. C. R. Daubert, Dr. M. A. Drake, Dr. Jan Genzer and Dr. Eva Johanes. Thank you for your help, motivation and support. A special thanks to Dr. Eva Johanes for taking so much time to teach and advise me on confocal microscopy techniques. I could not have done this without your help.

And to Paige Luck, many thanks to you. Your management skills and positivity have made the working environment of the lab a pleasant one. Thank you for always taking the time to train me on new equipment, even if I asked you to do this twice! You have become a dear friend to me over these years and I thank you for always lending an ear when I needed one.

To all of my current and former lab mates, Marghret Schneider, Ty Wagoner, Rini Triani, Phanin (Nin) Leksrisompong, Huiying Jennifer Lu, Hicran Koç, and Esra Çakir thank you for the science banter. These conversations helped so much to solve the countless everyday problems. Many thanks also to Chris Pernell, I greatly appreciate all of your

Rheology expertise, training and banter. And to Michelle Yates, thank you for helping me to navigate through the world of sensory.

And last, but certainly not least, to my husband Javier. Thank you for standing by my side though this roller-coaster journey. You were always there to laugh and cry with me through all of the successful and failed experiments. You are my rock and I could not have done this without you. Mua.

TABLE OF CONTENTS

LIST OF TABLES

CHAPTER 2

CHAPTER 3

CHAPTER 4

CHAPTER 5

LIST OF FIGURES

CHAPTER 2

CHAPTER 3

CHAPTER 4

CHAPTER 5

CHAPTER 1

Literature Review

1. Introduction

According to the U.S. Center for Disease Control, obesity is a health condition that is known to influence the onset of chronic health diseases including type 2 diabetes, heart disease and some types of cancer. As of 2010, roughly one third of the adult population in the U.S. was classified as obese; this is double that reported for the 1960's (Ogden and others 2012). Over the past decade, the prevalence of obesity seems to have stabilized (Ogden and others 2012). This stabilization however should not be considered as a sign that the fight for a healthy America is over, but rather that it has only just begun.

One way to combat obesity is to target some of the known contributing factors such as food caloric density. The International Food and Beverage Alliance was organized in 2008 to do just that. The International Food and Beverage Alliance is comprised of eleven major international food and beverage companies who have voluntarily committed to reducing the incidence of obesity and related diseases in the world's population through improving diet and activity. The first goal of the International Food and Beverage Alliance strategy to provide an improved diet to the consumer is to, "continue to reformulate products and develop new products". Reformulation of existing products for the reduction of fats or sugars however often leads to a change in the sensory attributes (e.g. texture profile) of the product.

Sensory texture is one of the main forces behind consumer preference of a product, which highly influences what the consumer will purchase and therefore consume in their diet. As demonstrated by Childs and Drake (2009), in the case of Cheddar Cheese, consumers are

not willing to sacrifice known sensory attributes of an existing product in exchange for the benefit of reduced fat. Thus, while a company may reformulate an existing product to reduce its caloric density, there is no guarantee that consumers will accept the product if its sensory attributes have been changed. An understanding of the factors involved in the textural properties of a food material could facilitate this reformulation process, allowing food manufacturers to reformulate existing products while minimally changing textural properties. Furthermore, this knowledge could enable manufacturers to create new products that have a targeted caloric density and targeted or "designed" texture. Our current understanding of what factors influence food texture however is very limited and it is this conundrum that has lead to the purpose of this theses. The primary purpose of this thesis was to develop model gel systems from a combination of whey and casein proteins that have a broad sensory texture spectrum and to determine if changes in microstructure could explain changes in texture. Chapters 4 and 5 explore the relationships between whey protein-casein gel texture and microstructure. Secondarily, this thesis sought to determine how functional filler particles might alter the texture properties of whey protein gels. Chapter 3 explores the effects of protein-phospholipid particles on whey protein gel properties.

1.1. Bovine milk composition and commercial products

1.1.1. Bovine milk composition

Bovine milk is a highly complex fluid system that contains water (87 %), carbohydrates (4.8%), fat (3.7 %), proteins (3.4%), and ash/minerals (0.7 %) (Deeth and Hartanto 2009). Consumption of bovine milk has been an accepted practice since the

domestication of sheep, goats and cattle around 8,000 BC (Kiple and Ornelas 2000, Fox 2003). Since this time, its commercial production has increased annually across the globe (FAOSTAT 2011). According to the Food and Agriculture Organization of the United Nations, nearly 614 metric tons of bovine milk were produced worldwide in 2011; 14 percent of which was produced in the United States of America alone. The high popularity of this commodity is due in part to its high nutrient content combined with our ability to transform it into a variety of different foods and products. These products include fermented beverages, yogurts, soft solid gels (i.e. cheese), and powders. For the purpose of this thesis, only the production of powders will be discussed in detail.

In order to understand why various processing techniques are used to generate different milk based powders, it is important to first understand how the milk constituents are organized in the fluid system. Based on the work of Jensen and others (1990), Jensen (1995) summarized the milk constituent organization as follows: "lipids in emulsified globules coated with a membrane, proteins in colloidal dispersion and as micelles, and most minerals and all lactose in true solution."

1.1.1.1. Casein

The caseins are an intrinsically unstructured group of proteins that constitute roughly 80 % of the total milk proteins. Historically, caseins are defined as the proteins which precipitate from milk at pH 4.6 (Fox 2003). This group of proteins includes α_{s1}- (~ 24 kDa), α_{s2}- (~ 25 kDa), β- (~ 24 kDa), and κ-casein (~ 19 kDa), which are present in concentrations of 12–15, 3–4, 9–11 and 2–4 g L^{-1} respectively (Huppertz 2013). Aside from differences in molecular weights, distinguishing features among the caseins are that the α_{s1}-, α_{s2}-, and β-

caseins are calcium sensitive and the κ- and α_{s2}-caseins have thiol groups capable of disulfide bonding (Huppertz 2013).

In natural milk, the four casein proteins associate via non-covalent interactions with each other and with calcium phosphate to form supramolecular colloidal particles called casein micelles (McMahon and Oommen 2013). Although the exact micelle structure has been a topic of debate for several decades, it is widely accepted that α_{s1}-, α_{s2}-, β- casein and calcium phosphate make up the micelle core while κ-casein resides at the surface, which provides steric hindrance preventing coalescence of the micelles (McMahone and Oommen 2013). The casein micelle size in fresh milk ranges from 25 to 300 nm with an average diameter of 200 nm (de Kruif 1998). If however the calcium phosphate within the micelle is removed, the micelle is destabilized and dissociates into smaller micelles that range from 8 – 80 nm in size (Dickinson and others 2001, Lucey and others 2000, Chu and others 1995, Nash and others 2005). These smaller micelles have a bimodal distribution where the larger aggregates make up only a small mass fraction of the micelles size distribution (HadjSadok and others 2008). HadjSadok and others (2008) speculated that the large micelles were complexes of fat and protein. HadjSadok and others (2008) investigated the physical and chemical properties of the smaller aggregates and found that caseins of theses small aggregates will remain in solution as individual molecules if the solute pH is far from the isoelectric point (~4.6) and the ionic strength is low. Moving the pH (< 6.0) toward the isoelectric point or screening electrostatic interactions with monovalent salt addition leads to association of the hydrophobic portion of the casein molecules and subsequent micelle formation (HadjSadok and others 2008).

1.1.1.2. Whey proteins

The whey proteins, also known as serum proteins, make up the remaining 20 % of milk proteins. They represent those that remain in milk serum after casein coagulation at pH 4.6 (Eigel and others 1984). The whey protein group is predominately comprised of β-lactoglobulin (70 %) and α-lactalbumin (25 %) with smaller fractions of blood serum albumin, immunoglobulins, and proteos peptones (5 % collectively) (Swaisgood 1982). Beta-lactoglobulin has been studied in depth and is the primary protein responsible for gelation of concentrated whey protein products. For the purposes of this thesis, only the physical and chemical characteristics of β-lactoglobulin will be discussed.

Sawyer (2013) has provided and excellent summary of research done to characterize β-lactoglobulin over the past several decades. The primary β-lactoglobulin protein sequence has 162 amino acid residues that are organized into α-helices (8 %), β-sheets (45 %) and random coils (47 %) in its secondary structure. The tertiary structure features an anti-parallel β-barrel motif where 8 β-sheet strands form the barrel and one β-sheet strand resides on the exterior of the barrel. A disulfide bond between residues 106 and 119 occurs between two of the barrel strands, along with a free thiol group at 121. A second disulfide bond is formed between another β-sheet stands (66) in the barrel and residue 160 of a random coil section. The β-sheet that is not part of the β-barrel motif interacts with the exterior β-sheet of other β-lactoglobulin monomers to form dimmers. This dimeric state is the prominent form of β-lactoglobulin in native milk. The dimeric quantinary structure is sensitive to heat, ionic strength and pH and can be altered to induced gelation. Specifics of gelation will be addressed in section 3.2.

1.1.1.3. Lipids

The milk lipids are located in either the milk fat globule or within the membrane surrounding it. Lipid classes include tri-, di- and monoglycerides (98.13 %), cholesteryl esters (0.02 %), free fatty acids (0.28 %), cholesterol (0.46 %), and phospholipids (1.11 %) (Bitman and Wood 1990). While no lipid class resides exclusively with the membrane or inside the globule, the glycerides are predominately found inside the fat globule, along with fat soluble vitamins, while the cholesterol and phospholipids are predominately found within the membrane (Fong et al 2007). Additionally, it is important to note that the size of the fat globule and membrane ranges between one and eight μm in raw milk (Walstra and Jenness 1984).

1.1.1.3.1. Phospholipids

Phospholipids, first discovered by Gobley in 1845, are a class of amphiphilic molecules found in cell membranes (Küllenberg and others 2012). In general their structure is comprised of a glycerol or sphingosine backbone with two fatty acids located at sn-1 and sn-2 positions, and a phosphoric acid at sn-3 position, which is esterified to an amino alcohol (Shin 2012). As stated previously (section 1.1.1.) bovine milk typically contains 3.5-4.7% fat; phospholipids account for 0.8 % of total milk fat (Fox 2003). Roughly 65% of the phospholipids in milk are associated with the milk fat globule membrane (Fox 2003) and make up one third of the milk fat globule membrane on a dry weight basis (Mudler and Walstra 1974). There is a substantial amount of research showing the health benefits of phospholipids (Küllenberg and others 2012). As such, ingredients containing a high

phospholipid content could be useful for nutrient delivery. The development of such an ingredient is detailed in section 1.2.3.

1.2. Powdered milk products and their manufacture

A number of different protein rich powders are commercially produced from bovine milk. The transformation of raw milk (i.e. milk that is fresh and has not been heat treated) into milk powder and various derivatives require a number of different sequential unit operations. For the purpose of this thesis, only the general unit operations required for the production of milk protein concentrate (MPC) and whey protein isolate (WPI) will be discussed.

1.2.1. Milk protein concentrate

Milk protein concentrate are complete dairy powders (e.g. they contain both casein and whey proteins) with a protein concentration that ranges between 40-89 % (US Dariy Council). Milk protein concentrate is produced from skim milk. A typical procedure for milk protein concentrate production from the raw milk state uses the following process according to Skanderby and others (2009). During milk harvest, the fluid product is easily contaminated with soil, bacterial spores and cell, and somatic cells, each of which reduces the raw milk quality. In order to attain a high quality end product, the level of these contaminates can be significantly reduced via centrifugation in a so called bactofuge in the first step of milk protein concentrate powder production. In this step, the relatively high density contaminates fall to the bottom and are removed from the milk serum . Centrifugation also causes the relatively low density fat globules to separate from the milk serum. Here fat can be skimmed from the top of the milk. Next, the milk is heat treated for

the inactivation of remaining pathogenic or spoilage microorganisms present after bactofuge treatment and homogenized to stabilize residual fat. Heat treated milk is then subjected to ultrafiltration. Ultrafiltration is a membrane separation process where a semi-permeable membrane with specific pore size is employed to separate fluid components by their size. In ultrafiltration, small molecules such as water, ions, and sugars pass through the membrane while large molecules (proteins, fat and bacteria) are retained, thereby concentrating the protein and retaining fat fractions of the skimmed and heated milk. At this point, the concentrated milk may be homogenized to prevent creaming of residual fat retained. Finally, the homogenized, condensed fluid is evaporated and spray dried to produce milk protein concentrate.

1.2.2. Whey protein isolate

Whey is the aqueous byproduct of casein and cheese production that is classified as sweet or acid depending on the primary process from which it was obtained. Sweet whey (pH 6.3 - 6) is the byproduct of rennet induced cheese manufacture; acid whey (pH 4.3 - 4) is the byproduct of casein and acid cheese (e.g. Cottage cheese) manufacture (Morr and Ha 1993). In general, whey composition consists of water, proteins, lactose, lipids and minerals where the protein concentration is roughly 10 % of the total solids (Mulvihill and Ennis 2003). Over the past several decades, several concentration processes have been developed to remove the water, lactose and mineral fraction and concentrate the protein fraction to yield a number of different whey protein products. Whey protein isolate (WPI) was the source of whey protein used in this thesis and therefore the discussion of whey protein products will be limited to WPI.

Whey is the starting material used to produce whey protein isolate (WPI). The final powdered WPI has a protein concentration that is greater than 90 % protein (Smith 2006). In order to increase the protein concentration to this level, several steps much take place that reduce the impurities, water, lactose and mineral concentrations. In general, a first step is to remove impurities such as cheese fines and residual fat from the whey via centrifugation followed by pasteurization to kill pathogenic organisms (Smith 2006). Next, the whey proteins are then separated from low molecular weight non-protein whey components typically by ultracentrifugation followed by diafiltration (Huffman 1996, Onwulata 2008). The small pore size of the ultrafiltration and diafiltration membranes allow small molecular weight compounds like minerals to pass through but retain large fat globules. Residual fats are removed by microfiltration. The water content of the whey is then reduced by evaporation followed by spray drying (Huffman 1996, Onwulata 2008). Another processing technique used to separate the protein fraction from whey is a stirred bed ion exchange process. In this process, the fluid whey flows over an ion exchanger and charged whey proteins adsorb onto the reactor. The pH of the retained protein is then adjusted causing their release from the reactor. The resulting slurry is then concentrated by ultra-filtration and spray dried (Morr and Ha 1993, Onwulata 2008). The composition of the final powdered product has > 90 % protein (Page 2006) and the remaining 10 % (moisture, lactose, mineral and lipid) varies according to the specific processes used to produce the starting material (e.g. type of bacterial culture used for pH reduction in cheese production) and whether or not the whey was pretreated for removal of residual lipids (Morr and Foegeding 1990).

1.2.3. Phospholipid particles

Relative to whole milk, buttermilk is a rich source of phospholipids due to its high milk fat globule membrane content (Elling and others 1996). Buttermilk is the by-product of butter production. The cream used in butter production is an oil-in-water emulsion stabilized by the milk fat globule membrane. During butter production, the milk fat globule membrane is disrupted as the cream is agitated to invert the oil-in-water emulsion into a water-in-oil emulsion. As this happens, the fat coalesces and serum, rich in water soluble compounds including the disrupted membrane, is released. This collected serum is sweet buttermilk. Although less common, Whey buttermilk has significantly higher phospholipid content than sweet buttermilk (Sodini and others 2006). In its production, Whey cream, collected from the concentrated fat phase of whey permeate (Halpin-Dohnalek and others 1989), is churned to make whey butter and the liquid collected from this process is whey buttermilk (Elling and others 1996). Costa and others (2010) found that subjecting the whey buttermilk to ultrafiltration and diafiltration in combination with super critical fluid extraction can increase the total phospholipid concentration of whey buttermilk by 500% on a dry weight basis.

There is a substantial amount of research showing the health benefits of phospholipids (Küllenberg and others 2012). In powder form, whey buttermilk can be used as phospholipid rich ingredient to fortify foods for added health benefits. Saffon and others (2011) has taken the functionality of this ingredient a step further by creating a particle composed of protein and phospholipid from the whey buttermilk powder. These particles can be used as "filler particles" in various food matrixes and have been dubbed "liposomal aggregates" by Nguyen (2013). This name however is a misnomer as it indicates that the

aggregate is a kind of liposome. Liposomes have specific structures where aliphatic molecules self assemble to form a sphere that acts as a shell in aqueous medium (Lasic and Needham 1995). No evidence was provided of the "liposomal aggregate" structure. As such, for the purposes of this thesis, these aggregates will be referred to a protein-phospholipid particles. There are three distinct protein groups in whey buttermilk: proteins of the milk fat globule membrane, caseins and immunoglobulin G light chains, and whey proteins. Caseins are the least abundant protein fraction. The protein-phospholipid particles are generated by denaturing the protein in the presence of buttermilk lipids. The composition of the protein-phospholid particle pellet obtained after centrifugation is 10 % total fat, 0.68 % phospholipids, 2% total protein with the remaining content being water (Nguyen 2013). The protein fraction is comprised of proteins from the milk fat globule membrane, caseins, and whey proteins. It should be noted however the protein content was measured by the bicinchoninic acid method using a bovine serum albumin standard curve. Kessler and Fanestil (1986) have found that, in the presence of bicinchoninic acid, phospholipids produce an absorbance peak similar to that of protein, which could cause erroneously high protein concentration results. Saffon and others (2014) successfully incorporated such particles into an acidified casein gel and found that they interacted with the network via thiol/disulfide exchange. To date, there are no reports on their incorporation into a whey protein gel network. Given the results of Saffon and others (2014) combined with those of Nguyen (2013), it is plausible that the protein-phospholipid particle could be used as a filler particle with the added benefit of nutrient delivery vesicle.

2. Food structure

2.1. Soft matter physics approach to food structure

Manufactured foods (i.e. foods that have been processed and are not in their natural state) are highly complex materials, composed of proteins, fats, carbohydrates and water molecules that interact with each other in unique ways to form a space filled network. This space filled network may be considered the food structure. Additionally, foods may be classified as fluids, semi-solids, soft-solids or solids (van Vliet and others 2009). While these designations are somewhat arbitrary, a fluid flows and soft and hard-solids maintain their shape under normal gravitational forces. Semi-solids have some flow by also maintain three-dimensional shape. For the purposes of this thesis, further discussion on food structures will focus solely on soft-solids. Soft-solid food materials are viscoelastic, self supporting systems which fracture with applied force. Their structural features may be viewed at various degrees of resolution, which range from the nano- to macroscopic length scale. The length scale of relevance is dependent upon both the complexity of the system and the macroscopic property of interest. During the past decade, researchers from the field of soft matter physics have suggested that soft-solid structures formed at the meso- length scale (between the nano- and macro- length scale) control macroscopic properties such as perceived texture (van der Sman and van der Goot, 2009, Ubbink and others 2008). From their perspective, it is suggested that structures within the meso length scale are not in an equilibrium state, a state which is characterized by events at the atomic level. Consequently, mesoscopic interactions are governed by entropy rather than chemical bonds making the material more susceptible to external forces (van der Sman 2012), such as those compressive and shearing forces exuded

during mastication. Structures at this length scale may be elucidated using various microscopic techniques.

2.2. Microscopy

Several imaging techniques have been used to elucidate the relative structural arrangements of phases (e.g. protein phase, fat phase, crystalline mineral compounds) within dairy based foods and model systems such as gels. The technique of choice is dependent on the desired resolution and the target constituent. As stated previously, structures of the meso-length scale are thought to govern macroscopic properties of soft-solid materials. Although there is no precise range that defines the meso-length scale, it typically refers to a resolution between ~ 100 nanometers and ~100 micrometers. Light microscopy and confocal scanning laser microscopy are two imaging instruments that can obtain a resolution within this range.

2.2.1. Light microscopy

2.2.1.1. Brightfield

Brightfield light microscopy is commonly used for imaging of cheese (Bowland and Foegeding 2001, Awad and others 2002, Arimi and others 2008). For analysis, rigid (frozen or embedded) cheese samples are thinly sliced (0.25 – 5 μm) using a microtome. Sliced samples are then fixed to a glass slide and stained to differentiate fat and protein rich areas. Oil red O dye is typically used for fat staining and Fast Green or toluidine blue is used for protein staining. It is important to note that while brightfield imaging is a quick and inexpensive imaging technique, there is potential for the fat component to dissolve or shrink during sample preparation resulting in artifacts (El-Bakry and Sheehan 2014).

2.2.1.2. Polarized light

In bright field microscopy, waves of incident white light, produced from a light source such as a halogen lamp, are used to illuminate a specimen. The waves of white first pass through a condenser, which focuses the light onto a small area of the sample (Murphy and Davidson 2013). Light waves vibrating in all planes pass through the specimen. The specimen diffracts the light, which is then collected by the objective that forms a magnified real image in the image plane of the eyepiece on the microscope (Murphy and Davidson 2013). In polarized microscopy, the light waves pass through a polarizer after the condenser and before the specimen. The polarizer only allows waves vibrating in a single plane to reach the specimen. As the polarized light enters an anisotropic crystal (material with directionally dependant uniformity) it is split into two rays that travel perpendicularly to each other. The split rays then pass through an analyzer which recombines the two rays to enable imaging (Murphy and Davidson 2013).

In dairy foods, polarized microscopy can be used to image materials with anisotropic ordering of molecules such as crystalline fat or mineral deposits (Flint 1994, Bolder and others 2006, Moris and others 1988, Brooker and others 1975). For crystalline fats, proof that luminescence under polarized light is due to the fat can be achieved by imaging the sample in a cooling, heating, cooling process. Above the melting point of the fat luminescence is lost but will return upon cooling the sample (Flint 1994). Bolder and others (2006) demonstrated the ordering of whey protein fibrils formed at pH 2 under polarized light. Calcium phosphate and non-phosphase crystals may also be imaged in cheese under polarized light (Morris and others 1988, Brooker and others 1975).

2.2.2. Confocal

Confocal scanning laser microscopy (CSLM) is a fluorescence based microscopic technique that enables three dimensional imaging of samples and can achieve a resolution as high as 250 nm (Paddock and Eliceri 2014). In principle, atoms of intrinsic fluorochromes and extrinsic fluorophores absorb light energy at a specific wavelength range and become excited. Excited electrons then emit light energy at a higher wavelength range as they return to the non-excited ground state. Emitted light energy is then detected and amplified to generate a two dimensional image. This process is then repeated several times, and with each time the focal plane is moved along the z-axis into the sample. Consecutive two dimensional focal plane images are then stacked, or compiled, to give one three dimensional image (Paddock and Eliceri 2014).

Intrinsic fluorochromes are fluorescence capable molecules inherent to a system. Example of intrinsic fluorochomes in dairy foods are the aromatic amino acid residues tryptophan, tyrosine, phenylalanine. Their excitation/emission spectra are 280, 274, 257 nm and 348, 303 and 282 nm respectively (Kulmyrzaev and others 2005, Karoui and others 2003, Christensen and others 2006). An extrinsic fluorophore is a fluorescent molecule associated with a non-fluorescent molecule that is added to a sample matrix for the purpose of identifying a specific biological entity. Several extrinsic fluorophores or stains have been successfully used for the identification of protein or fat phases of dairy products. Acridine orange (0.2% w/v), Nile Blue A (0.1% w/v), Rhodamine B (0.1% w/v), and Fast Green FCF non-covalently interact with the protein phase of a system (0.1% w/v) (Choi and others 2007, Guinee and others 2000, Auty and others 2001). Interestingly, Nile Blue A may also be used

to simultaneously elucidate the fat phase of a sample by excitation at 488 nm instead of 633 nm for the protein phase (Auty and others 2001). Nile red (0.1% w/v) is a commonly used non-covalent stain used for elucidation of the fat phase (Auty and others 2001).

In systems containing more than one type of protein, it may be desirable to distinguish between the two proteins. This may be achieved through the use of covalent stains. Amine reactive stains such as Texas Red-X carboxylic acid succinimidyl ester and Oregon Green 488 carboxylic acid succinimidyl ester have been used successfully for this purpose (Vasbinder and others 2004). Another approach would be to use covalently labeled antibodies of specific proteins. Although several such antibodies have been developed for the detection and identification of casein and whey proteins, reports for their use to elucidate structural components within a food matrix are limited as of the publication date for this research.

2.3. Dairy gel structures

2.3.1. Casein

The casein micelle exists as a dispersed colloid in native milk that is stabilized via steric hindrance and electrostatic repulsion due the presence of the κ-casein protruding from the micelle. Removal of either stabilizing mechanism induces flocculation of the micelles leading to the formation of a particulate disordered gel. Given the structural complexity of the casein micelle a simplified structural model, the casein brush model, is often used to describe the physico-chemical changes in the casein micelle that lead to flocculation (de Kruif and Holt 2003). In the casein brush model the exterior layer of κ-casein protruding

from the micelle is envisioned as a polymeric brush composed of many polyelectrolyte molecules (i.e. the κ-casein) that can be thought of as brush bristles *per se*. Reductions in brush density or thickness can lead to collapse of the brush. Micelles with a collapsed brush are no longer stabilized in solution by steric hinderance or electrostatic repulsive and consequently flocculate.

Brush density can be reduced by the enzymatic activity of Chymosin. Chymosin is a proteolytic enzyme in rennet used in traditional cheese production that specifically cleaves the phenylalanine$_{105}$-methionine$_{106}$ bond of κ-casein. This hydrolysis releases a portion (amino acid residues 106-169) of the κ-casein commonly referred to as the casein macropeptide into solution. The remaining *para*-κ-casein now has a hydrophobic region protruding from the micelle. Once 80-90% of the κ-casein has been cleaved, sufficient steric henderance is reduced and the micelles begin to flocculate due to attractive forces. The onset of flocculation is concurrent with brush collapse in the casein brush model (de Kruif and Holt 2003).

Brush thickness is dependent on the bristle charge density. As stated previously, the bristles represent κ-casein. In native milk, positively and negatively charged residues are distributed unevenly throughout the protein; 28 negatively charged amino acids reside within the residue regions of 1-20 and 115-169 while 17 positively charged amino acids are located within 1-115 segment (Swaisgood 2003). As pH decreases ionized carboxylic acid groups regain hydrogen ions leading to reduced charge density. Below pH 5 sufficient reduction in brush thickness has occurred and the brush begins to collapse leading to micelle flocculation (de Kruif and Holt 2003).

2.3.1.1. Cheddar cheese structure and texture

The casein gel network forms the basis for the production of natural cheese products. The natural cheese structure however is far more complex than the model systems discussed above (section 3.1) and is dependent on the processing techniques used. Therefore a brief discussion of cheese structure and its relationship with texture is pertinent. Cheddar cheese will be used as a case in point.

In general, the structure of Cheddar cheese is unique in that larger curds composed of overlapping, flattened and elongated smaller curd particles are cut and pressed together to extrude fluid (whey) and form a continuous protein matrix. In traditional Cheddar cheese, containing 33 - 36 % fat, fat globules exist as large aggregated clusters dispersed throughout the protein matrix (Emmons and others 1980). Dispersion of these clusters into smaller evenly distributed particles only marginally alters the texture (Emmons and others 1980). Bryant and others (1995) concluded that maintaining an appropriate level of protein disruption by controlling fat content was essential to produce cheese with acceptable textural qualities. In general, textural features of Cheddar cheese lie between the crumbly and plastic textures associated with Cheshire and Gouda respectively (Lawrence and others 2004). Definitions for these and other sensory attributes are located in Table 1 of Chapter 2.

Reduced fat Cheddar cheeses are form a more cohesive mass during mastication, and are more springy (i.e. they return to original shape after deformation) than their full fat version as determined by instrumental Texture Profiling Analysis (Gwatrney and others 2002). These changes in texture are associated with increased protein density of the matrix (Bryant and others 1995, Emmons and others 1980).

2.3.2. Whey protein gel structure

As stated previously (section 1.1.1.2.), β-lactoglobulin is the predominate protein in the whey (serum) proteins. Consequently, researchers have primarily focused on β-lactoglobulin when studying heat denaturation and aggregation mechanisms of whey proteins. Heat induced denaturation and subsequent aggregation of β-lactoglobulin into a gel network is a complex process that is highly dependent on environmental conditions. de Wit (2008) and de la Fuente (2002) have prepared excellent, in depth reviews on this subject matter. For the purposes of this thesis, only the critical events and key points will be highlighted.

In native milk, β-lactoglobulin exists as dimmers which first separate into monomers upon heating (de Wit 2008). At temperatures near 70 °C, the tertiary structure of the monomer begins to unfold exposing a thiol group and hydrophobic residues (Iametti and others 1996). This structural modification enables the β-lactoglobulin monomer to interact with neighboring reactive species to form non-native dimers via sulfhydryl oxidation or thiol-disulphide exchange to form disulfide bonds (Schokker and others 1999; Briggs and Hull 1945; Sawyer 1968, Gezimati, Creamer, and Singh 1997). The non-native dimmers then polymerize to form tetramers (Briggs and Hull 1945). If aggregation continues and the protein concentration is high enough, a gel will form. Gels formed at near neutral pH and low ionic strength are composed of thin-stranded networks and commonly referred to as fine stranded gels. Conversely, under conditions of high ionic strength or low pH, the tetramers will coalesce into larger particles which then flocculate to form a particulate gel network (Ikeda and Morris 2002). A summary of these whey protein gel structures and their

relationship to rheological properties and sensory texture attributes can be found in Chapter 2.

3. Potential for modification of whey and casein gel properties

3.1. Casein and whey interactions

Interactions between β-lactoglobulin and individual casein proteins or the casein micelle have been studied extensively. The following section will focus solely on β-lactoglobulin interactions with individual and mixed casein (i.e. sodium caseinate) protein solutions.

Caseins are holdase molecular chaperones (Holt and others 2013). Holdase molecular chaperones are proteins that can inhibit the stress induced (e.g. heat, pressure) aggregation of specific proteins by interacting with hydrophobic residues of the target protein (Hartl and others 2011). In this case, β-lactoglobulin is the target protein. The ability of caseins to inhibit aggregation of heat denatured β-lactoglobulin is dependent on several factors including pH, ionic strength of the solvent and molar ratio of the holdase molecular chaperone to its target proteins (Morgan and others 2005, Kehoe and Foegeding 2011, Yong and Foegeding 2008, Guyomarc'h and others 2009). In solutions of 0.2 M NaCl with a 0.5:1 molar ratio of β-lactoglobulin to α_s-casein (i.e. both α_{s1}- and α_{s2}-casein), the ability of α_s-casein to inhibit β-lactoglobulin aggregation is reduced by nearly 50 % as pH is increased from 7.0 to 7.5 (Morgan and others 2005). For solutions containing 5 % w/w β-lactoglobulin and 1 % w/w β-casein, aggregation of heat denatured (80 °C for 20 min) β-lactoglobulin is inhibited most effectively at a pH of 6.0 and to a lesser extent at pH 6.5 and pH 5.8 (Kehoe

and Foegeding 2011). Addition of mono- or divalent salts further decreases the β-casein chaperone activity under these conditions (Kehoe and Foegeding 2011). Additionally, in solutions containing 6 % w/w β-lactoglobulin at pH 6.0 and low ionic strength, heat induced (90 °C, 20 min) aggregation is inhibited at a molar ratio of 1.0:0.13 β-lactoglobulin to β-casein (Yong and Foegeding 2008). Further addition of β-casein to the solution leads to an even greater suppression of denatured β-lactoglobulin aggregation (Yong and Foegeding 2008). Finally, for κ-casein and whey protein isolate solutions (1.5 – 2.4 % w/w protein, 0.1 M NaCl at pH 7), κ-casein inhibits denatured whey protein aggregation exponentially with increasing κ-casein concentration, which reaches a plateau at ~1 % κ-casein (Guyomarc'h and others 2009).

Utilization of individual caseins for their chaperone activities however is impractical on an industrial scale. The use of a mixed casein solution such as sodium caseinate would be more cost effective. Guyomarc'h and others (2009) has investigated the effectiveness of sodium caseinate to inhibit denatured whey protein aggregation. In whey protein isolate solutions (1-2% w/w, 0.1 M NaCl, pH 7) heated to 80 °C for 24 hours, addition of caseinate increasingly decreases protein aggregate size, which reaches a plateau at around ~ 1% caseinate. The protein content of the aggregates are comprised of 80-90% w/w whey protein and 10-20% w/w κ- and α_s-casein (Guyomarc'h and others 2009). β-casein is not incorporated into the final aggregate. Conversely, aggregates of β-lactoglobulin formed in the presence of pure β-casein contain significant quantites of β-casein (Kehoe and Foegeding 2014). Guyomarc'h and others (2009) surmized that κ-, α_s-, and β-caseins of sodium casein compete for interaction with denatured β-lactoglobulin.

The potential to utilize the holdase chaperone behavior of caseins to alter food textures was realized by Yong and Foegeding and others (2010) in their literature review of casein chaperone activity. To date, exploration into the potential texture modification of whey protein gels by caseins has received little attention. This void in the literature presents one avenue of new research that is in line with the overall goal of this thesis. In Chapter 3, the affects of mixed caseins and casein micelles on the sensory texture, rheological properties and microstructure of whey protein gels are investigated.

3.2. Complex calcium crystals

Development of crystalline deposits on the surface and within natural and processed cheese products is a common phenomenon. These deposits are typically composed of calcium complexes, sodium citrate, lactose or tyrosine (Brooker 1975, Brooker 1979, Dox 1911, Flückiger and Schilt 1963, Rayan and others 1980, Yiu 1985, Klostermeyer and others 1984). Tyrosine crystals have been located in Roquefort and Emmental cheeses near surfaces that are exposed to air (*i.e.* cracks or holes generated by gas) (Dox 1911, Flückiger and Schilt 1963). Their formation is thought to stem from proteolysis within the substratum and accumulated tyrosine molecules are able to crystallize in the low moisture environment of cracked surfaces or air bubbles (Dox 1911). Crystalline tyrosine deposits observed in Emmental cheese have a clustered needle-like morphology, in which needle-like bundles radiate outward from a single nucleation point. Two typical crystalline deposits found in Cheddar cheese are calcium lactate and calcium phosphate (Brooker 1979). As elucidated by Brooker and others (1975), the calcium lactate crystals "consist of randomly arranged bundles of slightly curved, needle-like crystals", which have an irregular shape and

can grow up to 80 μm in diameter (Brooker 1979, Brooker 1975). On the other hand, calcium phosphate crystals can grow to 20-30 μm in diameter and appear in large numbers relative to the calcium lactate crystals (Brooker and others 1975). The calcium phosphate crystal morphology was described by Brooker (1979) as "numerous, closely packed, needle-like crystals (25nm in diameter and up to 4.5 μm long)." Crystalline deposits of sodium citrate have been identified by Rayan and others (1980) in processed cheese. The sodium citrate deposits also have a needle-like morphology; however, this crystal type appears alone instead of bundled like the aforementioned calcium crystals. The sodium citrate crystal morphology has a slightly oblong shape with a length of ~5 μm and diameter that is greater than the individual needles of the complex calcium or tyrosine crystals (Rayan and others 1980).

The specific location of complex calcium crystals within the natural cheese matrix is unclear. Brooker (1979) and Yui and others (1980) have found that complex calcium crystals in Cheddar Cheese tend to accumulate near grain boundaries and junction zones where as Lowrie et al (1982) found that crystals, vaguely identified as "salt" crystals, are evenly distributed throughout the matrix. Morris et al (1988) estimates that calcium phosphate crystals in cheddar cheese (4 weeks old) occupy a volume fraction of ~ 1.96 % while non-phosphate crystals occupy ~ 0.42 % volume fraction. The crystalline deposits in processed cheese appear to be equally distributed throughout the protein matrix (Guinee and others 2004).

Although it is well known that crystalline deposits in natural and processed cheese products develop during the aging process (Noël and others 1996, Brooker 1979), their

affects on sensory or fracture properties are rarely considered. Schär and J. O. Bosset (2002) have indicated that salt crystals in processed cheese affect cheese texture but do not provide details as to what attributes are impacted by their presence. In a sensory and rheological analysis of aged Parmigianino Reggiano cheese (12, 18 and 28 months), Noël and others (1996) hypothesized that structural changes occur during the aging process that allow cracks to propagate more quickly through the cheese material. These structural changes were presumed to be a result of dehydration and proteolysis during the aging process. It is interesting to note however that although Noël and others (1996) reported that crystalline deposits within cheese samples of this study more than doubled with age, no consideration was given of their possible affects on fracture properties (i.e. brittleness, fracture strain, fracture stress) of the cheese.

Green and others (1985) examined crack propagation in Cheddar (28 weeks) cheese due to various force applications including bite and compressive forces, using scanning electron microscope. For bite force, a single person bit into cheese cubes (15 x 15 x 15 mm) using their front teeth until fracture occurred. For compressive force, cubes were compressed at rate of 50 mm/s using an Instron machine until fracture. Fractured surfaces of bitten Cheddar cheese samples showed that the top and bottom teeth penetrated into and cut the top and bottom thirds of the sample with a high enough force to fracture the remaining center third of the sample. From the teeth penetration points, cracks propagated through the center matrix section along a high fat plane. Minimal crack propagation from this fractured surface radiated into the cheese matrix. For compression force testing, crack propagation occurred

along grain boundaries and an abundance of cracks were observed to radiate from the fractured surface into the cheese interior.

In normal mastication of soft solid foods, such as cheese cubes, samples are more likely to be placed between the back molars for fracture than between the front teeth. In considering the greater surface area of the molar tooth relative to the front tooth, it could be argued that a greater degree of compressive normal force is applied to a food sample when it is compressed between the molars. Thus, crack propagation in Cheddar cheese induced by bite force between the molars may also occur along the grain boundaries like that seen for the instrumental normal force compression. In considering the observations of Green et al (1985) in conjunction with those of Brooker (1979) and Yui and others (1980), that complex calcium crystals in Cheddar Cheese tend to accumulate near grain boundries and junction zones, the following question is raised; Do complex crystalline inclusions alter the breakdown properties of a protein matrix? This question is addressed in Chapter 4.

4. Sensory analysis

Sensory texture acceptance is a critical factor that influences consumer preference of a food material (Cardello 1995). A variety of analytical techniques have been developed in the field of sensory science to describe the various attributes perceived during the oral processing of a food material. In particular, Quantitaive Descriptive Analysis (QDA) is a technique designed to quantitavily discriminate texture attribute intensity differences between several sample treatments (Stone 1992). For this analysis, a sensory panel comprised of 10 – 12 members is guided by a panel leader to develop a common language

that describes the perceived sensory textures of the samples and the order in which they are perceived. The panel also generates definitions for the terminology developed and a standardized procedure for assessment of each attribute. A number of the commonly assessed attributes, definition(s), and their evaluation protocol has been summarized by Pascua and others (2013). This summary can be found in Table 1 in Chapter 2 of this thesis. Finally, the intensity of each attribute is quantitatively assessed using a line scale In this thesis, the Spectrum^{TM} method (Meilgaard and others 1999) of descriptive analysis was used to characterize gel texture attributes. This method follows a similar procedure to the QDA except that the intensity of each attribute is quantitatively assessed using a line scale with word anchors.

Sensory analysis by a trained panel is expensive and time consuming. Often times, researchers will suggest the use rheological analyses to infer sensory texture of a material. While several rheological tests (see section 6) have found good correlations with some sensory texture attributes, instrumental tests simply cannot emulate the dynamic conditions exerted onto a material during oral processing, and therefore cannot provide complete information on masticatory attributes (Bourne 2002). (A description of the dynamic oral processing events can be found in Chapter 2, section 1). As such, for a thorough understanding of the descriptive texture profile of a material there is no substitution for sensory analysis by a human panel.

5. Rheology

Rheology is the study of deformation and flow of matter (Steffe 1996). As a whole, "Rheometry helps in understanding the responses of food structure to applied forces or

deformation and also provides information on the dependence of food structure on overall composition and interaction between the components" (Miri 2010). In solid materials, rheological tests use the relationship of stress and strain parameters to evaluate material properties before fracture in the linear and non-linear regions. The stress parameter (σ) is defined as force per unit area and the strain (ε) parameter is defined as the deformation per unit length (Steffe 1992). When the stress is applied perpendicular to the material surface it is a normal stress, whereas if applied parallel to the material surface it is shear stress. Regardless of which direction the stress is applied, if the stress and strain responses are proportional to each other then the stress-strain relationship is linear and the material is said to obey Hooke's law (Steffe 1992). Perfectly elastic solid materials follow Hooke's law. Rubber is an example of a Hookian solid. In fluids, a relationship is drawn between shear stress and shear strain rate to evaluate the viscous nature of the material. If the stress-strain rate respose is linear the fluid follows Newton's law (Steffe 1992). Most food oils are examples of Newtonian fluids. Soft solid foods are rarely purely elastic or viscous. Soft-solid food materials typically have both a viscous and elastic nature and therefore are considered viscoelastic materials. Under very small deformations, viscoelastic soft-solid materials exhibit a Hookian response at a given shear strain rate (in most cases applied in oscillation). This region of the stress-strain curve represents the linear viscoelastic region (LVR). As the strain or strain rate is increased, there will be a point where the stress-stain response is no longer linear. This region of the curve is appropriately called the non-linear viscoelastic region.

A number of rheological tests have been developed to probe material properties at both high and low strain levels. These tests may be fundamental or empirical. In empirical testing, sample shape and deformation are conducted such that precise values of stress, strain and strain rate cannot be calculated - so true material properties cannot be calculated. These tests are most useful for gauging force-deformation relationships of material that are highly heterogeneous or use in quality control. A ganache filled tempered chocolate is an example of a highly heterogeneous food material. On the other hand, fundamental tests are conducted using test geometries and applied forces and deformations such that fundamental material properties can be calculated. Furthermore, in most fundamental tests the samples are assumed to be isotropic and homogeneous on a scale relative to the dimensions of the testing apparatus.

5.1. Small strain Rheology

In small strain Rheology, material properties are evaluated at very small deformations within the LVR (Steffe 1992). Small amplitude oscillatory shear (SAOS) is a common small strain test that measures shear stress, shear strain, and phase angle (between stress and strain oscillations) at various strain rates. These values are used to calculate the storage modulus (G′) and loss modulus (G″) of a material. The storage modulus represents the ability of the material to elastically store energy. The loss modulus represents dissipated energy. The phase angle represents the degree of material viscoelasticity at a given frequency. The instrument works by applying a constant controlled stress or strain to the specimen at increasing frequency and the respondent magnitude of strain or stress is measured. One important restriction for this test is that the applied stress or strain must be within the linear

viscoelastic region of the material. To determine the LVR, stress or strain is applied at an increasing magnitude and constant frequency. The LVR is where the stress and strain response is linear over a range of frequencies.

One application of small strain rheological methods is in determining the effects of filler particles (van Vliet 1988). Values for G′ can be used to determine if a filler particle is active or inactive within a particular material. Filler particles are discrete entities embedded in a continuous matrix. Particles are either inactive, not interacting with the continuous matrix, or active and interacting with the surrounding matrix (van Vliet 1988). The G′ of filled gels (also called composite materials) will depend on if the filler particle is active or inactive. Inactive filler particles decrease G′ by essentially causing voids in the matrix and decreasing the density of load-bearing elements. Active filler particles increase, decrease or do not change G′ of the filled gel depending on if the filler particles have G′ values that are, higher, lower or the same as the matrix, respectively (van Vliet 1988).

The small angle oscillatory shear test described above is used in Chapter 3 to determine whey protein-phospholipid particle interaction with the whey protein gel matrix.

5.2. Large strain Rheology

Large strain rheological tests of soft-solid viscoelastic materials evaluate the stress and strain relationships in various regimes of the stress-strain curve (Steffe 1992). Uniaxial compression is often used to measure stress – strain relationships on bulk materials. Unlike small angle oscillatory shear testing, obtaining viscoelastic information is more difficult and tests are often conducted at one rate of deformation (usually given as crosshead speed of the instrument). Uniaxial compression is under normal force so the proportionality constant is

the Young's Modulus (E). As the strain is increased, the stress-stain curve moves through the non-linear region until catastrophic failure occurs at the fracture point. The stress and strain values at the point of fracture are two important parameters used to characterize the material.

A relatively new, and empirical measure, is to determine post-fracture patterns in force – deformation relationships. A decrease in measured force occurs after fracture and stress and strain values are no longer valid because the material has been broken and the area of the material used to calculate stress and strain values is no longer known. The post-fracture curve pattern characterizes the breakdown pattern of the material where a steep drop in force represents fast breakdown and a slow pattern represents slow breakdown (van den Berg and others 2007). According to van den Berg and others (2007) crack propogation speed of the material post catastrophic failure can be inferred from the slope of the post fracture curve. A steep slope represents a free running crack where as a slope closer to zero is indicative of a slower breakdown via multi-point fractures or yielding of the material. Evaluation of the post-fracture curve under normal force has been used in several studies of phase separated protein-polysaccharide model gels, cheddar cheese and cheese analog under (van den Berg 2007, Çakır and others 2012, Patton 2013).

6.2.1. Torsional fracture

Diehl and others (1979) were the first to apply torsion analysis to foods. In this test, a pure shear force is applied to a capstan shaped specimen by twisting at a specified rate until fracture. The fracture stress and fracture strain of the specimen are calculated from the maximum torque and rotational angle reached respectively. A unique feature of this test is

that the conditions of pure shear in twisting causes shear, normal and tensile forces to be equally distributed throughout the specimen during deformation. This enables the specimen to fail under the type of stress (tensile or shear) that the material has the least resistance against (Deihl and others 1979). If the specimen fractures at a 45 ° angle, failure was due to tensile stress. If a horizontal fracture occurs, shear stress was the cause of failure (Deihl and others 1979).

Rheological measures fundamental food material properties that can provide information about the food structure and also which shows good correlations with some sensory texture attributes. A thorough discussion on sensory texture and food structure relationships is given in Chapter 2.

References

Arimi JM, Duggan E, O'Sullivan M, Lyng JG, O'Riordan ED. 2008. Effect of refrigerated storage on water mobility and microwave expansion of imitation cheese containing resistant starch. J Food Eng 89(3):258-66.

Auty MAE, Twomey M, Guinee TP, Mulvihill DM. 2001. Development and application of confocal scanning laser microscopy methods for studying the distribution of fat and protein in selected dairy products. J Diary Res 68:417-27.

Awad RA, Abdel-Hamid LB, El-Shabrawy SA, Singh RK. 2002. Texture and microstructure of block type processed cheese with formulated emulsifying salt mixtures. LWT-Food Sci Tech 35:54-61.

Bitman J, Wood DL. 1990. Changes in milk phospholipids during lactation. J Dairy Sci. 73:1208-16.

Bolder SG, Hendrickx H, Sagis LM, van der Linden E. 2006. Fibril assemblies in aqueous whey protein mixtures. J Agr Food Chem 54(12):4229-34.

Bourne M. 2002. Correlation between physical measurements and sensory assessments of texture and viscosity. In: Bourne M, editor. Food texture and viscosity: concept and measurement, 2nd edition. San Diego:Academic Press, p 293-323.

Bowlan EL, Foegeding EA. 2001. Small strain oscillatory shear and microstructural analyses of a model processed cheese. J Dairy Sci 84(11):2372-80.

Briggs DR, Hull R. 1945. Studies on protein denaturation. I. Electrophoretic study kinetics at neutrality of heat denaturation of β-lactoglobulin. J Amer Chem Soc 67(11):2007-14.

Brooker BE, Hobbs DG, Turvey A. 1975. Observations on the microscopic crystalline inclusions in Cheddar cheese. J Dairy Res 42(2):341-48.

Brooker BE. 1979. Milk and its products. In: Vaughn JG, editor. Food Microscopy. London:Academic Press. p 273-311.

Bryant A, Ustunol Z, Steffe J. 1995. Texture of Cheddar cheese as influenced by fat reduction. J Food Sci 60(6):1216-19.

Çakır E, Daubert CR, Drake MA, Vinyard CJ, Essick G, Foegeding EA. 2012. The effect of microstructure on the sensory perception and textural characteristics of whey protein/κ-carrageenan mixed gels. Food Hydrocolloid 26(1):33-43.

Cardello AV. 1994. Consumer expectations and their role in food acceptance. In: MacFie HJH, Thomson DMH, editors. Measurement of food preferences. New York:Blackie Academic. p 253-97.

Childs JL, Drake MA. 2009. Consumer perception of fat reduction in cheese." J Sensory Stud 24(6):902-21.

Choi J, Horne DS, Lucey JA. 2007. Effect of insoluble calcium concentration on rennet coagulation properties of milk. J Dairy Sci 90(6):2612–23.

Christensen J, Nørgaard L, Bro R, Engelsen SB. 2006. Multivariate autofluorescence of intact food systems. Chem Rev 106(6):1979-94.

Chu B, Zhou Z, Wu G, Farrell HM. 1995. Laser light scattering of model casein solutions: effects of high temperature. J Colloid Int Sci 170:102-12.

Costa MR, Elias-Argote XE, Jiménez-Flores R, Gigante ML. 2010. Use of ultrafiltration and supercritical fluid extraction to obtain a whey buttermilk powder enriched in milk fat globule membrane phospholipids. Int Dairy J 20(9):598-602.

Deeth HC. Hartanto J. 2009. Chemistry of milk-Role of constituents in evaporation and drying. In: Tammie AY, editor. Dairy powders and concentrated products. UK:Blackwell Publishing Ltd. p 1-22.

de Kruif. 1998. Supra-aggregates of casein micelles as a prelude to coagulation. J Dairy Sci 81:3019–28.

de Kruif CG, Holt C. 2003. Casein micelle structure, functions and interactions. In: Fox PF, McSweeney PLH, editors. Advanced Dairy Chemistry Vol1: Proteins, 3rd edition. New York:Kluwer Academic/Plenum. p 233-76.

de la Fuente MA, Singh H, Hemar Y. 2002. Recent advances in the characterization of heat-induced aggregates and intermediates of whey proteins. Trend Food Sci Tech 13(8):262-74.

de Wit JN. 2009. Thermal behaviour of bovine β-lactoglobulin at temperatures up to 150 C. A review. Trends Food Sci Tech 20(1):27-34.

Dickinson E, Semenova MG, Belyakova LE, Antipova AS, Il'in MM, Tsapkina EN, Ritzoulis C. 2001. Analysis of light scattering data on the calcium ion sensitivity of caseinate solution thermodynamics: relationship to emulsion flocculation. J Colloid Int Sci 239: 87-97.

Diehl KC, Hamann DD, Whitfield JK. 1979. Structural failure in selected raw fruits and vegetables. J Texture Stud 10(4):371-400.

Dox AW. 1911. The occurrence of Tyrosine crystals in Roquefort cheese. J Am Chem Soc 33(3):423-25.

Eigel WN, Butler JE, Ernstrom CA, Farrell HM Jr., Harwalkar VR, Jenness R, Whitney RMcL, 1984. Nomenclature of proteins of cow's milk: fifth revision, J Dairy Sc, 67(8):1599-1631.

El-Bakry M, Sheehan J. 2014. Analysing cheese microstructure: A review of recent developments. J Food Eng 125:84-96.

Elling JL, Duncan SE, Keenan TW, Eigel WN, Boling J. 1996. Composition and microscopy of reformulated creams from reduced-cholesterol butteroil. J Food Sci 61:48-53.

Emmons DB, Kalab M, Larmond E, Lowrie RJ. 1980. Milk gel structure. X. Texture and microstructure in Cheddar cheese made from whole milk and from homogenized low-fat milk 1. J Texture Stud 11:15-34.

Flint O. 1994. Food Microscopy. Oxford:BIOS scientific publishers limited. p 125.

Flückiger E, Schilt P. 1963. Beitrag zur kenntnis der salzsteinbildung in mmmentalerkäsen. Milchwissenschaft 18:437-42.

Fong BY, Norris CS, MacGibbon AKH. 2007. Protein and lipid composition of bovine milk-fat-globule membrane. Int Dairy J 17(4):275-88.

FAOSTAT. 2011. Food and Agriculture Organization of the United Nations. website: faostat.fao.org accessed 01-14-14.

Fox PF. 2003. Milk proteins: General and historical aspects. In: Fox PF, McSweeny PLH, editors. Advanced dairy chemistry, Vol 1:Proteins, 3rd ed. New York:Kluwer Academic/Plenum Publishers. p 1-48.

Gezimati J, Creamer LK, Singh H. 1997. Heat induced interactions and gelation of mixtures of bovine β-lactoglobulin and α-lactalbumin. J Agr Food Chem 45:1130-36.

Green ML, Marshall RJ, Brooker BE. 1985. Instrumental and sensory texture assessment and fracture mechanisms of Cheddar and Cheshire cheese. J Texture Stud 16:351-64.

Guinee TP, Auty MAE, Mullins C, Corcoran MO, Mulholland EO. 2000. Preliminary observations on effects of fat content and degree of fat emulsification on the structure-functional relationship of Cheddar-type cheese. J Texture Stud 31:645-63.

Guinee TP, Carić M, Kalab M. 2004. Pasteurized processed cheese and substitute/imitation cheese products. In: Fox PF, McSweeney PLH, Cogan TM, Guinee TP, editors. Cheese: Chemistry, physics and microbiology, Vol 2. Amsterdam:Elsevier. p 349-94.

Guyomarc'h F, Nono M, Nicolai T, Durand D. 2009. Heat-induced aggregation of whey proteins in the presence of κ-casein or sodium caseinate. Food Hydrocolloid 23(4):1103-10.

HadjSadok A, Pitkowski A, Nicolai T, Benyahia L, Moulai-Mostefa N. 2008. Characterisation of sodium caseinate as a function of ionic strength, pH and temperature using static and dynamic light scattering. Food Hydrocolloid 22(8):1460-66.

Halpin-Dohnalek MI, Marth EH. 1989. Fate of Staphylococcus aureus in Whey, Whey Cream, and Whey Cream Butter. J Dairy Sci 72(12):3149-55.

Hartl F, Ulrich AB, Hayer-Hartl M. 2011. Molecular chaperones in protein folding and proteostasis. Nature 475(7356):324-32.

Holt C, Carver JA, Ecroyd H, Thorn DC. 2013. Invited review: Caseins and the casein micelle: Their biological functions, structures, and behavior in foods. J Dairy Sci 96(10):6127-46.

Huffman LM. 1996. Processing whey protein for use as a food ingredient. Food Technol. 2:49-52.

Huppertz T. 2013. Chemistry of the caseins. In: McSweeney PLH, Fox PF, editors. Advanced dairy chemistry, Vol 1A: Proteins: Basic aspects, 4th edition. Boston:Springer US. p 135-60.

Iametti S, de Gregori B, Vecchio G, Bonomi F. 1996. Modifications occur at different structural levels during the heat denaturation of β-lactoglobulin. Eur J Biochem 237:106-12.

Ikeda S, Morris VJ. 2002. Fine-stranded and particulate aggregates of heat-denatured whey proteins visualized by atomic force microscopy. Biomacromolecule 3(2):382-89.

Jensen RG, Fenis AM, Lammi-Keefe CJ, Henderson RA. 1990. Lipids of bovine and human milks: a comparison. J. Dairy Sci 73:223-40.

Jensen RG. 1995. Introduction. In: Jensen RG, editor. Handbook of milk composition. San Diego:Academic Press p 1-3.

Karoui R, Mazerolles G, Dufour E. 2003. Spectroscopic techniques coupled with chemometric tools for structure and texture determinations in dairy products. Int Dairy J 13(8):607-20.

Kehoe JJ, Foegeding EA. 2011. Interaction between β-casein and whey proteins as a function of pH and salt concentration. J Agr Food Chem 59(1):349-55.

Kessler RJ, Fanestil DD. 1986. Interference by lipids in the determination of protein using bicinchoninic acid. Analytical Biochem 159(1):138-142.

Kiple KF, Ornelas KC. 2000. Milk and dairy products. In: Kiple KF, Ornelas KC, editors. The cambridge world history of food, Vol 1. Cambridge:Cambridge University Press. p 692-702.

Klostermeyer H, Uhlmann G, Merkenich K. 1984. Formation of crystals in processed cheese. 2. Identification of a new citrate. Milk Sci Int 39(4):195-97.

Küllenberg D, Taylor LA, Schneider M, Massing U. 2012. Health effects of dietary phospholipids. Lipids Health Dis 11(3):1-16.

Kulmyrzaev AA, Levieux D, Dufour E. 2005. Front-face fluorescence spectroscopy allows the characterization of mild heat treatments applied to milk. Relations with the denaturation of milk proteins. J Agr Food Chem 53(3):502-07.

Lasic DD, Needham D. 1995. The “stealth" liposome: a prototypical biomaterial. Chem Rev 95(8): 2601-28.

Lawrence RC, Gilles J, Creamer LK, Crow VL, Heap HA, Honoré CG, Johnston KA, Samal PK. 2004. Cheddar cheese and related dry-salted cheese varieties. In: Fox PF, editor. Cheese: chemistry, physics and microbiology 3rd edition, Vol 2. Boston:Elsevier. p 71-102.

Lowrie RJ, Kalab M, Nichols D. 1982. Curd granule and milled curd junction patterns in Cheddar cheese made by traditional and mechanized processes. J Dairy Sci 65(7):1122-29.

Lucey JA, Srinivasan M, Singh H, Munro PA. 2000. Characterization of commercial and experimental sodium caseinates by multiangle laser light scattering and size-exclusion chromatography. J Agr Food Chem 48(5):1610-16.

McMahon DJ, Oommen BS. 2013. Casein micelle structure, functions, and interactions. In: McSweeney PLH, author. Advanced dairy chemistry, Volume 1A. Boston, Mass: Springer US. p. 185-209.

Meilgaard M, Civille GV, Carr BT. 1999. The spectrum descriptive analysis method. Sensory Eval Tech 4:189-253.

Miri T. 2010. Viscosity and oscilatory rheometry. In: Norton IT, Spyropoulos F, Cox P, editors. Practical food rheology: an interpretive approach. Hoboken:John Wiley & Sons p 7-28.

Morr CV, Ha EYW. 1993. Whey protein concentrates and isolates: processing and functional properties. Critical Rev Food Sci Nutr 33(6):431-76.

Morr CV, Foegeding EA. 1990. Composition and functionality of commercial whey and milk protein concentrates and isolates: A status report.Food Tech 44(4):100-12.

Morris HA, Holt C, Brooker BE, Banks JM, Manson W. 1988. Inorganic constituents of cheese: analysis of juice from a one-month-old Cheddar cheese and the use of light and electron microscopy to characterize the crystalline phases. J Dairy Res 55(2): 255-68.

Mulder H, Walstra P. 1974. The milk fat globule. Emulsion science as applied to milk products and comparable foods. No. 4. Wageningen:Centre for Agricultural Publishing and Documentation.

Mulvihill DM. Ennis MP. 2003. Functional milk proteins: production and utilization. In: McSweeney PLH, Fox PF, editors. Advanced dairy chemistry Vol 1. Boston:Springer US p 1175-1228.

Murphy DB, Davidson MW. 2013. Fundamentals of light microscopy and electronic imaging, 2nd edition. Hoboken:John Wiley & Sons.

Nash W, Pinder DN, Hemar Y, Singh H. 2002. Dynamic light scattering investigation of sodium caseinate and xanthan mixtures.Int J Bio Macromolecule 30:269–71.

Nguyen TMT. 2013. The Effects of microfluidization and homogenization on the composition and structure of liposomal aggregates from whey buttermilk and commercial buttermilk. PhD diss., California Polytechnic State University.

Noël Y, Zannonis PM, Hunter EA. 1996. Texture of Parmigiano Reggiano cheese: Statistical relationships between rheological and sensory variates. Lait 76(3):243-54.

Ogden CL, Carroll MD, Kit BK, Flegal KM. 2012. Prevalence of obesity in the United States, 2009-2010. NCHS Data Brief No. 82.

Onwulata CI. 2008. Milk whey processes: current and future trends. In: Onwulata CI, Huth PJ, editors. Whey processing, functionality, and health. Ames:Wiley-Blackwell. p 369-91.

Paddock SW, Eliceiri KW. 2014. Laser scanning confocal microscopy: History, applications, and related optical sectioning techniques. In: Paddock SW, editor. Confocal Microscopy New York:Springer. p 9-47.

Page J. 2004. Whey and lactose: Natural milk products. In: Page J, Meyer D, Haines B, Lagrange V, Kenney A, editors. Reference manual for US whey and lactose products. Arlington, VA: US Dairy Export Council. p 11-14.

Pascua Y, Koç H, Foegeding EA. 2013. Food structure: Roles of mechanical properties and oral processing in determining sensory texture of soft materials. Cur Opin Colloid Inter Sci 18(4):324-33.

Patton JQ. 2013. Development and Application of Whey Protein Particles for the Improvement of Low Fat Cheddar Cheese Texture. Thesis, North Carolina State University.

Rayan AA, Kalab M, Errlstrom CA. 1980. Microstructure and rheology of process cheese. Scanning Electron Microsc 3:635-43.

Saffon M, Britten M, Pouliot Y. 2011. Thermal aggregation of whey proteins in the presence of buttermilk concentrate. J Food Eng 103(3):244-50.

Saffon M, Jiménez-Flores R, Britten M, Pouliot Y. 2014. On the use of buttermilk components as aggregation nuclei during the heat-induced denaturation of whey proteins. J Food Eng 132:21-8.

Sawyer L. 2013. β-Lactoglobulin.In: McSweeney PLH, Fox PF, editors. Advanced dairy chemistry, Vol 1A. Boston:Springer US. p 211-59.

Schär W, Bosset JO. 2002. Chemical and physico-chemical changes in processed cheese and ready-made fondue during storage. A review. LWT-Food Sci Tech 35(1):15-20.

Schokker EP, Singh H, Pinder DN, Norris GE, Creamer LK. 1999. Characterization of intermediates formed during heat-induced aggregation of β-lactoglobulin AB at neutral pH. Int Dairy J 9:791-800.

Shin. 2010. Lipids. In: Wang, editor. Food chemistry. New York:Nova Science Publishers.

Skanderby M, Westergaard V, Partidge A, Muir DD. 2009. Dried milk products. In: Tammie AY, editor. Dairy powders and concentrated products. Hoboken:John Wiley & Sons. p 180-234.

Smith K. 2006. Production technologies. In: Bishop R, Page J, Meyer D, Haines B, Lagrange V, Kenney A, editors. Reference manual for US whey and lactose products. Arlington, VA: US Dairy Export Council. p 19-25.

Sodini I, Morin P, Olabi A, Jiménez-Flores R. 2006. Compositional and functional properties of buttermilk: A comparison between sweet, sour, and whey buttermilk. J Dairy Sci 89(2):525-36.

Steffe JF. 1996. Rheological methods in food process engineering. East Lansing:Freeman press. p 418.

Stone H. 1992. Quantitative descriptive analysis. ASTM International. In: Hootman RC, editor. Manual on descriptive analysis testing for sensory evaluation, Vol. 13. ASTM International. West Conshohocken:American Society for Testing & Materials. p 15-21.

Swaisgood HE. 1982. Chemistry of Milk Protein. In: Fox PF, editor. Developments in dairy chemistry Vol 1. Applied Science Publishers LTD. p 1-59.

Swaisgood, HE. 2003. Chemistry of the caseins. In: Fox PF, McSweeney PLH, editors. Advanced Dairy Chemistry Vol 1, 3rd edition. New York:Kluwer Academic/Plenum. p 139-201.

Ubbink J, Burbidge A, Mezzenga R. 2008. Food structure and functionality: a soft matter perspective. Soft Matter 4:1569–81.

van der Sman RGM, van der Goot AJ. 2009. The science of food structuring. Soft Matter 5:501–10.

van der Sman RGM. 2012. Soft matter approaches to food structuring. Adv Colloid Interface Sci 176:18-30.

van Vliet T. 1988. Rheological properties of filled gels. Influence of filler matrix interaction. Colloid Poly Sci 266(6):518-24.

van Vliet T, van Aken GA, de Jongh HHJ, Hamer RJ. 2009. Colloidal aspects of texture perception. Adv Colloid Int Sci 150:27-40.

Vasbinder AJ, van de Velde F, de Kruif CG. 2004. Gelation of casein-whey protein mixtures. J Dairy Sci 87(5):1167-76.

Walstra P, Jenness R.1984. Milk fat globules. In: Walstra P, Jenness R, editors. Dairy chemistry and physics. New York:Wiley. p 254-78.

Yiu SH. 1985. A fluorescence microscopic study of cheese. Food Microstruct 4:99-108.

Yong YH, Foegeding EA. 2008. Effects of caseins on thermal stability of bovine β-lactoglobulin. J Agr Food Chem 56(21):10352-58.

Yong YH, Foegeding EA. 2009. Caseins: utilizing molecular chaperone properties to control protein aggregation in foods. J Agr Food Chem 58(2):685-93.

CHAPTER 2

Food structure: roles of mechanical properties and oral processing in determining sensory texture of soft materials

The contents of this chapter have been published in:

Current Opinion in Colloid & Interface Science, 2013, 18(4): 324-333

Y Pascua[1], Hicran Koç[2] and E. A. Foegeding[1*]

[1]Department of Food, Bioprocessing, and Nutrition Sciences, North Carolina State University, Box 7624, Raleigh, NC 27695-7624. hkoc@ncsu.edu, ymthibau@ncsu.edu, eaf@ncsu.edu

[2]PepsiCo Advanced Research, 7701 Legacy Drive, Plano, TX. 75024

Current Opinion in Colloid & Interface Science 18 (2013) 324–333

Contents lists available at SciVerse ScienceDirect

Current Opinion in Colloid & Interface Science

journal homepage: www.elsevier.com/locate/cocis

Food structure: Roles of mechanical properties and oral processing in determining sensory texture of soft materials

Yvette Pascua [a], Hicran Koç [b], E. Allen Foegeding [a,*]

[a] Department of Food, Bioprocessing, and Nutrition Sciences, North Carolina State University, Box 7624, Raleigh, NC 27695-7624, United States
[b] PepsiCo Advanced Research, 7701 Legacy Drive, Plano, TX 75024, United States

ARTICLE INFO

Article history:
Received 2 February 2013
Received in revised form 8 March 2013
Accepted 12 March 2013
Available online 10 April 2013

Keywords:
Sensory texture
Food structure
Oral processing

ABSTRACT

There is a desire to alter food composition to make foods healthier and at the same time not diminish sensory quality. This requires an understanding of key elements of food structure associated with texture perception. Texture, in part, is perceived during oral processing of food. Knowledge of structure–oral processing–texture interrelations could be utilized to develop or prevent specified textural attributes. Overall, the investigation of structure–oral processing–texture interrelations is just starting as a research focus. Factors including non-universal and inconsistent sensory terminology, omission of consideration for structural changes incurred by oral processes, and the lack of cross-disciplinary investigations hamper progress in this field. Consideration of these factors in future investigations on sensory texture will increase the applicability of their findings and bring us closer to understanding the contribution of food structure to sensory texture.

© 2013 Elsevier Ltd. All rights reserved.

1. Introduction

Consumers' expectations from a food product are desirable sensory perception (liking) and healthy components at a reasonable cost. The current desire to alter food composition for health concerns (reduction in salt, fat, and calories and increase in bioactive compounds) has brought to light the challenges involved in altering composition and maintaining consumer acceptance. For example, while a reduction of fat in Cheddar cheese is desirable, consumers are not willing to sacrifice texture and flavor for fat reduction [1].

Texture is one of the most important factors determining food choice, especially for foods with semi-solid or solid textures [2••]. Unlike aroma and taste, where sensations are associated with specific molecular structures, food texture is a cognitive property we assign to foods on the basis of how our senses interact with the food by vision, touch and oral processing. It is defined as "all the mechanical, geometrical and surface attributes of a product perceptible by means of mechanical, tactile and, where appropriate, visual and auditory responses" [3]. Three important concepts can be elicited from this definition as stated by Szczesniak [4•]: Texture is 1) a sensory property of food that is perceived by humans; possibly involving several senses; 2) a multi-parameter property; and 3) originates from food structure at different length scales (molecular, microscopic, macroscopic). As texture perception is a cognitive perception derived from many inputs, it can be understood based on physical and physiological measurements that allow us to explain how food structure breaks down and is sensed during oral processing.

Food structure represents the molecules comprising a food and their interactions over a wide range of length scales (Fig. 1). Depending on the product and its components, one or more of the length scales can control the properties of the food [5]. Some examples of relevant length scales in, for example, a beverage designed for meal replacement would be: 1) flavor compounds at <1 nm forming a true solution, 2) casein micelles at 150 to 200 nm forming a sol [6], and 3) oil droplets of 1 μm representing an emulsion (Fig. 1). A relatively new approach is to view foods as a form of soft matter and use those principles to understand food properties [5,7•,8,9]. Foods are considered to be mixed, disperse systems and recognized as one of the most complex forms of soft matter [7•,8].

One element of soft matter physics is that structures formed at the mesoscale (between molecular nanoscale and macroscale) control the macroscopic properties of materials [7•]. Therefore, structure at the relevant length scale should be finely controlled to generate foods with textures designed to achieve desirable properties [10•]. The only way this goal can be achieved is by understanding how structure (at the appropriate length scale) is converted into sensory texture with oral processing. This involves the structures inherent to the food material and how they are transformed and sensed during consumption.

2. Oral processing and sensory perception of food

Food texture is perceived during the conversion of food structure into a bolus through a complex series of oral manipulations including ingestion, processing and swallow (Fig. 2) [11]. During oral processing,

* Corresponding author at: North Carolina State University, Department of Food, Bioprocessing and Nutrition Sciences, 236 Schaub Hall, Raleigh, NC 27695-7624, United States. Tel.: +1 919 513 2244; fax: +1 919 513 8023.
E-mail addresses: ymthibau@ncsu.edu (Y. Pascua), hkoc@ncsu.edu (H. Koç), eaf@ncsu.edu, allen_foegeding@ncsu.edu (E.A. Foegeding).

1359-0294/$ – see front matter © 2013 Elsevier Ltd. All rights reserved.
http://dx.doi.org/10.1016/j.cocis.2013.03.009

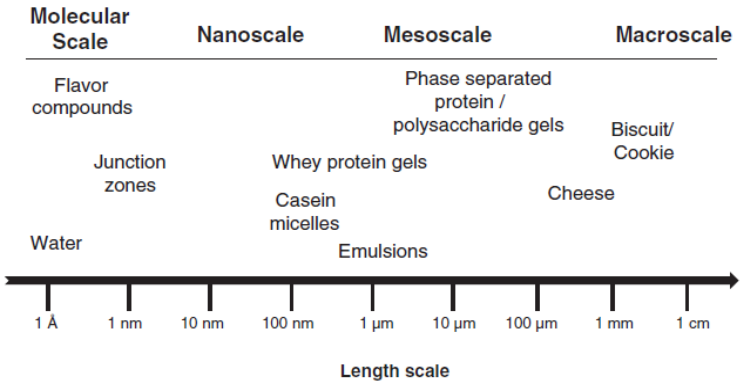

Fig. 1. Some structural elements in foods and relevant length scales. Adapted from Ref [5] with permission of The Royal Society of Chemistry.

structure is broken down with force applied by teeth and/or tongue (mechanical breakdown) and lubricated (possibly hydrated or dissolved) with saliva [12,13]. Oral processing includes a rhythmic motor activity of the jaw controlled by the central nervous system and modulated by sensory feedback from mechanoreceptors located in the lips, oral mucosa, and periodontal ligaments as well as spindles and Golgi tendon organs in the jaw muscles [14,15]. Oral processing varies among individuals due to differences in anatomical characteristics of the masticatory apparatus and physiological factors [16,13].

Hutchings and Lillford [17] proposed a conceptual model for oral processing where food structure is broken down and formed into a lubricated mass until the time that a swallowing threshold is reached. Saliva as a lubricant lowers the friction by softening the fragments of food and adheres food particles together to form a cohesive bolus [18••]. Structure breakdown continues until fragments reach a critical particle size (0.82–3.04 mm), depending on structural and mechanical characteristics of the food [19,20]. Swallowing is triggered when the physical character of the food bolus reaches a certain state such that the bolus can be transported through the soft tissues of the pharynx and esophagus safely [18••,21]. Swallowing initiation is possibly a process that takes several bolus properties into account [21].

Food structure determines mechanical properties and mechanical properties determine processes needed before swallowing [22]. Fluids are characterized by rheological and tribological properties [23,24••]. In the model shown in Fig. 2, fluids with little to no adhesion move rapidly along the dashed arrows due to minimal need for processing. Semi-solids having a substantial yield stress are processed by palating (tongue compressive movements). Forces originating from the compression between tongue and hard palate are perceived by tongue receptors and result in tactile sensations [25••,26••]. Soft and hard solids are chewed with rhythmic jaw movements to reduce the particle size and prepare for swallowing.

Oral processing of foods has been investigated by various approaches including measuring electrical activities of masticatory muscles (electromyography), jaw movements (jaw tracking) and force during chewing or biting, as well as observation of tongue and soft tissues by videofluorography and ultrasonic echo-sonography [16,27,28,12]. This has historically been of interest to researchers focused on biological questions such as dental, anatomical and neurobiological

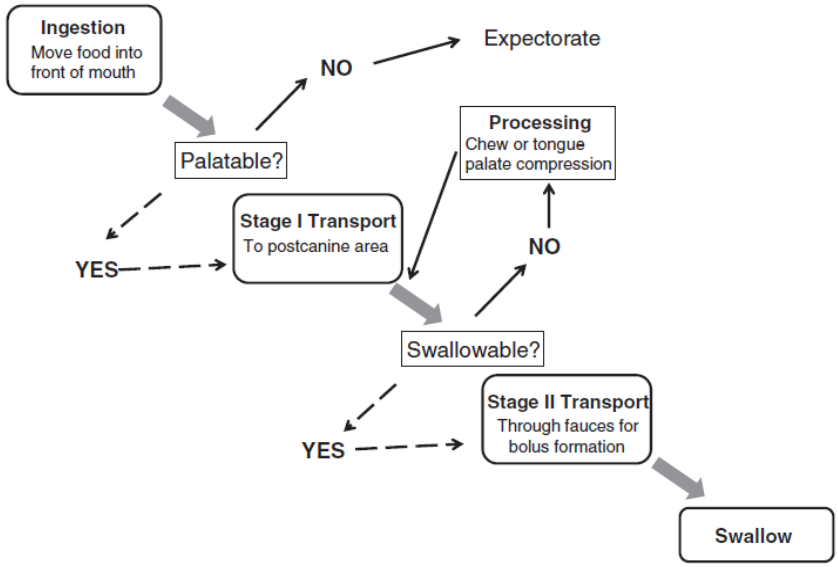

Fig. 2. Oral processing of food based on a modification of the Process Model for Feeding found in [11]. Adapted from [11] with permission of John Wiley and Sons.

Table 1
Texture terminology for semisolids and solids.

Attribute	Definition/Evaluation	Material/Reference
A. Non-oral		
1-Spreadability	Initial stage force (time and effort) needed/Spread the sample with a knife	Cream cheese [73], Feta cheese [74]
2-Consistency	Speed of fall of the product from a spoon/Visual observation from thin to thick	Semisolid dairy desserts [75]
B. Tongue-palate compression		
1-Springiness/Rubberiness	The degree or rate at which the sample returns to its original size, shape after partial compression/Between the tongue and palate[a]/Between teeth[b]/After biting, assessed during first 2–3 chews[c]	Whey protein gel[a] [54], semisolid and soft-solid foods[a] [76], cheese[b] [77], protein gels (egg white and fish, turkey, beef and pork muscles)[b] [78], processed cheese[c] [79]
2-Compressibility	The degree to which the sample deforms or compresses before fracture/Partial compression between the tongue and hard palate	Whey protein gels [54]
3-Surface slipperiness	The degree to which the sample piece was perceived as slippery/Feeling of sample on tongue prior to mastication	Whey protein gels [54]
C. First bite/first chew		
1-Hardness/Firmness	1) Force required to/Bite completely through the sample between molars (for solids)[a]/Compress sample between tongue and palate during compression (for semi-solids)[b]/Compress sample between fingers until fracture[c] 2) Extent of initial resistance/First bite with incisors[d] 3) Solid, compact sensation; holds its shape/NA[*e] 4) Hardness sensation perceived/During mastication[f]	Whey protein gels[a] [54], mixed whey protein/κ-carrageenan gels[a] [63], semisolid and soft-solid foods[a] [76], cheese[a] [77], caramel[a] [80], biopolymer gels[b] [48], mixed whey protein–polysaccharide gels[b] [53], cream cheese[b] [73], agarose gel[c] [81], processed cheese[d] [79], yogurt[e] [82], caramel[f] [80]
2-Moisture release	Extent to which moisture is released from the sample/First bite with the molars	Mixed whey protein/κ-carrageenan gels [63], whey protein gels [54]
3-Fracturability/Crumbliness	Degree to which the sample fractures into pieces/First bite with the molars	Whey protein gels [54], cheese [83]
4-Deformability/Cohesiveness	The degree to which the sample deforms or compresses before fracture/Bite completely through with the molars	Semisolid and soft-solid foods [76], agar gels [81], cheese [83]
D. Mastication (evaluated during or after a degree of chewing)		
1-Hardness	Resistances perceived/Palate sample until disintegration	Gelatin gels [48], polysaccharide gels [48]
2-Crumbliness	1) Sample falls apart in pieces/Compression between tongue and hard palate[a] 2) The extent by which structure breaks apart in the mouth/Assessed during the first 2–3 chews[b]	Mixed protein/polysaccharide mixed gels[a] [53], cheddar cheese[b] [84]
3-Particle size	Size of breakdown particles (small to large)/After 8–10 chews	Whey protein gels [54]
4-Particle size distribution	Degree of homogeneity in the particle distribution size distribution/After 8–10 chews	Whey protein gels [54]
5-Adhesiveness/Stickiness	1) Evaluate the force required to remove sample adhered to the mouth/With the tongue during eating[a] 2) Degree to which sample sticks to teeth and palate, oral cavity/After mastication just before swallowing[b]/palate without squeezing the sample[c]/NA[d]/During 5–8 chews[e] 3) Food is pulled apart by downward movement of the tongue and the resulting threads are sensed as sticky by tongue, palate and throat, making swallowing difficult/Mouthfeel sensed via tongue movements[f]	Semisolid and soft-solid foods[a] [76], cheese[a] [77], caramel[a] [80], feta cheese[b] [74], cream cheese[c] [73], yogurt[d] [82], yogurt[d] [85], sauces[d] [33,86], whey protein gels[e] [54], cheese[e] [83], custard dessert and mayonnaise, custard dessert[f] [31,83]
6-Cohesiveness of mass/Mass-forming	Degree to which sample holds together in a mass/Compression with tongue against palate at least 5 times[a]/NA[b]/Probably judged toward the end of the chewing[c]/As chewing progress (5–8 chews)[d]	Cream cheese[a] [73], yogurt[b] [82], processed cheese[c] [79], whey protein gels[d] [54], cheese[d] [83]
7-Rate/Degree of breakdown	1) Rate at which the sample breaks into smaller and smaller particles (slow to fast)/Chew 5–8 times and evaluate[a] 2) Amount of breakdown as a result of mastication (meltability/dissolvability)/Chew the sample 5 times and evaluate the chewed mass[b]	Whey protein gels[a] [54], cheese[b] [83]
8-Toughness	Effort to bite and utilize; strong coherence/NA	Mixed whey protein–polysaccharide gels [53]
9-Curdiness	Amount of lumps present in the sample/NA	Yogurt [82]
10-Chewiness	1) The total amount of work necessary to chew a sample to a state ready for swallowing/End of mastication[a] 2) The effort needed to break down the structure/Judge in the middle phase of mastication[b] 3) Number of chews required to prepare sample for swallowing/End of mastication[c]	Semisolid and soft-solid foods[a] [76], processed cheese[b] [79], protein gels (egg white and fish, turkey, beef and pork muscles)[c] [78]
11-Gumminess	Springy and rubbery characteristics of the sample/Compress sample between tongue and palate, then move tongue against palate	Cream cheese [73]
12-Tenderness/Chewiness (time–intensity)	Product of hardness, cohesiveness, and springiness relating to chewing time and number of chews or energy required to chew and prepare for swallowing/From first bite through swallowing	Meat [41–43]

Table 1 (*continued*)

Attribute	Definition/Evaluation	Material/Reference
D. Mastication (evaluated during or after a degree of chewing)		
13-Viscosity	Resistance to flow in the mouth/Manipulate the sample in the mouth with the tongue for exactly 15 s, then swallow (time–intensity before and after swallow)[a]/NA[b]	Pudding and crème[a] [44], yogurt[b] [82]
14-Thickness	1) Thickness, firmness/NA[a] 2) The thickness of the food in the mouth/After the food is compressed via up and down motions of tongue against palate[b] 3) Mechanical property perceived/When compressing the product between the mouth and the palate[c] 4) Perceived thickness in the mouth/NA[d] 5) The viscosity or readiness to flow/Evaluated by manipulation in the mouth[e] 6) ISO(1993)[f] or NA[g]	Yogurt[a] [82], Custard dessert[b] [33,86], custard dessert and mayonnaise[b] [87], Semisolid dairy desserts[c] [75], yogurt[d] [85], puddings[e] [88], cream cheese[f] [73], creamlike products, semisolid high fat products (butter, cream cheese), frozen foods (ice creams, ice milk, sherbert)[g] [30]
15-Smoothness	1) Perceived smoothness in the mouth from smooth to rough/NA[a] 2) Degree to which food contains granules/Judge by moving tongue parallel to palate[b] 3) The absence of detectable particles from gritty to smooth/Evaluate by pushing the sample to the roof of the mouth[c] 4) Sensation/Property of moving food bolus with the tongue along the palate or teeth (Smooth — jelly, grainy — semolina)[d] 5) The degree to which the mass of particles feels smooth/Judge after 8–10 chews[e] 6) NA[f]	Yogurt[a] [85], custard dessert[b] [33,86], puddings[c] [88], mayonnaise[d] [87], whey protein gels[e] [54], creamlike products, semisolid high fat products (butter, cream cheese), frozen foods (ice creams, ice milk, sherbert)[f] [30], yogurt[f] [82]
16-Melting/Dissolving/Difficulty to dissolve, Meltdown Rate/rate of melt	1) Rate and degree that the sample breaks down due to salivary, mechanical action/Assess speed in which sample disappears during mastication[a] 2) Food becomes thin and spreads throughout the mouth/Judge at different rates (slow-quick) during palating[b]/Probably judged toward the end of the chewing[c] 3) The degree of melting (from "not melted" to "melted")/Move the sample around in mouth with the tongue until it melted[d] 4) Rate of the created sensation of a sample melting in the mouth/NA[e]	Yogurt[a] [85], puddings[a] [88], custard dessert[b] [33,86], custard dessert and mayonnaise[b] [87], processed cheese[c] [79], cream cheese[d] [73], table spreads[d] [89], yogurt[e] [82]
17-Fattiness/Greasiness/Oiliness	1) Fat and oil layer on oral tissues lubricating the food transport and simulating saliva production/NA[a] 2) Perceived amount of fat/grease in the sample/Judged at the end of the chewing sequence[b]	Yogurt[a] [82], custard dessert[a] [33,86], processed cheese[b] [79]
18-Creaminess	1) Creamy texture/NA[a] 2) Range of sensation typically associated with fat content such as full and sweet taste, compact, smooth, not rough, not dry, with a velvety (not oily) coating/NA[b] 3) Texture associated with cream that has been whipped/Assessed during the first 2 to 3 chews[c] 4) Overall intensity of the perceived creaminess based on each assessor's own concept (could include appearance, flavor and texture)/NA[d] 5) Personal assessment of the overall creaminess of the sample/NA[e] 6) NA[f]	Cream cheese[a] [73], Yogurt[a] [85], custard dessert[b] [33,86], custard dessert and mayonnaise[b] [87], processed cheese[c] [79], yogurt[d] [82], chocolate mousses and artificial creams[e] [90], creamlike products, semisolid high fat products (butter, cream cheese), frozen foods (ice creams, ice milk, sherbert)[f] [30]
19-Velvetiness	A silky, velvety sensation that slides on the surface of the tongue and the roof and sides of the mouth	Yogurt [82]
20-Juiciness (time–intensity)	Time intensity measurement/First bite through swallowing	Beef [43]
21-Roughness	1) Rough feeling on the tongue and palate/NA[a] 2) Roughness sensed on teeth, palate, tongue, typically caused by products such as walnuts, spinach, wine/NA[b]. 3) The product gives a grainy oral texture (smooth–grainy)/NA[c]	Cream cheese[a] [73], yogurt[a] [85], custard dessert[b] [33,86], semisolid dairy desserts[c] [75]
22-Dryness/Mouth-drying	1) Dry feeling in the mouth/Judge during compression between tongue and hard palate[a]/NA[b]/after expectoration[c] 2) Food seems to absorb saliva, making it difficult to swallow/After expectoration[d]	Yogurt[a] [85], yogurt[b] [82], puddings[c] [88], custard dessert[d] [33,86],
23-Powdery/Chalkiness	1) Presence of small particles/NA[a] 2) A chalky, cloying powdery sensation in the mouth/NA[b]	Yogurt[a] [85], yogurt[b] [82]
24-Grittiness/Graininess	1) Amount of sandy particles present in the sample/NA[a] 2) Degree to which small, gritty, sand-like particles are perceived/Place bite size of sample between molar teeth, chew and evaluate[b]	Yogurt[a] [82], protein gels (egg white and fish, turkey, beef and pork muscles)[b] [78]
25-Slipperiness	Sample sliding through oral cavity/Judge during palateing[b]/NA[a]	Mixed whey protein–polysaccharide gels[a] [53], yogurt[b] [85]
26-Featheriness	A light sensation created by a sample that contains trapped air, reminiscent of whipped products/NA	Yogurt [82]
27-Airiness/Denseness	1) Perceived by tongue as airy/foamy and disintegrates easily after the food is compressed against the palate[a]/NA[b] 2) The compactness of the sample from airy to compact/NA[c]	Custard dessert[a] [33,86], custard[b] [87], puddings[c] [88]

(*continued on next page*)

Table 1 (*continued*)

Attribute	Definition/Evaluation	Material/Reference
D. Mastication (evaluated during or after a degree of chewing)		
28-Toothpacking	The amount of product packed in and between molars/Evaluation of residues after swallowing	Caramel [80]
29-Particle size	Size of the residual particles in the mass/After thorough manipulation	Cream cheese [73]
30-Spreadability	The extent of sample spreads/Between tongue and palate	Mixed whey protein–polysaccharide gels [53]
E. Residual		
1-Mouthcoating	1) Perception of a thin layer covering the palate, oral cavity, mouth/Evaluation of residues after swallowing[a] 2) The extent to which the sample clings to the inside of the mouth (roof, teeth, tongue, gums)/Judged in the middle phase of mastication[b]	Whey protein gels[a] [54], semisolid dairy desserts[a] [75], yogurt[a] [82], yogurt[a] [85], puddings[a] [88], processed cheese[b] [79]
2-Slime producing	Product leaves a feeling of thick mucus in the mouth that is difficult to remove or swallow, typically caused by dairy products/Afterfeel	Custard dessert [33,86]

* NA — Not applicable (when the evaluation method was not stated in the reference). Superscripts link evaluation with reference.

issues. Oral processing techniques have been used to investigate food texture and was recently reviewed [29•]. Our understanding of oral processing and how it relates to texture perception continues to improve; however, the question still remains: Are the current techniques providing us the information we need? Especially in investigations that cover how oral processing adjusts to specific elements of food structure and how specific texture terms are perceived.

3. Sensory texture — terminology and evaluation

Texture is a multi-parameter property describing the various sensory attributes experienced in extra-oral manipulation (spreading and touching) and during consumption of a food product. Although there are standard techniques, such as Quantitative Descriptive Analysis and Spectrum™ for descriptive analysis of texture, variations exist in the attributes used, their definitions, and their evaluation techniques, even for the same product types. Table 1 illustrates attributes that have been used to describe textural properties of various semi- and soft-solids at different stages including non-oral, tongue-palate compression, first chew, mastication and residual. Some attributes such as hardness or firmness are relatively less complex and can be explained by mechanical properties (i.e. those describing the force needed to cause fracture, yielding of flow). The definitions and evaluation of hardness are fairly similar among these studies. On the other hand, some terms such as adhesiveness, cohesiveness, creaminess, tenderness and juiciness are more complex and are not directly connected to one mechanical measurement. These properties originate from sensations which are related to bulk (rheological), surface (adhesive) and frictional (tribological) properties of a food when it is undergoing oral processing to produce a bolus capable of being swallowing and requires dynamic elements of potentially several material properties and sensory perceptions. For example, Kokini and Cussler [30••] investigated the material properties responsible for creaminess of various commercial semi-solid products (Table 1, section D-14, 15, 18) and correlated creaminess with thickness and smoothness. Also, they explained that thickness and smoothness were related to viscosity and the frictional forces on the tongue, respectively. Reviews by de Wijk et al., [31••] and Frost and Janjoj [32] give detailed insight into mechanisms responsible for creaminess, which is a key driver for sensory acceptance of semi-solids. Another example is stickiness, which results from surface and rheological properties of foods [33,34]. However, using an adhesiveness measurement determined by pressure-sensitive adhesive techniques (e.g., tack test) can be misleading regarding oral perception of stickiness; because it can change dramatically throughout oral processing due to saliva as a lubricant and solvent. Thus, the effect of saliva should be considered in order to understand the mechanism of stickiness, which requires information from time–intensity sensory perception and oral processing in addition to physical properties. The complex nature of such sensory perceptions has led to sensory evaluations that vary greatly in their techniques and terminology in attempts to fully and accurately describe the perception of dynamic sensations.

The lack of a commonly accepted lexicon of sensory terminology produces the complicating factor of one term having various meanings. Table 1 offers a collective view of the broad range of terminology used to describe different food products and their respective evaluation techniques. As shown in Table 1, a large number of attributes are used to describe sensory perception of texture. In some cases, the attribute name and definition are similar across studies; however, it is assessed by different oral manipulations. This prevents comparisons between investigations because the oral processes used to scale the term are different. For example, springiness/rubberiness (Table 1, section B-1) is generally assessed as the degree or rate at which the sample returns to its original size and/or shape after partial compression. It can be related to the recoverable energy in physical terms. When fat is reduced in Cheddar cheese, texture becomes springier, which is not desirable by consumers [35]. It has also been assessed during the first 2–3 chews. Therefore with springiness, one approach is measuring a pre-fracture deformation while the other is assessing during and/or after fracture deformations — for the same textural term. Moreover, in other cases, the same definitions can be associated with different terms such as deformability/cohesiveness (Table 1, section C-4), or the same attribute may be defined and described in various ways such as creaminess (Table 1, section D-18). In addition, if we look at the terms and evaluation techniques further, only a few of the textural attributes (Table 1, section D-12, 20) are considered as a dynamic property and evaluated as a function of time (time–intensity), even though texture is a dynamic attribute due to continuous changes in food structure during eating.

The dynamic nature of food texture was highlighted in "the mouth process model" proposed by Hutchings and Lillford [17] discussed earlier. The paths for loss of structure and increase in lubrication over time clearly indicated the dynamic and complex nature of texture perception with the continuous changes from food to bolus. This raises the question of: Are we evaluating textural attributes properly with descriptive analysis methods that somewhat arbitrarily assign a certain number of chews before scoring the attribute? The approach of traditional descriptive analysis is to statically measure the intensity of attributes at various stages during oral processing such as after first chew, mastication for a designated number of chews, and after swallowing. In contrast, time–intensity methods allow panelists to scale their sensations over time and it provides rate-related, duration and intensity information [36–38]. Temporal dominance is a type of time–intensity method where dominant sensations (the most striking perception at a given time) are selected by panelists from predetermined attributes and evaluated individually over time [39]. Descriptive methods can be

combined with time–intensity methods for texture evaluation. Some examples of such studies are gelatin hardness [40], meat tenderness [41–43], viscosity of chocolate puddings [44], and juiciness of meat [43]. Development, training and application of time intensity descriptive evaluation of food texture can be challenging and requires a large amount of time and cost investments. However, it is an important analysis that can give insight to the perception of complex textural attributes. In addition to time intensity studies and oral processing, understanding sensory texture also requires comprehensive research on physical and chemical properties of foods (involving rheology, fracture properties and food structure) [2••]. In the following sections, food structures in relation to sensory perception and structure breakdown will be discussed.

4. Food structures and associated textural properties

4.1. Food structures

The structure of everyday foods is complex and therefore difficult to understand in regards to elements generating specific textural properties. To gain a fundamental understanding of food structure–texture relationships, model biopolymer gels are often used. Our database *per se* of textural properties for these models is far from complete, let alone their structure–texture relationships. It is plausible that omission of structural evolution during mastication is one of the major reasons for this structure–texture disconnect. Our discussion of structure–texture relationships will be limited to soft-solids.

Structure analysis via microscopic techniques typically takes place on a static food sample that has not undergone mastication, omitting the dynamic nature of sensory texture analysis. During oral processing of a soft or hard solid that requires chewing, the sample is placed between the molars and crushed to fracture. The fractured particles are coated with saliva and either returned to the molars for further size reduction or positioned at the back of the mouth for bolus formation [45]. At each step of the processes just described, applied shear and normal forces, and possibly thermal and enzymatic effects, cause changes in sample structure. For example, consider a viscoelastic solid material such as cheese or mixed biopolymer gel. As the sample is crushed, applied normal and shear forces are exerted until fracture occurs or the molars come into close contact with each other having squeezed out the sample. Based on the energy balance model proposed by van Vliet [46], the energy supplied to deform a material may be stored elastically, used for fracture, or dissipated through frictional or viscous movements. Frictional or viscous movements that occur during first bite deformation would correspond with structural rearrangements of the material. van den Berg [47••] investigated structural changes in a protein continuous, phase separated gel composed of whey protein isolate (WPI) and locust bean gum using rheomicroscopy. Gel structure was imaged before and after stages of compression. After compression, locust bean gum inclusions became interconnected and the protein walls between inclusions became thinner. This change in microstructure resulted from compression to a true strain of 0.63. It is reasonable to think that microstructural changes would be even greater at much higher normal strains such as that experienced during the first bite.

Temperature-associated transitions (e.g., melting) and enzymatic degradation of foods also alter food structure during mastication. During this time, thermal and enzymatic actions begin to modify the food, which alter its perceived texture throughout the oral process. For example, Muñoz et al. [48] investigated temporal hardness (Table 1, section D-1) in gelatin, κ-carrageenan and alginate gels. A trained sensory panel was instructed to compress samples between the tongue and hard palate for an initial firmness reading, then palate the sample and simultaneously rate its perceived firmness until disintegration. Gelatin hardness decreased more rapidly during palating than either κ-carrageenan or alginate gels. This was a consequence of melting of the gelatin structure by elevated mouth cavity temperatures [48]. Also, starch-containing foods will undergo enzymatic breakdown that will reduce its hardness [49]. These findings raise the question: Is oral sensory hardness perceived at first bite or first palate the complete perception of hardness or just a first impression?

Even though we do not have a comprehensive understanding of structure–texture relationships, strong evidence exists for some associations including hardness, moisture release, and crumbliness. Sensory hardness or firmness is probably the most widely investigated sensory term used to describe the texture of soft and hard solids (and sometimes semi-solids). Degrees of network connectivity and polymer concentration have been associated with both sensory and instrumental gel hardness. Structural changes of fish gelatin gels followed using atomic force microscopy as gelatin concentration increases show that above concentrations of 1% gelatin, network connectivity (junction zone density) also increases [50]. This corresponds with an increasing instrumental gel hardness measured as the peak force during compression to 40% of the gel original height. A similar association is found for ι- and κ-carrageenan gels [51]. For both gels, junction density increases by addition of calcium or potassium ions. This increase is related to increasing gel hardness measured instrumentally as the peak force obtained when a probe of 10 mm diameter is punched 15 mm through a sample. In agarose gels, increasing polymer concentrations causes increases in hand sensory gel hardness (Table 1, section C-1) measured as 'the amount of force required to compress sample to fracture.' In alginate gels, both increasing polymer concentration and cross-link density cause an increase in fracture stress [52]. In the small sampling of studies above, although measurements for sensory and instrumental hardness are inconsistent, they collectively provide a reasonable connection between *initial* hardness (sensory or instrumental) and polymer concentration and/or degree of network connectivity.

The sensation of moisture release (Table 1, section C-2) is described as the amount of fluid expressed from the sample as it is compressed on first bite or during chewing and has been related to food microstructure and instrumental measures of water holding properties [53••,54]. Serum release during deformation and water holding are correlated with gel permeability. In low acyl gellan gum gels, cryo-scanning electron microscopy images suggest the potential for two co-existing networks, each with discrete pore size distributions [55]. It is thought that a primary network of large pores (1 μm) and thick interconnecting network strands co-exist with a web-like structure of smaller pores (0.1 μm). It is proposed that the primary structure provides a main frame support to external forces, while the web like structure controls water holding properties. Likewise, for whey protein gels, as pore sizes increase due to a structural shift from fine stranded to particulate, gel permeability increases [56] and the water holding capacity of the gel decreases [57]. In phase separated mixed WPI/polysaccharide gels, gels with bicontinuous and coarse stranded structures release significantly more serum during compression than protein continuous or homogeneous microstructures, resulting in increases in watery perception during palating [53••]. This is due to increased permeability of the bicontinuous and coarse stranded gel structures that facilitate serum flow through the matrix. Together, these studies provide strong support for the link of sensory perception for watery mouthfeel/moisture release and gel porosity. Because bolus formation is influenced by moisture released from a food [58], such knowledge would benefit the development of foods aimed at aiding bolus formation processes.

Crumbliness (Table 1, section C-3) is defined as the degree to which a sample falls into pieces upon fracture. Although it is not clear what structural features contribute to this, it is likely that failure mechanisms and energy dissipation during deformation contribute to this texture perception. At the microscopic level, crumbliness in wet soft-solids is related to the breakdown pattern after fracture and critical speed of fracture [47••]. A sharp decrease in the slope of normalized force–deformation curves after fracture is associated with a crumbly texture, whereas a gradual decrease occurs for gels having low levels of crumbliness [47••]. Crumbly gels can use their

high elastic energy for a fast fracture by free running cracks. Crumbliness is also related to recoverable energy; crumbly gels have higher, 70–85% recoverable energies compared to 30–40% for non-crumbly gels (percent recoverable energy was defined as the 'ratio of the energy released as mechanical work during the decompression over the energy invested during the compression') [47••]. Crumbly gels also exhibit low serum release (water flowing out during compression), which is related to porosity of the gel network. For phase separated WPI/polysaccharide gels, van den Berg et al. [47••] found that low serum release during deformation was a prerequisite for crumbliness. If energy supplied to the microstructure during deformation was dissipated though viscous flow, the phase separated gels had low crumbliness. In other words, gels with high elastic components have high crumbly scores. Based on this study, gels with homogeneous and protein continuous structures have higher elastic components than bicontinuous and coarse stranded structures and are more crumbly. Whether or not the extrapolation of these structural associations with perceived crumbliness to other foods is possible remains to be proven.

Although progress has been made towards understanding what fundamental physical features contribute to relatively simple textures, the need remains for more exploration into structure–texture relationships for complex texture attributes such as tenderness. As illustrated above, food structures change throughout the chewing process. Tenderness is defined as the product of hardness, cohesiveness and springiness (Table 1, sec D-12). It is evaluated from the first bite through to swallowing. Based on its definition, to understand tenderness we must first understand hardness, cohesiveness and springiness, and how changes in relative magnitudes of these terms determine tenderness.

4.2. Food structure design

A thorough understanding of how structural properties of gels translate into textural properties is best approached by starting with a single biopolymer and using various mechanisms to change structure and determine textural and oral processing outcomes. Whey protein isolate or β-lactoglobulin gels come closest to achieving that goal. Gels were historically called "fine stranded" or "particulate" based on appearance of primary aggregates (or gel strands) under transmission electron microscopy [59]. Work by Ako et al. [60] proposed the designation of "micro-phase separation" to indicate structures observed on the μm scale in particulate gels. Moreover, Ako et al. [60] demonstrated that a state diagram can be developed to show the transition between homogeneous (at the μm scale) and micro-phase separated structures as a function of pH, or ionic strength at a given pH. At pH 2.0 the structure shifts to fibrils with lengths in the μm range and widths of ~8 nm, resembling β-amyloid fibers [61]. Of the three structures, most sensory investigations have focused on particulate and fine stranded structures with little known about sensory texture of fibril gels. Gwartney et al. [54] investigated the textural properties of fine stranded and particulate gels formed from 12% w/v protein, 25 mM NaCl, pH 7 solutions. Fine stranded gels were translucent and had high water holding properties. Gel texture was described as high springiness, compressibility and firmness with a slippery mouthfeel prior to mastication. During mastication, the gels had low moisture release, crumbliness and their chewed particles had smooth surfaces. Particulate gels were formed by adding 10 mM calcium chloride in addition to the 25 mM NaCl used in forming fine stranded gels. Particulate gels were opaque with low water holding properties. Gel texture was described as low in springiness, slipperiness, firmness and compressibility. During mastication, particulate gels exhibited high moisture release and crumbliness, which is opposite to that for phase separated WPI/polysaccharide gels [53••], and chewed particles had a rough surface.

A series of studies using WPI/polysaccharide mixtures have aided our understanding of how microstructure determines sensory texture. van den Berg et al. [47••,53••] investigated semi-solid structures formed by cold gelation of whey protein isolate and polysaccharides, while Çakir et al. [62,63] formed soft-solid structures using heat-induced gelation and WPI/κ-carrageenan mixtures. The combination of using micro-phase separation to shift from stranded to particulate protein structure [60] and addition of a polymer (κ-carrageenan) to induce polymer–polymer phase separation produced a range of microstructures. Microstructure morphologies were classified based on the nomenclature of van den Berg et al. [53••] as: homogeneous, protein continuous, bicontinuous, coarse stranded or κ-carrageenan continuous, based on how structures appeared when imaged with confocal microscopy. Changes in microstructure coincided with changes in large deformation rheological properties. Starting with homogeneous gels and adding κ-carrageenan shifted the microstructure to protein continuous with a coinciding increase in fracture stress [62]. Adding more κ-carrageenan shifted the structure to bicontinuous and did not modify or decrease fracture stress. Fracture stress then decreased significantly as microstructure shifted from bicontinuous to κ-carrageenan continuous. Fracture stress of particulate whey protein isolate gels increased as the microstructure was shifted to a coarse stranded structure with κ-carrageenan addition, followed by a sharp decrease with a shift to a carrageen-continuous structure. Fracture stress was correlated with sensory firmness defined as the 'force required to fracture the sample with the molars.' Conversely, in the van den Berg et al. [47••,53••] studies, similar changes in microstructure did not have coinciding changes in fracture stress. This difference could be due to 1) van den Berg et al. [53••] using a range of hydrocolloids to produce each phase separated microstructure, 2) van den Berg et al. [53••] gels had lower protein (3% vs. 13%) concentrations, forming weaker gels that were palated rather than chewed, 3) gel mechanisms were different (cold set vs. heat set) and/or 4) characteristic length scales smaller than those observed in confocal microscopy were responsible.

In considering the mechanical and textural structure relationships found in these studies for phase separated gels, it is reasonable to think that the same would apply to other protein–polysaccharide gels where similar microstructures are observed. However, to ascertain this hypothesis, we first need to have a good understanding of the large strain, fracture and sensory texture properties of single component biopolymer (homogeneous) gels such as pectins, alginate, agarose or gellan gum. Based on search results using Google Scholar and Web of Science search engines, there has been substantial progress in the measurement and understanding of mechanical properties and structural features of the junction zone character for several biopolymers, but surprisingly, the same cannot be said for their associated sensory texture properties.

4.3. Structure breakdown during oral processing and food texture perception

Understanding sensory texture based on how food is sensed during oral processing is important to answer the questions of how and what structural changes are perceived as textural properties. Physical sensations produce the overall perception and are affected by the extent and type of processes in the mouth. In the case of semi-solids, attributes perceived at early stages of mastication are less affected by the extent of oral manipulation [64,26••]. However, due to the dynamic nature of oral processing, food structures and surfaces are continually changing, making assessments of structural changes perceived at later stages more challenging. Consequently, only those textural properties for which we have a reasonable understanding of how they are perceived have been investigated.

Sensory attributes are perceived in a certain order during oral processing and depend on complex oral movements. In the case of semi-solids, for example, *thickness* is sensed through compression

forces during flow of the food. Perception of thickness occurs quickly and when the sample is more intact [26••]. *Smoothness* is perceived when a sample layer between tongue and palate has been thinned enough through squeezing forces and/or amylase activity [25••]. Perception of *creaminess* is slower and requires less compressive movement, and can be related to the formation of a viscous coating on the tongue surface [26••,25••]. *Creaminess* perceptions are quality indicators of semi-solids and are associated with good lubrication behavior. High fat content, smaller fat droplets, and smaller food particles enhance lubrication and perception of creaminess. These sensations are explained by in-mouth coalescence of fat, induced by shear or surface interactions, by which frictional forces is reduced [65–67].

In the case of solids; hardness, adhesiveness, crunchiness and tenderness are among the most important sensory attributes and have been investigated with oral processing.

Hardness (Fig. 3) is one of the most studied sensory attributes regarding oral processing. Increased hardness of model foods (gelatin jellies and caramels) results in increases in chewing time, muscle activity, and jaw movement during oral processing [68•]. Similarly, sensory hardness of mixed WPI/κ-carrageenan gels is associated with muscle activities and the number of cycles [69]. In addition to these model systems, hardness of rich tea type biscuits (short bread type cookie) is explained with muscle activity in the first five chewing cycles [12]. *Adhesiveness* (Fig. 3) is a complex attribute and occurs by a combination of factors that determine adhesion (surface and rheological properties) and lubrication (saliva contribution) of food materials. Caramels formulated at increased levels of adhesiveness, but with similar hardness, cause increases in jaw-opening and jaw-closing muscle activity, opening duration, and jaw movements [70]. Chewing frequency is another mastication parameter affected by changes in adhesiveness. For example, fat reduction in cheese results in less adhesive texture, which is associated with increased chewing frequency [70]. *Crunchiness* (Fig. 3) is an attribute associated with hard solids such as crackers and biscuits. Crunchiness of biscuits is related to muscle activity during intermediate chewing cycles [12]. *Tenderness* (Fig. 3) is an attribute determining meat quality and has been investigated with time intensity sensory measurements and oral processing. The first and subsequent chews contribute to the perception of meat tenderness [71]. This confirms that tenderness indicates the ease of chewing and preparing the meat for swallowing.

Particle and moisture *mouthcoating* (Fig. 3) are residual attributes evaluated for both semi-solids and solids and can affect the quality of the product. Residual attributes are associated with jaw movements in the last cycles of the chewing sequence for mixed WPI/κ-carrageenan gels [69]. The amount of oral coating after swallowing of semi-solids can be important in perception of texture. Prinz et al. [72•] investigated the amount of oral coating collected with rinse water after swallowing. Turbidity of the first rinse was strongly correlated to sensory attributes associated with fat content and viscosity of food such as thickness, creaminess and fattiness. This technique is proposed as a useful method to study texture.

5. Conclusions

There are a limited number of investigations relating food structure to oral processing and sensory texture perception of semi-solid and solid foods. The fact that some investigations show that sensory attributes are perceived at different stages of the chewing sequence suggests a more thorough investigation of the rate of structural breakdown is needed to understand sensory texture. Current findings and understanding in the food texture research highlight some important points to rethink and question, as follows:

1) Are textural attributes evaluated properly with descriptive analysis methods that assign a certain number of chews before scoring the attribute? Individuals will vary greatly in the number of chews for the same food product, so fixing chews at an arbitrary number does not imply the same degree of structural breakdown and lubrication.
2) There is a need for a common sensory language. If not an accepted language, then at least an accepted reference language for food texture to facilitate comparisons among investigations.
3) Another gap in the area is fundamental physical understanding of complex sensory attributes. What makes a matrix more cohesive, adhesive or with a higher degree of mouthcoating is known to a limited extent.
4) Microscopic techniques that show dynamic changes at the mesoscale need to be coupled with changes in sensory perception.
5) More investigations are needed that couple characterization of structure, oral processing and sensory texture.

In general, attributes evaluated during tongue-palate compression and first-chew are successfully explained and related to structural and mechanical properties. On the other hand, attributes determined during mastication or after some degree of mastication have been difficult to predict based on current knowledge of structures and mechanical properties. This is probably because of the involvement of saliva, surface interactions, and the bolus formation process in evaluating these terms. To achieve this goal, physiological measures are needed to provide a better understanding of these sensations and how they relate to physical properties of food structure and food structure breakdown.

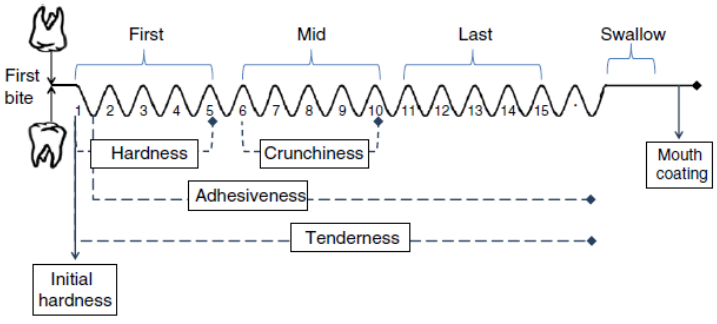

Fig. 3. Texture perception time line of semi-solids during oral processing. Progression of jaw opening and closing during chew cycle represented by valleys and peaks respectively. Boxed terms indicate texture assessment at a single point (ending at arrow) or over a period of chews (on dotted lines). Diamonds indicate end of texture assessment. Based on Refs. [12,63].

References and recommended reading*,**

[1] Childs JL, Drake MA. Consumer perception of fat reduction in cheese. J Sens Stud 2009;24:902–21.

[2] van Vliet T, van Aken GA, de Jongh HHJ, Hamer RJ. Colloidal aspects of texture perception. Adv Colloid Interface 2009;150:27–40. Colloidal aspect of texture perception is explained for liquids, semi-solids and hard solids.

[3] ISO. Sensory analysis: vocabulary (ISO 5492); 1992 [Geneva, Switz].

[4] Szczesniak AS. Texture is a sensory property. Food Qual Prefer 2002;13:214–25.

[5] Ubbink J, Burbidge A, Mezzenga R. Food structure and functionality: a soft matter perspective. Soft Matter 2008;4:1569–81.

[6] Dalgleish DG, Corredig M. The structure of the casein micelle of milk and its changes during processing. Annu Rev Food Sci Technol 2012;3:449–67.

[7] van der Sman RGM, van der Goot AJ. The science of food structuring. Soft Matter 2009;5:501–10. This is an interesting article on food structure from the viewpoints of soft matter physics and molecular gastronomy. It covers qualitative description of food structure by SAFES (systematic approach to food engineering systems), which characterizes food structures by phase, composition, aggregation state, and state diagrams (temperature vs. moisture content).

[8] Mezzenga R, Schurtenberger P, Burbidge A, Michel M. Understanding foods as soft materials. Nat Mater 2005;4:729–40.

[9] Norton JE, Norton IT. Designer colloids—towards healthy everyday foods? Soft Matter 2010;6:3735–42.

[10] Aguilera JM, Lillford PJ. Structure–property relationships in foods. In: Aguilera JM, Lillford PJ, editors. Food materials science: principles and practice. New York: Springer Sci; 2008. p. 229–53. A good chapter on structure-function relationship from a food material science perspective.

[11] Hiiemae K. Mechanisms of food reduction, transport and deglutition. How the texture of food affects feeding behavior. J Texture Stud 2004;35:171–200.

[12] Brown WE, Eves D, Ellison M, Braxton D. Use of combined electromyography and kinesthesiology during mastication to chart the oral breakdown of foodstuffs: relevance to measurement of food texture. J Texture Stud 1998;29:145–67.

[13] van der Bilt A. Human oral function: a review. Braz J Oral Sci 2002;1:7–18.

[14] Essick G, Trulsson M. Tactile sensation in oral region. In: Squire LR, editor. Encyclopedia of neuroscience. Maryland Heights. MO: Springler-Verlag; 2008. p. 3999–4005.

[15] Lavigne G, Kim JS, Valiquette C, Lund JP. Evidence that periodontal pressoreceptors provide positive feedback to jaw closing muscles during mastication. J Neurophysiol 1987;58:342–58.

[16] Woda A, Foster K, Mishellany A, Peyron M. Adaptation of healthy mastication to factors pertaining to the individual or to the food. Physiol Behav 2006;89:28–35.

[17] Hutchings JB, Lillford PJ. The perception of food texture: the philosophy of the breakdown path. J Texture Stud 1988;19:103–15.

[18] Lucas PW, Prinz JF, Agrawal KR, Bruce IC. Food physics and oral physiology. Food Qual Prefer 2002;13:203–13. This article is one of the fundamental studies in the food physics and physiology of chewing that gives an overview of the fracture of food during mastication. Also, it explains the swallowing process and factors involved with theoretical models of mastication.

[19] Jalabert-Malbos ML, Mishellany-Dutour A, Woda A, Peyron MA. Particle size distribution in the food bolus after mastication of natural foods. Food Qual Prefer 2007;18:803–12.

[20] Prinz JF, Lucas PW. Swallow thresholds in human mastication. Arch Oral Biol 1995;40:401–3.

[21] Peyron MA, Gierczynski I, Hartmann C, Loret C, Dardevet D, Martin N, et al. Role of physical bolus properties as sensory inputs in the trigger of swallowing source. PLoS One 2011;6:1–8.

[22] Foegeding EA, Daubert CR, Drake MA, Essick G, Trulsson M, Vinyard CJ, et al. A comprehensive approach to understanding textural properties of semi- and soft-solid foods. J Texture Stud 2011;42:103–29.

[23] Shama F, Sherman P. Identification of stimuli controlling the sensory evaluation of viscosity II. Oral methods. J Texture Stud 1973;4:111–8.

[24] Chen J, Stokes JR. Rheology and tribology: two distinctive regimes of food texture sensation. Trends Food Sci Technol 2012;25:4–12. A critical review on the application of rheology and tribology concepts in understanding oral processing and sensory perception. It explains the importance of bulk phase properties on textural features sensed at early stages of oral processing. Also, the influence of lubrication on texture sensations perceived during oral processing is discussed.

[25] van Aken GA, Vingerhoeds MH, de Hoog EHA. Food colloids under oral conditions. Curr Opin Colloid Interface Sci 2007;12:251–62. An excellent article giving critical information on oral physiology, changes during oral processing, structure breakdown and sensory perception.

[26] de Wijk RA, Janssen AM, Prinz JF. Oral movements and the perception of semi-solid foods. Physiol Behav 2011;104:423–8. A very interesting article covering instrumental, sensory and physiological studies and explaining the importance of oral movements on the perception of textural attributes associated with semi-solids.

[27] Boyar MM, Kilcast D. Food texture and dental science. J Texture Stud 1986;17:221–52.

[28] Hylander WL, Johnson KR. Modeling relative masseter force from surface electromyograms during mastication in non-human primates. Arch Oral Biol 1993;38:233–40.

[29] Chen J. Food oral processing—a review. Food Hydrocolloids 2009;23:1–25. A comprehensive review of oral processing and food texture.

[30] Kokini JL, Cussler EL. Predicting the texture of liquid and melting semi-solid foods. J Food Sci 1983;48:1221–5. One of the earliest attempts in relating textural properties of liquids and semi-solids to frictional properties (tribology) and understanding the physical meaning of creaminess.

[31] de Wijk RA, Terpstra MEJ, Janssen AM, Prinz JF. Perceived creaminess of semi-solid foods. Trends Food Sci Technol 2006;17:412–22. This article provides a great insight into understanding of perceived creaminess of semi-solid foods. They explain creaminess perception using multidisciplinary research methods (physico-chemistry, oral physiology, psychophysiology and psychology).

[32] Frost MB, Janjoj T. Understanding creaminess. Int Dairy J 2007;17:1298–311.

[33] Dunnewind B, Janssen AM, van Vliet T, Weenen H. Relative importance of cohesion and adhesion for sensory stickiness of semisolid foods. J Texture Stud 2004;35:603–20.

[34] Weenen H, van Gemert LJ, van Doorn JM, Duksterhuis GB, de Wijk RA. Texture and mouthfeel of semisolid foods: commercial mayonnaises, dressings, custard desserts and warm sauces. J Texture Stud 2003;34:159–79.

[35] Rogers NR, Drake MA, Daubert CR, McMahon DJ, Bletsch TK, Foegeding EA. The effect of aging on low-fat, reduced-fat, and full-fat Cheddar cheese texture. J Dairy Sci 2009;92:4756–72.

[36] Lawless HT, Heymann H. Sensory evaluation of food: principles and practices. New York: Springer; 2010.

[37] Cliff M, Heymann H. Development and use of time–intensity methodology for sensory evaluation: a review. Food Res Int 1993;26:375–85.

[38] Peyvieux C, Dijksterhuis G. Training a sensory panel for TI: a case study. Food Qual Prefer 2001;12:19–28.

[39] Pineau N, Schlich P, Cordelle S, Mathonnière C, Issanchou S, Imbert A, et al. Temporal dominance of sensations: construction of the TDS curves and comparison with time–intensity. Food Qual Prefer 2009;20:450–5.

[40] Larson-Powers N, Pangborn RM. Paired comparison and time–intensity measurement of the sensory properties of beverages and gelatins containing sucrose or synthetic sweeteners. J Food Sci 1978;43:41–6.

[41] Butler G, Poste LM, Mackie DA, Jones A. Time–intensity as a tool for the measurement of meat tenderness. Food Qual Prefer 1996;7:193–204.

[42] Duizer LM, Gullett EA, Findlay CJ. The relationship between sensory time–intensity, physiological electromyography and instrumental texture profile analysis measurements of beef tenderness. Meat Sci 1996;42:215–24.

[43] Zimoch J, Gullett EA. Temporal aspects of perception of juiciness and tenderness of beef. Food Qual Prefer 1997;8:203–11.

[44] Pangborn RM, Koyasako A. Time-course of viscosity, sweetness and flavor in chocolate desserts. J Texture Stud 1981;12:141–50.

[45] Iami A, Tanaka M, Tatsuta M, Kawazoe T. Ultrasonographic images of tongue movement during mastication. J Osaka Dent Univ 1995;29:61–9.

[46] van Vliet T. On the relation between texture perception and fundamental mechanical parameters for liquids and time dependent solids. Food Qual Prefer 2002;13:227–36.

[47] van den Berg L, Carolas AL, van Vliet T, van der Linden E, van Boekel MAJS, van de Velde F. Energy storage controls crumbly perception in whey proteins/polysaccharide mixed gels. Food Hydrocolloids 2008;22:1404–17. Energy stored elastically or lost to viscous flow during compression alters failure mechanisms of WPI/polysaccharide gels, which is related to perceived texture of crumbliness. These findings lead to a better understanding of what mechanical properties control crumbly perception in phase separate mixed WPI/polysaccharide gels.

[48] Muñoz AM, Pangborn RM, Noble AC. Sensory and mechanical attributes of gel texture. II. Gelatin, sodium alginate and kappa-carrageenan gels. J Texture Stud 1986;17:17–36.

[49] Janssen AM, van de Pijpekamp AM, Labiausse D. Differential saliva-induced breakdown of starch filled protein gels in relation to sensory perception. Food Hydrocolloids 2009;23:795–805.

[50] Yang H, Wang Y. Effects of concentration on nanostructural images and physical properties of gelatin from channel catfish skins. Food Hydrocolloids 2009;23:577–84.

[51] Thrimawithana TR, Young S, Dunstan DE, Alany RG. Texture and rheological characterization of kappa and iota carrageenan in the presence of counter ions. Carbohydr Polym 2010;82:69–77.

[52] Zhang J, Daubert CR, Foegeding EA. Fracture analysis of alginate gel. J Food Sci 2005;70:425–31.

[53] van den Berg L, van Vliet T, van der Linden E, van Boekel MAJS, van de Velde F. Breakdown properties and sensory perception of whey proteins/polysaccharide mixed gels as a function of microstructure. Food Hydrocolloids 2007;21:961–76. Protein continuous, bicontinuous, and coarse stranded microstructures with distinct textures can be generated in phase separated WPI/polysaccharide gels. These findings show the potential to alter sensory properties via microstructure manipulation.

[54] Gwartney EA, Larick DK, Foegeding EA. Sensory texture and mechanical properties of stranded and particulate whey protein emulsion gels. J Food Sci 2004;69:333–9.

[55] Mao R, Tang J, Swanson BG. Water holding capacity and microstructure of gellan gum. Carbohydr Polym 2001;46:365–71.

[56] Verheul M, Roefs SPFM. Structure of whey protein gels, studied by permeability, scanning electron microscopy and rheology. Food Hydrocolloids 1998;12:17–24.

[57] Barbut S. Effect of sodium level on the microstructure and texture of whey protein isolate gels. Food Res Int 1995;28:437–43.

[58] Engelen L, de Wijk RA. Oral Processing and Texture Perception. In: Chen J, Engelen L, editors. Food oral processing: fundamentals of eating and sensory perception. Chicester: John Wiley & Sons; 2012. p. 157–76.

* of special interest.

** of outstanding interest.

[59] Clark AH, Judge FJ, Richards JB, Stubbs JM, Suggett A. Electron microscopy of network structures in thermally-induced globular protein gels. Int J Pept Protein Res 1981;17:380–92.
[60] Ako K, Nicolai T, Durand D, Brotons G. Micro-phase separation explains the abrupt structural change of denatured globular protein gels on varying the ionic strength or the pH. Soft Matter 2009;5:4033–41.
[61] Gosal WS, Clark AH, Pudney PDA, Ross-Murphy SB. Novel amyloid fibrillar networks derived from a globular protein: β-lactoglobulin. Langmuir 2002;18:7174–81.
[62] Çakır E, Foegeding EA. Combining protein micro-phase separation and protein–polysaccharide segregative phase separation to produce gel structures. Food Hydrocolloids 2011;25:1538–46.
[63] Çakır E, Daubert CR, Drake MA, Vinyard CJ, Essick G, Foegeding EA. The effect of microstructure on the sensory perception and textural characteristics of whey protein/κ-carrageenan mixed gels. Food Hydrocolloids 2012;26:33–43.
[64] de Wijk RA, Engelen L, Prinz JF. The role of intra-oral manipulation in the perception of sensory attributes. Appetite 2003;40:1–7.
[65] de Wijk RA, Prinz JF. Mechanisms underlying the role of friction in oral texture. J Texture Stud 2006;37:413–27.
[66] Dresselhuis DM, de Hoog EHA, Cohen Stuart MA, Vingerhoeds MH, van Aken GA. The occurrence of in-mouth coalescence of emulsion droplets in relation to perception of fat. Food Hydrocolloids 2008;22:1170–83.
[67] Malone ME, Appelqvist IAM, Norton IT. Oral behaviour of food hydrocolloids and emulsions. Part 1. Lubrication and deposition considerations. Food Hydrocolloids 2003;17:763–73.
[68] Foster KD, Woda A, Peyron MA. Effect of texture of plastic and elastic model foods on the parameters of mastication. J Neurophysiol 2006;95:3469–79. This investigation evaluates mastication parameters for model foods with different rheological properties, hardness and elasticity.
[69] Çakır E, Vinyard CJ, Essick G, Daubert CR, Drake MA, Foegeding EA. Interrelations among physical characteristics, sensory perception and oral processing of protein-based soft-solid structures. Food Hydrocolloids 2012;29:234–45.
[70] Çakir E, Koç H, Vinyard CJ, Essick G, Daubert CR, Drake M, et al. Evaluation of texture changes due to compositional differences using oral processing. J Texture Stud 2012;43:257–67.
[71] Mioche L, Bourdiol P, Monier S. Chewing behaviour and bolus formation during mastication of meat with different textures. Arch Oral Biol 2003;48:193–200.
[72] Prinz JF, Huntjens LL, de Wijk RA. Instrumental and sensory quantification of oral coatings retained after swallowing semi-solid foods. Arch Oral Biol 2006;5:1071–9. A very interesting study on the quantification of oral coatings retained after swallowing semi-solid foods. It relates the amount of oral coating (by measuring turbidity of rinse water after swallowing) to the textural properties as a new tool to understand texture.
[73] Brighenti M, Govindasamy-Lucey S, Lim K, Nelson K, Lucey JA. Characterization of the rheological, textural, and sensory properties of samples of commercial US cream cheese with different fat contents. J Dairy Sci 2008;91:4501–17.
[74] Wium H, Qvist KB, Gross M. Uniaxial compression of UF-feta cheese related to sensory texture analysis. J Texture Stud 1997;28:455–76.
[75] Bayarri S, González-Tomás L, Hernando I, Lluch MA, Costell E. Texture perceived on inulin-enriched low-fat semisolid dairy desserts rheological and structural basis. J Texture Stud 2011;42:174–84.
[76] Meullenet JF, Lyon BG, Carpenter JA, Lyon CE. Relationship between sensory and instrumental texture profile attributes. J Sens Stud 1998;13:77–93.
[77] Bryant A, Ustunol Z, Steffe J. Texture of cheddar cheese as influenced by fat reduction. J Food Sci 1995;60:1216–9.
[78] Montejano JG, Hamann DD, Lanier TC. Comparison of two instrumental methods with sensory texture of protein gels. J Texture Stud 1985;16:403–24.
[79] Fagan CC, Everard C, O'Donnell CP, Downey G, Sheehan EM, Delahunty CM, et al. Evaluating mid-infrared spectroscopy as a new technique for predicting sensory texture attributes of processed cheese. J Dairy Sci 2007;90:1122–32.
[80] Steiner AE, Foegeding EA, Drake MA. Descriptive analysis of caramel texture. J Sens Stud 2003;18:277–89.
[81] Barrangou LM, Drake MA, Daubert CR, Foegeding EA. Sensory texture related to large-strain rheological properties of agar/glycerol gels as a model food. J Texture Stud 2006;37:241–62.
[82] Ciron CIE, Gee VL, Kelly AL, Auty MAE. Effect of microfluidization of heat-treated milk on rheology and sensory properties of reduced fat yoghurt. Food Hydrocolloids 2011;25:1470–6.
[83] Brown JA, Foegeding EA, Daubert CR, Drake MA, Gumpertz M. Relationships among rheological and sensorial properties of young cheeses. J Dairy Sci 2003;86:3054–67.
[84] Everard CD, O'Callaghan DJ, Howard TV, O'Donnell CP, Sheehan EM, Delahunty CM. Relationships between sensory and rheological measurements of texture in maturing commercial cheddar cheese over a range of moisture and pH at the point of manufacture. J Texture Stud 2006;37:361–82.
[85] Alting AC, van de Velde F, Kanning MW, Burgering M, Mulleners L, Sein A, et al. Improved creaminess of low-fat yoghurt: the impact of amylomaltase-treated starch domains. Food Hydrocolloids 2009;23:980–7.
[86] de Wijk RA, van Gemert LJ, Terpstra MEJ, Wilkinson CL. Texture of semi-solids; sensory and instrumental measurements on vanilla custard desserts. Food Qual Prefer 2003;14:305–17.
[87] Engelen L, van den Keybus PAM, de Wijk RA, Veerman ECI, Amerongen AVN, Bosman F, et al. The effect of saliva composition on texture perception of semi-solids. Arch Oral Biol 2007;52:518–25.
[88] Elmore JR, Heymann H, Johnson J, Hewett JE. Preference mapping: relating acceptance of "creaminess" to a descriptive sensory map of a semi-solid. Food Qual Prefer 1999;10:465–75.
[89] Tuorila H, Vainio L. Perceived saltiness of table spreads of varying fat compositions. J Sens Stud 1993;8:115–20.
[90] Kilcast D, Clegg S. Sensory perception of creaminess and its relationship with food structure. Food Qual Prefer 2002;13:609–23.

CHAPTER 3

Use of protein-phopholipid particles as fillers in whey protein gels

Abstract

Novel processing technologies have been developed to produce a whey protein particle embedded with dairy phospholipids. In considering the health benefits of dairy phospholipids, this complex particle has the potential to serve as a functional food ingredient in the form of a filler particle. Filler particles can greatly influence the textural properties of a particular matrix depending on their interaction with the matrix, phase volume and rigidity. The objectives of this study were to characterize whey protein-phospholipid particles, determine their status as an active or inactive filler particle, and determine their effects on texture properties of whey protein gels.

Particle composition was determined using proximate analysis. Fat distribution within the particle and particle size were determined using confocal microscopy and a laser diffraction based particle size analyzer respectively. Whey protein gels with increasing phase volume (ϕ of 0, 0.06 and 0.12) were characterized using small and large strain rheological techniques.

Whey protein-phospholipid particles were composed of 84.72 ± 1.65 % protein, 9.77 ± 2.51 % lipid, 0.69 ± 0.04 % ash and 4.82 % carbohydrate, on a dry weight basis, with average diameters of 8.63 ± 0.67 μm. Lipid rich regions were distributed throughout the particle and at the particle surface. Particles were actively incorporated into the whey protein matrix and, relative to whey protein gels of equivalent protein concentration, had reduced gel stiffness (Young's Modulus), strength (fracture stress), and deformability (fracture strain), while causing the gel to break into numerous pieces upon fracture. These results show that

the whey protein-phospholipid particle may be used as an active filler and nutriceutical ingredient to deliver phospholipid health benefits in a whey protein matrix.

Key words

Whey protein; Phospholipid; Filler particle; Functional foods; Dairy

1. Introduction

Dietary phospholipids influence a spectrum of health conditions, ranging from colon cancer to Alzheimer's disease, by altering the fatty acid composition of cell membrane phospholipids within specific cell types (Küllenberg and others 2012). Dairy phospholipids in particular have been shown to protect against gastrointestinal injury in patients at risk for aspirin ulcers (Cryer and others 2011), suppress colon carcinogenesis (Berra and others 2002), and reduce memory impairment due to stress (Schubert 2011) among other health benefits. Functional foods, those with ingredients/components associated with specific health benefits, are a rapidly growing sector of the food industry. Therefore food companies are incorporating bioactive compounds, such as soluble fiber, polyphenols, plant sterols or omega-3-fatty acids, into various food matrices to attain a desired health benefit. This results in a convenient nutraceutical delivery system. In considering their many health benefits, dairy phospholipids may also act as a nutraceutical ingredient in functional foods.

Technology for the generation of a whey protein aggregate containing buttermilk phospholipids has been developed (Saffon and others 2011; Nguyen 2013). In this process,

buttermilk concentrate prepared from ultra-centrifuged skimmed buttermilk is combined with whey protein concentrate of equal protein concentration (9.6 %) at ratios of 25:75; 50:50; 75:25 or 100:0. The whey protein:buttermilk concentrate solution pH is then adjusted to 4.6 and heated under shear conditions at 90 °C for 25 min. Heat treated solutions are then homogenized (5 passes) at 65.5 MPa. Protein-phospholipid particles are collected by centrifuging at 15,000 x g for 20 min at 20 °C. As a nutraceutical ingredient, this complex whey protein-phospholipid particle can be added to various food systems in the form of a filler particle. Filler particles are typically incorporated into food matrices for the purposes of texture modification or fat replacement. Their affect on texture or material properties is dependent on several factors including particle phase volume, particle rigidity and surface activity. Particle surface activity will dictate if the particle is *active* or *inactive* within a particular matrix. When the particle surface has a high chemical affinity for the surrounding matrix, the particle is considered active and acts to reinforce or strengthen the matrix network (van Vliet 1988, Chen and Dickinson 1999). Conversely, if the particle surface has little chemical affinity for the matrix, it is considered inactive and will not strengthen the network (van Vliet 1988, Chen and Dickinson 1999).

The degree of filler particle interactions with the matrix will also influence the failure mechanisms of the composite material. At the point of catastrophic failure, cracks propagate through a material taking the path of least resistance (Anderson 1995). In a composite material with an active filler, the crack will propagate from the matrix, through the filler particle and continue on to the matrix. In the presence of an inactive filler however, the propagating crack will divert its pathway, moving around the filler particle within the weakly

associated filler matrix boundary then continue on into the matrix (Normand and others 2001). This crack pathway diversion forms voids within the composite during deformation, which shifts the material facture mechanism from brittle-like to pseudo-ductile (Norton and Firth 2001).

In considering the potential impact filler particles may have on the textural properties of a particular matrix, it is important to know if the filler of interest is active or inactive within a given system. The objectives of this study were to characterize protein-phospholipid particles, determine their status as an active or inactive filler particle, and determine their effects on textural properties of whey protein gels.

2. Materials and Methods

2.1. Materials

Whey protein isolate (WPI) was donated by Davisco Foods Inc. (Le Sueur, MN, U.S.A.) and contained 94.55 % (w/w) protein (N x 6.38) as determined by nitrogen content determined by inductively coupled plasma spectroscopy. Whey buttermilk powder (WBP) was provided by Dr. Rafael Jiménez-Flores of California Polytechnic State University. Sodium acetate, ethyl alcohol, ethyl ether, petroleum ether, Sigmacote® and Fast Green FCF were purchased from Sigma-Aldrich Corp. (St. Louis, Mo., U.S.A.). Hydrochloric acid (HCl) (37%, FCC, ACS, NF) was purchased from Mallinckrodt Baker (Paris, Ky., U.S.A.). Sodium hydroxide (NaOH) (ACS pellets), Nile Red and acetone were purchased from Fisher

Scientific Inc. (Fair Lawn, N.J., U. S. A.). Deionized water used for solution preparations had a resistance of >17 MΩ.

2.2. Protein-phospholipid particle preparation

Protein-phospholipid particles were prepared from whey buttermilk solution (5 % (w/v) protein). Solutions were formed by mixing whey buttermilk powder in 0.1 M sodium acetate at room temperature (21 ± 1 °C) for 5 hr, then stored overnight at 4 ± 1 °C for complete protein hydration. Solutions were brought to room temperature (21 ± 1 °C) and pH was adjusted to 4.6 using 6 M HCl. The solution (1 L) was stirred at 200 rpm, using a mechanical overhead stirrer (model RZR 2021) with impeller attachment (Heidolph Instruments GmbH & Co., Elk Grove Village, Il., U.S.A.), and heated in a 95 ± 1 °C water bath until it reached 80 ± 1 °C. Heated solutions were immediately transferred to an 80 ± 1 °C waterbath and held for 25 min with constant stirring (200 rpm). Solutions were cooled to 4 ± 1 °C and subjected to two passes through a Panda 2K laboratory homogenizer (GEA Niro Soavi North America, Bedford, N.H., U.S.A.) at a pressure of 140 bars. Homogenized solutions were centrifuged using a Sorvall RC 5B centrifuge (DuPont Instruments, Newtown, Conn., U.S.A.) at 2,000 x *g* for 10 min. The pellet containing protein-phospholipid particles was washed three times by re-suspending the particles in deionized water and centrifuging. The washed pellet was held at 4 ± 1 °C until used.

2.3. Gel preparation

Whey protein gels were prepared at 12, 16, and 21 % (w/w) protein and pH 6. Filled gels were made by mixing 12% (w/w) protein solutions with different phase volumes (ϕ of 0, 0.06 and 0.12) of protein-phospholipid particles. It was assumed that the WPI and water constituted one phase and the protein-phospholipid particle constituted a second phase. WPI was dispersed in deionized water at ~80% of final volume. Protein-phospholipid particles were added to WPI solutions and mixed using a magnetic stirrer until homogeneous. Solution pH was adjusted to 6 using 6 M HCl, brought to final volume and degassed for one hour. Degassed solutions were poured into glass tubes (19 mm diameter x 180 mm height) that were stoppered on one end with a rubber plug and coated with Sigmacote® siliconizing release agent. Glass tubes were covered with aluminum foil to prevent evaporation and heated in a water bath at 80 ˚C for 30 min. Immediately after heating, gels were cooled in ice water and held for 24 hr at 4 ˚C. Three replications were prepared for each treatment.

2.4. Composition analysis

Protein was determined by inductively coupled plasma spectroscopy (N x 6.38). The total moisture content (% w/w) was measured by the Forced Draft Oven method (AOAC International 977.11) whereby samples were dried in a 105 °C oven for 16 h. Total fat was determined using the Mojonnier method (AOAC 991.20. 662). Two samples per replicate were analyzed for moisture. Three samples per replicate were analyzed for protein and fat.

2.5. Particle size analysis

The protein-phospholipid particle size distribution was measured by laser light scattering using a Mastersizer 3000 (Malvern Instruments, Malvern, UK), equipped with a 4 mW He/Ne laser (λ = 633 nm) and a 10 mW LED (λ = 470 nm) according to a modified method of Lopez and others (2010). The protein-phospholipid particle (pellet diluted 1:100 in deionized water) was added to the measurement cell containing deionized water at room temperature (21 ± 1 °C) until a 10 % obscuration was reached. The solution was stirred at 2400 rpm during analysis. Size distribution was characterized by the volume-weighted average diameter (d_{43}).

2.6. Imaging

Confocal Laser Scanning Microscopy (CSLM) was used to image protein-phospholipid particles according to a modified method of Gallier and others (2010). The protein-particle pellet was diluted 1:100 (w/v) in deionized water. Nile Red (0.1 % (w/v) in acetone) was added (4:100 (v/v)) to diluted particles to stain the lipid regions followed by addition of Fast Green FCF (0.1 % (w/v) in deionized water, added at a ratio of 6:100 (v/v)) to stain the protein regions. A 5 µL aliquot of stained particle solution was then placed in the center of a glass bottom microwell dish (35 mm petri dish, 14 mm Micro well, Nr 1.5 cover glass (0.15 to 0.19 mm)) (MatTek Corp., Mass., U.S.A.). To fix the sample, 195 µL of agarose (0.5 % (w/v) in deionized water) that had been heated to 90 °C and cooled to 35 °C was added to the microwell dish, gently mixed with the sample, and cooled to room temperature. Samples were imaged using an inverted Leica TCS SP1 CSLM (Leica Inc.,

Bannockburn, Il., U.S.A.) with 63 X, C-Apochromat water immersion objective (N.A. = 1.2). The Nile Red probe was excited at 488 nm and emission collected between 500 and 600 nm. The Fast Green FCF probe was excited at 633 nm and emission collected between 655 and 755 nm.

2.7. Rheology

2.7.1. Small strain rheology

Dynamic oscillatory measurements were performed on a stress controlled rheometer (StressTech, Rheologica Instruments AB, Lund, Sweden) using a serrated parallel plate geometry (20 mm diameter, 1 mm gap). Measurements were made under the strain controlled mode to prevent sample damage. Gels cut to a 3 mm height were loaded onto parallel plate and exposed edges of sample were covered with a thin layer of mineral oil to minimize evaporation. A stress sweep (1 Hz) was performed at 21 °C between a stress level of 1 to 1000 Pa to determine the linear viscoelastic region. A frequency sweep between 0.01 and 10 Hz was performed at 21 °C at a stress level selected within the linear viscoelastic region.

2.7.2. Large strain rheology

Torsional fracture. Gels were equilibrated to room temperature (21 ± 2 °C) and prepared for torsion analysis using the method of Truong and Daubert (2000) and evaluated by the method of Diehl and others (1979). Briefly, gel cylinders (19 mm diameter) were cut to a length of 28.7 mm and notched plastic disks (Gel Consultants. Raleigh, N.C., U.S.A.) were

glued to each end of the sample ends using cyanoacrylate glue (Loctite 401: Loctite Corp. Rocky Hill, Conn., U.S.A.). The cylinders were mounted on a modified milling machine and ground to a capstan shape with a minimum center diameter of 10 mm. Samples were mounted onto a Haake VT-550 rotational viscometer (Gerbruder Haake GmbH, Karlsruhe, Germany) with a torsion testing attachment and twisted at a strain rate of 0.26 1/s until fracture. The maximum torque (M) and corresponding time value (t) were used to calculate the angular deformation (ϕ) of sample where $\phi = \gamma_t$ and γ_t is the uncorrected strain. The true shear stress (σ_t) and true shear strain (γ_{true}) of sample at fracture were calculated using equations developed by Diehl and others (1979), Eqs. (1), (2), (3):

$$\sigma_\tau = \frac{2KM}{\pi r_{\min}^3} \tag{1}$$

$$\gamma_t = \frac{2K\phi}{\pi r_{\min}^3 Q} \tag{2}$$

$$\gamma_{true} = \ln\left[1 + \frac{\gamma_t^2}{2} + \gamma_t\left(1 + \frac{\gamma_t^2}{4}\right)^{1/2}\right] \tag{3}$$

where the shape factor constant (K) is 1.08, M is the maximum torque, r_{min} is the minimum radius in the middle of the capstan shaped sample, and Q is a curvature section constant (8.45 x10^{-6} m^{-3}).

Uniaxial compression. Young's Modulus (E) and fractured gel morphology were determined under uniaxial compression. For all tests, gel cylinders (19 mm diameter) were cut to a length of 21.5 mm and compressed at room temperature (21 ± 2˚C) using an Instron universal testing instrument type 5565 equipped with a 5 kN load cell (Instron Engineering Corporation., Mass., U.S.A). Samples were compresses at a rate of 50 mm/min between plates lubricated with mineral oil had a diameter of 5 cm. This diameter was greater than the maximum diameter of samples after compression. Compression was stopped at 90% of the original sample height. Young's Modulus was determined from the slope of the linear region in the force deformation curve by applying a linear regression was applied up to 5 % strain. The force-deformation curve was determined by plotting the true stress and true strain during compression, which were calculated according to the following Eqs. (4) and (5):

$$Ture\ stress = \left(\frac{F}{A}\right)\left(\frac{L}{L_i}\right) \qquad (4)$$

$$True\ strain = \ln\left(\frac{L}{L_i}\right) \qquad (5)$$

where F is the force during compression, A is cross sectional the area of the initial sample, L_i is the initial sample height and L is the sample height.

3. Results

3.1. Composition and particle size

Protein-phospholipid particle composition consisted of 84.72 ± 1.65 % (w/w) protein, 9.77 ± 2.51 % (w/w) lipid, 0.69 ± 0.04 % (w/w) ash and 4.82 % (w/w) carbohydrate by difference on a dry weight basis. Particle size of the protein-phospholipid particle ranged broadly from 0.6 μm to 106 μm and had a bimodal size distribution. The average particle sizes of the first and second peaks were 2.15 ± 0.16 and 8.63 ± 0.67 μm respectively (Figure 1).

3.2. Imaging

Confocal laser scanning microscopy was used to elucidate the relative protein and fat distributions of the protein-phospholipid particle. In the confocal image, red colored areas indicate lipid rich regions whereas blue colored areas indicate protein rich regions. Areas of no color are void of lipid and protein. Lipid rich regions were present at the particle surface (Figure 2) and three-dimensional imaging of the particle (data not shown) showed that spherical lipid rich regions were predominately embedded within the particle interior. Small lipid particles not incorporated into the protein particle were also present.

3.3. Rheology

Small and large strain rheological properties of composite whey protein gels were measured. The initial whey protein concentration was 12 % (w/w). Aggregate addition of ϕ

= 0.06 and ϕ = 0.12 decreased the overall amount of protein contributed from WPI but, due to the protein content of the particles, increased the total protein concentration of the composite system to 16 and 21 % (w/w) respectively. Therefore, WPI gels with 16 and 21 % (w/w) protein were used as controls. These will be referred to as whey protein control gels throughout this paper.

3.3.1. Small strain rheological properties

The mechanical spectra of all treatments were typical for that of a gel; having a storage modulus (G′) greater than the loss modulus (G″) over all frequencies tested and a relatively linear dependence on frequency (Figure 3A and 3B). G′ increased with increasing protein-phospholipid particle volume fraction. G′ also increased for whey protein control gels as protein concentration increased. G′ of composite gels was less than that of the whey protein control gels at equivalent protein concentrations.

3.3.2. Large strain and fracture rheological analysis

3.3.2.1. Fracture stress and fracture strain

All samples experienced tensile failure based on the failure plane occuring at a 45 degree angle relative to the plane parallel to the gel cylinder diameter (Diehl and others 1979). Increasing protein-phospholipid particle volume fraction and/or total protein concentration increased fracture stress (Table 1). This response is typical for active filler particles (van Vliet 1988) and also supports small strain data presented earlier. Composite gel strength however was less than that of the whey protein control gel at equivalent protein

concentrations. Fracture strain (Table 1) was reduced with increasing particle volume fraction in the composite gels. Contrarily, in the control gels, fracture strain was increased by protein addition; the 16 % (w/w) protein control gel had a higher fracture strain than the 21 % (w/w) protein control gel.

3.3.2.2. Young's Modulus

Mathematically, Young's Modulus (E) represents the change in stress relative to the change in strain a material exhibits during the initial (linear region) phase of compressive deformation. The relative difference in E between treatments can be visualized in the linear regions of force-deformation curve (Figure 4). E increased with increasing protein concentration and with protein-phospholipid particle volume fraction (Table 1). At equivalent protein concentrations, however, E was lowered by incorporation of protein-phospholipid particles.

3.3.2.3. Force-deformation curve and after fracture breakdown

During compression, all gels experienced abrupt tensile failure (vertical fracture). Typical true stress and strain curves are presented in Figure 4. Interestingly, it was observed that the number of fractured pieces increased with protein-phospholipid particle addition (Figure 5). Composite gels fractured into multiple (>10) pieces and had a stranded macroscopic appearance.

4. Discussion

Protein-phospholipid particle production was similar to methods used in the production of the more familiar microparticulated whey protein (MWP) particles. In this process, a protein rich fluid, such as whey protein concentrate, is heated under conditions of high shear to induce heat denaturation and aggregation of the protein and simultaneously breakup the aggregates (Havea and others 2009). The heated fluid may then be homogenized under high pressure (commonly referred to as microfluidization) to further reduce protein aggregate size (Dissanayake and T. Vasiljevic 2010). Simplesse is an example of a commercially produced MWP product (Singer and others 1988). Because our process for protein-phospholipid particle production was similar to that for MWP particles, the protein-phospholipid particle may be considered as a type of MWP particle and will therefore be compared to such to facilitate discussion.

Total fat content (9.8 % (w/w)) of the protein-phospholipid particle was within the range typically reported for other MWPs (Table 2). On the other hand, the protein concentration (84.72 % (w/w)) was substantially greater than that for other MWP particles (Table 2). Lactose, a disaccharide, was not measured in this study. As a carbohydrate, the maximum level of lactose in the protein-phospholipid particle could be that of the carbohydrate levels (4.82 % (w/w)), which were determined by difference in proximate analysis. This maximum level was more than three times less than the lowest reported lactose concentration of other MWPs (Table 2). The same was true for the ash content. It is likely that compositional differences stem from the different starting materials used in the production of the various MWPs.

The fat of the particle was present at the particle surface and within the particle interior. This observation is consistent with the physical character of other particles formed from similar starting material (whey:buttermilk concentrate). Saffon and others (2014) studied the formation of "pre-formed" complex particles formed in a solution of buttermilk protein concentrate powder dissolved in fresh whey. Their study showed that fat containing, non-soluble, protein particles are formed at the pasteurization step of buttermilk production and that these particles are then concentrated in the buttermilk protein concentrate powder. These particles are 15-30 μm in size with lipid rich regions distributed on the surface and throughout a protein aggregate (Gallier and others 2010). When these "pre-formed" particles are heated in the presence of whey protein and buttermilk constituents, they act as nuclei to interact with denatured whey proteins and milk fat globule membrane components via thiol/disulfide interchange to form larger particles that also have lipid rich regions at the surface and within aggregated protein particle. The larger particles are then reduced in size via microfluidization to an average diameter of 7.3 μm (Saffon and others 2014).

The average particle sizes of the first and second peaks were 2.15 ± 0.16 and 8.63 ± 0.67 μm respectively (Figure 1). The smaller particles (2.15 μm) were lipid rich spheres not incorporated into the protein-phospholipid particle, which were observed during image analysis (data not shown). The larger particles (8.63 μm) were the protein-phospholipid aggregates. Their particle size was within the normal range reported for other MWP particles (Table 2). Particles that are < 10 μm impart a smooth mouthfeel (Spiegel 1999) and can be easily incorporated into dairy based products such as ice cream, and soft or semi-hard cheese (Steffl and others 1997; Schreiber and others 1998; Koxholt and others1999). Based on the

protein-phospholipid particle size distribution (Figure 1), approximately one half of the particles prepared in this study would give a smooth mouthfeel.

When incorporated into a given matrix the particle size, phase volume, rigidity and surface activity of filler particles influence the composite material properties. Increasing the protein-phospholipid particle volume fraction in the whey protein gel caused an increase in the elastic modulus of the gel (Figure 3). This suggests that the whey protein-phospholipid particle interacted with the matrix to reinforce the network and therefore acted as an active filler in the whey protein network (van Vliet 1988). The surface activity of a filler particle dictates whether or not the particle will be active or inactive within a given system. Thus, in a hydrophilic matrix, particles with a hydrophobic surface would not strongly interact with the matrix and therefore be considered an inactive filler. In this case, hydrophobic regions (lipid rich regions) were observed at the surface of the protein-phospholipid; however the degree of particle hydrophobicity was not measured. It is hypothesized that the degree of lipid rich regions at the surface of the particle were not sufficient to over-ride interactions between the whey protein matrix and the protein rich (hydrophilic) regions of the particle.

Reports for MWP particles formed from fresh whey proteins and whey protein concentrate also conclude that MWP particles actively participate in whey protein gel matrices (Renard and others 2002, Purwanti and others 2012) and acidified casein matrices (Saffon and others 2013). The MWP particle most similar to the protein-phospholipid particle used in this study has only been evaluated for activity in an acidified casein network. There are no reports to date on the activity of this type of particle in a whey protein network. In the case of the casein network, Saffon and others (2013) incorporated particles prepared

from a 25:75 mixture of whey:buttermilk concentrate powder into an acidified casein matrix (yogurt) that was prepared from skim milk powder. Protein (20, 40, 60, 80 and 100 % (w/w)) from the skim milk powder was substituted for an equivalent amount of protein contributed by the whey-buttermilk particles. This substitution caused the yogurt gel firmness to decrease where firmness was determined by the maximum force achieved when a cylindrical probe penetrated the gel to a depth of 20 mm. On the other hand, Saffon and others (2013) showed that the whey-buttermilk particles interacted with caseins via thiol/disulfide interchange. This interaction indicated that the particle was an active filler; however, their experimental design was not adequate to show filler effects based on filled gel models. When determining filler particle activity, the filler and matrix are considered as two phases. If the modulus of the composite increases when the filler phase volume is increased then the filler is said to be active within the matrix (van Vliet 1988, Chen and Dickinson 1999). In the experimental design of Saffon and others (2013), the protein particle was used as a protein substitute for skim milk powder protein and the phase volume of the filler and matrix were not considered. Overall, Saffon and others (2013) concluded that although the whey-buttermilk particle interacted with the network, and hypothesized that when incorporated into the casein network, the particle reduced the casein network density leading to reduced gel hardness. This is contradictory to our findings for the protein-phospholipid particle in the whey protein matrix. Our findings show that the particle interacted with the whey protein gel network and enhanced the network strength.

As hypothesized previously, the surface activity (which was not measured) of the protein fraction of the protein-phospholipid particle had a greater influence on the particle

interaction with the matrix than did the lipid fraction. This is in contrast to findings of Sağlam and others (2014) for corn oil-whey protein particles formed in the presence of an emulsifier that were incorporated into a whey protein gel network. These emulsified particles also had lipid rich regions (formed from residual emulsifier Polyglycerol Polyricinoleate) at the particle surface but the particle did not actively participate in whey protein gel network. Sağlam and others (2014) evaluated whey protein gels (4 – 24 % w/w) at pH 5.5 and 6.8 with increasing particle volume fraction (0.11 to ~0.65). Replacement of whey protein in the continuous phase with filler particle prevented gelation when the initial protein concentration of the continuous phase was less than 12 % w/w. Had the particles sufficiently interacted with the matrix, the composite gels would have had an increasing modulus with increasing volume fraction; instead particle addition prevented gelation.

The active incorporation of protein-phospholipid particles into the whey protein network influenced the large strain rheological properties of the composite gels. Both E and fracture stress increased with increasing protein-phospholipid particle volume fraction. Likewise these properties increased with increasing protein concentration in the control gels. At equivalent protein concentrations, however, whey protein control gels had a higher E and fracture stress than that of the composite gel. These findings are in line with other studies on MWP particles, which report that whey protein gel hardness (force before fracture), stiffness (E) (Purwanti and others 2011, Purwanti and others 2012), and shear modulus (Sağlam and others 2014) are reduced by replacement of protein from WPI with protein from MWP particles. Also, Renard and others (2002) found that MWP particles were disruptive to β-lactoglobulin gels because they flocculated and formed heterogeneities within the matrix

causing a reduced gel strength. One explanation for the lower composite gel fracture stress could be that the particles are inhomogeneities within the system that act as stress raisers to increase the local stress concentration and thereby cause the material to fail at a lower stress (Anderson 1995).

The observed changes in large strain rheological properties suggests that protein-phospholipid particle addition changed the whey protein gel texture. During mastication, soft solid foods are compressed between the back molar teeth until fracture. As such, large strain rheological testing more closely resembles oral processing events than small strain testing and shows better correlations with first bite sensory textures (Foegeding and others 2003). Fracture strain is associated with the sensory texture attribute compressibility/deformability (degree to which sample deforms before fracture) while fracture stress is related to sensory texture attribute of hardness (force required to fracture a sample on the first bite) (Gwartney and others 2004, Çakır and others 2012). Also, gel stiffness may be gauged by measurement of Young's Modulus (E), which is related to the sensory texture attribute of firmness (gel hardness before fracture) (Çakır and others 2012). Thus, protein-phospholipid particle addition to a whey protein gel reduced gel stiffness (E), hardness (fracture stress), and deformability (fracture strain) relative to whey protein gels of equivalent protein concentration.

The total sensory experience of oral processing however is far more complex and dynamic and can be broken down into three phases: first bite, mastication and residual. Mechanical properties up to the point of fracture help us to gauge texture perception during the first bite phase. Fracturability is defined as the "degree to which the sample fractures into

pieces" upon the first bite between the molars (Pascua and others 2013). This sensory texture attribute is a breakdown property. To date, published information on how filler particles impact the breakdown properties of model soft solid gels is limited. Therefore we felt it pertinent to comment on the changes in breakdown properties caused by filler particle incorporation. As described previously (section 3.3.2.3), protein-phospholipid particle addition to the whey protein gel increased gel fracturability. When failure occurs at the point of fracture, a crack will propagate through the material. Crack propagation begins at the site of an imperfection within the material (Carlson and others 2012). In theory, a higher number of imperfection sites would lead to a greater number of cracks propagating through the material. Although analyses employed in this investigation did not evaluate crack propagation mechanisms, the observed increase in fracturability (i.e. greater number of propagating cracks) suggests that the whey-phospholipid particles are sites of imperfections that initiate crack propagation.

5. Conclusions

The objectives of this study were to characterize protein-phospholipid particles, determine their status as an active or inactive filler particle, and determine their effects on textural properties of whey protein gels. It was shown that protein-phospholipid particles have a relatively high protein, average fat, and low ash and carbohydrate concentrations as compared to other MWP particles. The fat was distributed on the particle surface and throughout the particle interior. The protein-phospholipid particle acted as an active filler

within the whey protein matrix and greatly impacted whey protein gel texture properties as determined by instrumental analyses. Relative to whey protein gels of equivalent protein concentration, protein-phospholipid particles reduced gel stiffness (E), hardness (fracture stress), deformability (fracture strain) and increased gel fracturability. These results show that the protein-phospholipid particles could be used as an active filler particle and nutraceutical ingredient to deliver phospholipid health benefits in a whey protein matrix.

References

Anderson TL. 1995. Fracture Mechanics:Fundamentals and Applications. 2nd edition. Boca Raton:CRC press. p 688.

Berra B, Colombo I, Sottocornola E, Giacosa A. 2002. Dietary sphingolipids in colorectal cancer prevention. Eur J Cancer Prev 11(2):193-97.

Çakır E, Daubert CR, Drake MA, Vinyard CJ, Essick G, Foegeding EA. 2012. The effect of microstructure on the sensory perception and textural characteristics of whey protein/κ-carrageenan mixed gels. Food Hydrocolloid 26(1):33-43.

Carlson RL, Kardomateas GA, Craig JI. 2012. Fracture mechanics. In: Carlson RL, author. Mechanics of failure mechanisms I n structures. New York:Springer. p 13-17.

Chen J, Dickinson E. 1999. Effect of surface character of filler particles on rheology of heat-set whey protein emulsion gels. Colloid Surf B:Biointerfaces 12(3):373-81.

Cryer B, Bhatt DL, Lanza FL, Dong JF, Lichtenberger LM, Marathi UK. 2011. Low-dose aspirin-induced ulceration is attenuated by aspirin–phosphatidylcholine: A randomized clinical trial. Am J Gastroenterol 106(2):272-77.

Diehl KC, Hamann DD, Whitfield JK. 1979. Structural failure in selected raw fruits and vegetables1. J Texture Stud 10(4):371-400.

Dissanayake M, Vasiljevic T. 2009. Functional properties of whey proteins affected by heat treatment and hydrodynamic high-pressure shearing. J Dairy Sci 92(4):1387-97.

Dissanayake M, Kelly AL, Vasiljevic T. 2010. Gelling properties of microparticulated whey proteins. J Agr Food Chem 58(11):6825-32.

Foegeding AE, Brown J, Drake MA, Daubert CR. 2003. Sensory and mechanical aspects of cheese texture. Int Dairy J 13(8):585-91.

-Flores R, Everett D. 2010. Using confocal laser scanning microscopy to probe the milk fat globule membrane and associated proteins. J Agr Food Chem 58(7):4250-57.

Gwartney EA, Larick DK, Foegeding EA. 2004. Sensory texture and mechanical properties of stranded and particulate whey protein emulsion gels. J Food Sci 69(9):333-39.

Havea P, Baldwin AJ, and Carr AJ. 2009. Specialized and novel powders. In: Dairy powders and concentrated products. A.Y. Tamime Ed. Blackwell publishing Ltd. United Kingdom. pp 268-288.

Koxholt K, McIntosh T, Eisenmann P. 1999. Enhanced stability of ice cream by using particulated whey proteins. Eur Dairy Mag 10:14–15.

Küllenberg D, Taylor LA, Schneider M, Massing U. 2012. Health effects of dietary phospholipids. Lipid Health Dis 11(3):1-16.

Norton IT, Frith WJ. 2001. Microstructure design in mixed biopolymer composites. Food Hydrocolloid 15(4):543-53.

Normand V, Plucknett KP, Pomfret SJ, Ferdinando D, and Norton IT. 2001. Large deformation mechanical behavior of gelatin–maltodextrin composite gels. J App Poly Sci 82(1):124-35.

Nguyen TMT. 2013. The Effects of Microfluidization and Homogenization on the Composition and Structure of Liposomal Aggregates from Whey Buttermilk and Commercial Buttermilk. PhD diss., California Polytechnic State University.

Pascua Y, Koç H, Foegeding EA. 2013. Food structure: Roles of mechanical properties and oral processing in determining sensory texture of soft materials. Curr Opin Colloid Inter 18(4):324-33.

Purwanti N, Smiddy M, van der Goot AJ, de Vries R, Alting A, Boom R. 2011. Modulation of rheological properties by heat-induced aggregation of whey protein solution. Food Hydrocolloid, 25(6):1482-89.

Purwanti N, Moerkens A, van der Goot AJ, Boom R. 2012. Reducing the stiffness of concentrated whey protein isolate (WPI) gels by using WPI microparticles. Food Hydrocolloid 26(1):240-48.

Renard D, Robert P, Faucheron S, Sanchez C. 1999. Rheological properties of mixed gels made of microparticulated whey proteins and β-lactoglobulin. Colloid Surf B:Biointerfaces 12(3):113-21.

Renard D, Lavenant L, Sanchez C, Hemar Y, Horne D. 2002. Heat-induced flocculation of microparticulated whey proteins (MWP); consequences for mixed gels made of MWP and β-lactoglobulin. Colloid Surfaces B: Biointerface 24:73-85.

Saffon M, Britten M, Pouliot Y. 2011. Thermal aggregation of whey proteins in the presence of buttermilk concentrate. J Food Eng 103(3):244-50.

Saffon M, Richard V, Jiménez-Flores R, Gauthier SF, Britten M, Pouliot Y. 2013. Behavior of heat-denatured whey: buttermilk protein aggregates during the yogurt-making process and their influence on set-type yogurt properties. Food 2(4):444-59.

Saffon M, Jiménez-Flores R, Britten M, Pouliot Y. 2014. On the use of buttermilk components as aggregation nuclei during the heat-induced denaturation of whey proteins. J Food Eng 132:21-8.

Sağlam D, Venema P, de Vries R, van den Berg M, van der Linden E. 2014. Whey protein particles modulate mechanical properties of gels at high protein concentrations. Food Hydrocolloid 38:163-71.

Schreiber R, Post F, Kessler HG. 1998. Einbau von molkenproteinaggregaten in schnittkäse. Teil 2: Einfluß von größe, Struktur und zusammensetzung der molkenprotein-aggregate. Deut Milchwirtschaft 49:1071–74.

Schubert M, Contreras C, Franz N, Hellhammer J. 2011. Milk-based phospholipids increase morning cortisol availability and improve memory in chronically stressed men. Nutr Res 31(6):413-20.

Singer NS, Yamamoto S, Latella J. 1988. Protein product base. European Patent Application EP250623.

Spiegel T. 1999. Whey protein aggregation under shear conditions–effects of lactose and heating temperature on aggregate size and structure. Int J Food Sci Tech 34(5-6):523-31.

Steffl A, Krause I, Nussbaum S, Freitsmiedl C, Kessler HG. 1997. Einbau von partikulierten molkenproteinen in weichkäse - Einflüsse auf zusammensetzung, ausbeute und reifung. Deut Molkerei Zeitung 118:1041–42.

Truong VD, Daubert CR. 2000. Comparative study of large strain methods for assessing failure characteristics of selected food gels. J Texture Stud 31(3):335-53.

van Vliet T. 1988. Rheological properties of filled gels. Influence of filler matrix interaction. Colloid Poly Sci 266(6):518-24.

Table 1. Large strain rheological properties of whey protein gels (12, 16 and 21 % (w/w) whey protein) and composite gels with $\phi = 0.06$ and $\phi = 0.12$ protein-phospholipid particles.

Total protein concentration (% w/w)	ϕ	**Fracture stress (kPa)**	**Fracture strain**	**Fracture Modulus (kPa)**	**Young's modulus (kPa)**
12	0.00	12.7 ± 0.40	2.00 ± 0.00	6.5 ± 0.10	17.6 ± 1.80
16	0.00	57.5 ± 1.40	2.20 ± 0.00	25.9 ± 0.10	447 ± 22.1
	0.06	26.3 ± 0.60	1.80 ± 0.00	14.9 ± 0.60	47.9 ± 2.20
21	0.00	187 ± 2.00	2.13 ± 0.00	87.7 ± 0.80	1090 ± 38.1
	0.12	53.8 ± 1.10	1.00 ± 0.00	52.7 ± 1.40	304 ± 6.10

Table 2. Protein-phospholipid particle and microparticulated whey protein particle compositions on a dry weight basis

Constituent	Starting material			
	whey buttermilk concentrate	whey:whey buttermilk concentrates (25:75)	whey protein concentrate (Simplesse 100)	fresh whey protein
Protein	84.7	57.3	50.1	68.8
Total fat	9.80	12.7	4.37	4.15
Ash	0.70	4.9	nd	4.69
Carbohydrate by difference	4.80	nd	nd	nd
Lactose	nd	18.8	35.5	20.9
Avg. particle size (μm)	8.6	7.3	1.5	10
Reference	This investigation	Saffon and others (2011)	Renard and others (1999)	Dissanayake and others (2009)

*nd – not determined

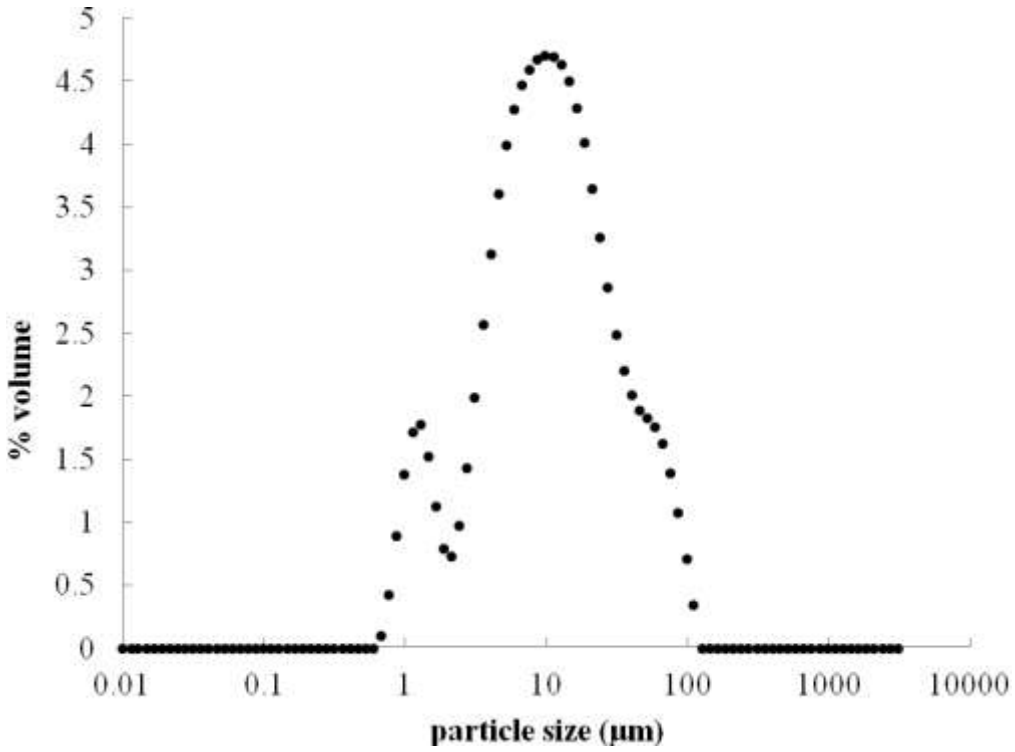

Figure 1. Protein-phospholipid particle size distribution

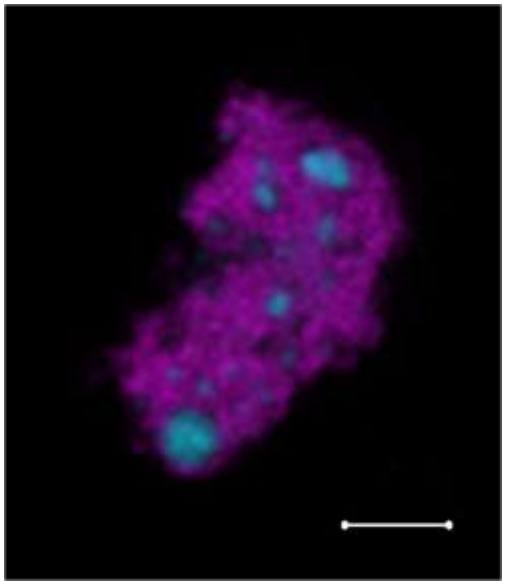

Figure 2. Confocal images of protein-phospholipid particle cross-section. Purple areas indicate protein and blue areas indicate lipid rich regions. Scale bar represents 5 μm.

A.

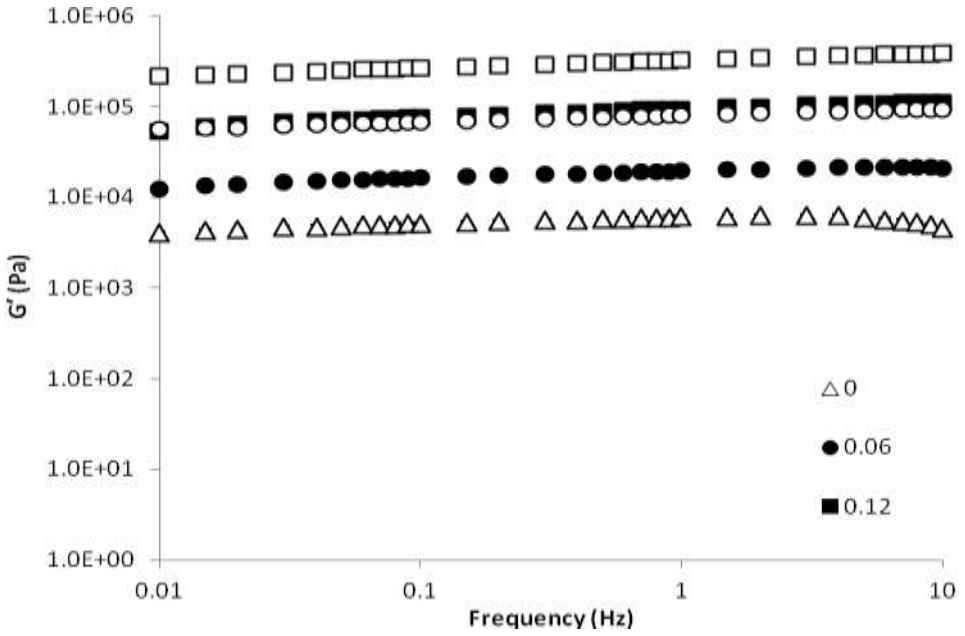

B.

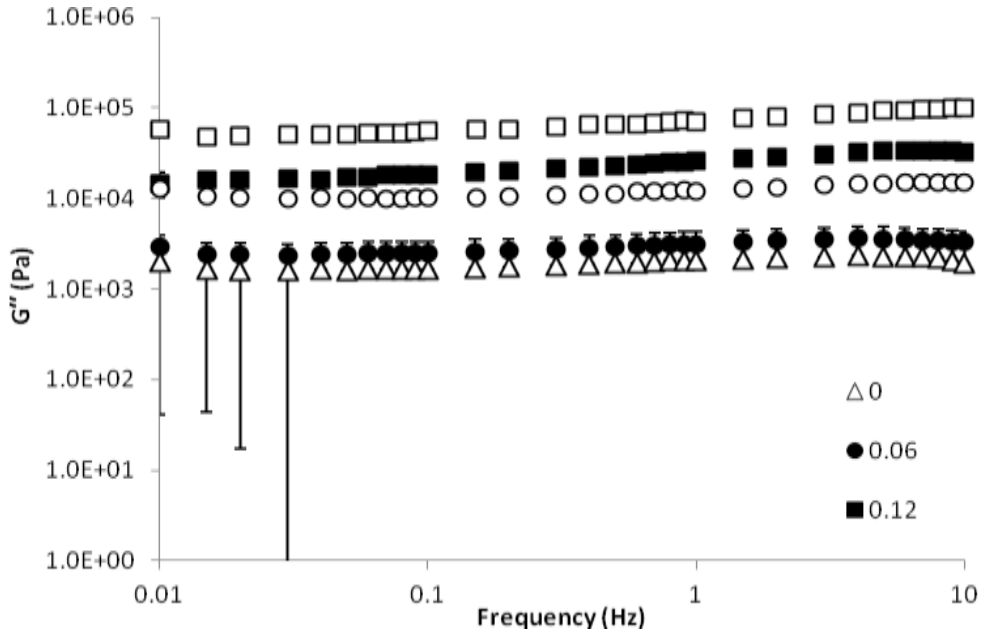

Figure 3. Storage (G′) and loss (G″) modulus of whey protein gels with ϕ = 0, 0.06 and 0.12 protein-phospholipid particle. Closed symbols represent gels with filler particle.

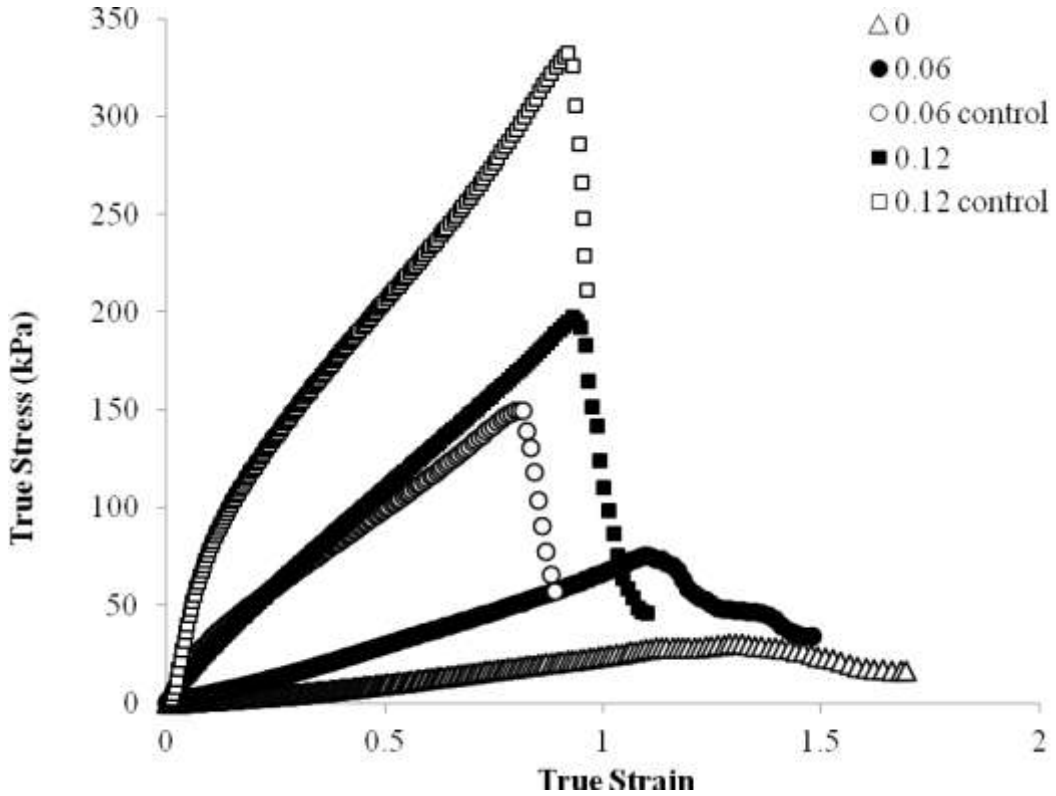

Figure 4. Typical force-deformation curves for whey protein control gels (12, 16 and 21 % (w/w) whey protein) and composite gels with $\phi = 0.06$ and $\phi = 0.12$ protein-phospholipid particles. Corresponding images show typical morphology of fracture gels.

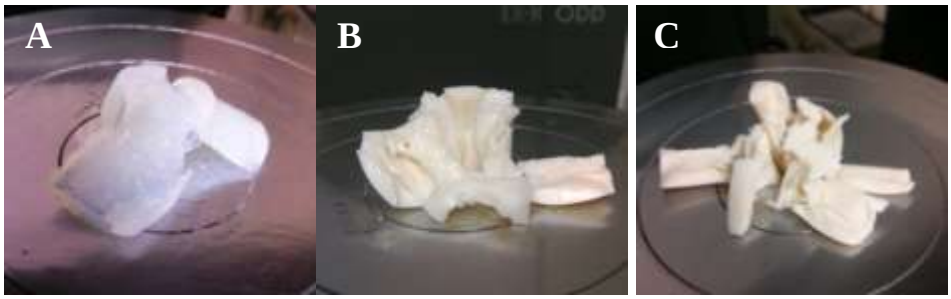

Figure 5. Images of whey protein gels with A) $\phi = 0$, B) $\phi = 0.06$ and C) $\phi = 0.12$ protein-phospholipid particles. Images show that gels with protein-phospholipid particles broke into several pieces after fracture whereas gels without particles broke into a few pieces.

CHAPTER 4

Modification of whey protein gel sensory texture, rheological properties and microstructure by casein addition

Abstract

The objective of this study was to determine the effects of casein micelles and dispersed casein on the sensory texture and material properties of whey protein isolate gels. Secondarily, we sought to determine if whey protein-casein gel microstructures could be correlated with changes in sensory texture and material properties. Heat set gels were made from whey proteins alone or combined with casein in micellar or dispersed form at pH 6 and 5.5. Replacing the whey protein with casein drastically reduce gel strength but minimally altered recoverable energy. Instrumentally measured water holding capacity was decreased by casein addition. Breakdown patterns were shifted from brittle-like to ductile-like for dispersed casein at pH 5.5 or micellar casein at pH 6. Additionally, whey protein-casein gels broke down more rapidly into a more cohesive mass during mastication than did the whey protein gels without casein. Shifts in microstructure observed by confocal microscopy could not explain the changes in mechanical or sensory textures. Overall, it was demonstrated that mechanical and sensory properties of whey protein gels can be altered to a more cheese-like pattern using caseins as a texture modifier while maintaining a high total protein concentration.

1. Introduction

There is an increasing demand for high protein snack foods that are low in fats and sugars. Milk proteins (casein and whey proteins) provide an excellent platform for the development of such food items due to their diverse textural potential. In the current market, whey proteins are incorporated into a myriad of different foods from several food sectors

(Page 2004). They are added to foods to specifically enhance or alter some physical or sensory property of the food, such as increasing the water holding, whipability, or viscosity of the product or to provide a nutritional protein source (Page 2004). In others words, food processors typically consider whey proteins as additives and not the primary ingredient of a product. Considering that whey proteins alone can form soft solid gels, a potential application is as the main structure forming component in products such as high protein, hand-held snack foods.

β-lactoglobulin, the predominate globular protein in whey, can form soft solid gels that have a broad textural range depending on the type of microstructure formed (Gwartney and others 2004). The type of microstructure formed is highly dependent on both pH and ionic strength of the solvent used (Ako and others 2009). When heated in solution at concentrations >10 % w/w protein, near neutral pH and low ionic strength, a fine stranded gel is formed, which appears homogeneous at the microscopic length scale. Gwartney and others (2004) characterized the fine stranded gel produced from 12 % (w/w) whey protein, pH 7 and 25 mM NaCl solutions. Texturally, the gel was described as springy and firm with low moisture release during mastication. The gel had a slippery mouthfeel and exhibited a low degree of crumbliness. Physically, the gel had high water holding capacity and a translucent appearance. Under conditions of high ionic strength or low pH however, denatured whey proteins aggregate to form protein dense clusters that are a few microns in diameter resulting in microphase separation (Ako and others 2009). At protein concentrations > 2 % (w/w) and NaCl concentration > 0.1 M, the microphase separated solution forms a gel that is commonly referred to as particulate. Gwartney and others (2004)

evaluated the sensory texture of particulate gels formed form a 12 % (w/w) whey protein, pH 7, 25 mM NaCl and 10 mM calcium chloride solution. Particulate gels were described as highly deformable and crumbly with a grainy mouthfeel. Physically, the particulate gels had low water holding capacity and were turbid in appearance.

Interactions between β-lactoglobulin and casein (κ-, β-, and α_{s1}- and α_{s2}) proteins have been studied extensively. In native milk (i.e. unheated milk at natural pH), the caseins are organized into micelles, where κ-casein predominately resides at the micelle surface with the hydrophilic C-terminal section protruding into solution (McMahone and Oommen 2013). When the milk is heated, denatured β-lactoglobulin aggregates with κ-casein to form appendages at the casein micelle surface (Mottar and others 1989) via hydrophobic interactions (Haque and others 1987) and disulfide bonding (Jang and Swaisgood 1990). On the other hand, isolated β– and α_s-caseins (i.e. both α_{s1}- and α_{s2}-casein) exhibit holdase chaperone activity in the presence of heat denatured whey proteins to inhibit their aggregation with neighboring denatured whey proteins (Bhattacharyya and Das 1999, Yong and Foegeding 2008, Kehoe and Foegeding 2014). In dispersed casein mixtures such as sodium caseinate, κ-, α_s-, and β-caseins compete for interaction with denatured β-lactoglobulin (Guyomarc'h and others 2009). The protein profile of aggregates formed by the heat treatment (80 °C) of whey protein isolate solution (1-2 % (w/w), 0.1 M NaCl, pH 7), in the presence of sodium caseinate consists of 80-90% (w/w) whey protein and 10-20 % (w/w) κ- and α_s-caseins (Guyomarc'h and others 2009). Beta-caseins were not incorporated into the final aggregate under these conditions. This is in contrast to results found by Kehoe and Foegeding (2014). Protein aggregates formed by heat denaturation of β-lactoglobulin in

the presence of pure β-casein contained both β-lactoglobulin and β-caseins in significant quantities (Kehoe and Foegeding 2014).

Interactions between β-lactoglobulin and the casein micelle significantly influence the texture properties of cheese. The β-lactoglobulin/κ-casein complexation increases steric hindrance and surface hydrophobicity of the micelle (Mottar and others 1989) thereby reducing chymosin hydrolysis rate (Reddy and Kinsella 1990) and curd fusion (Guinee and others 1995) in the production of natural cheese. Consequently, the textural properties of natural cheese products are altered (Mottar and others 1989, Reddy and Kinsella 1990). Research into the effects of casein addition on whey protein gel texture however is limited. In considering the known whey-casein interactions, whey protein gel properties may be altered by incorporation of casein micelles or dispersed casein proteins, and thereby expand the textural range of whey protein based gels. The objective of this study was to determine the effects of casein micelles and dispersed casein on the sensory texture and material properties of whey protein isolate gels. Secondarily, we sought to determine if casein interactions with whey proteins would lead to changes in whey protein gel microstructure that could be correlated with changes in sensory texture and material properties.

2. Materials and Methods

2.1. Materials

Whey protein isolate (WPI) was donated by Davisco Foods Inc. (Le Sueur, Minn, U.S.A.). Milk protein isolate (MPI) was donated by Idaho Milk Products (Jermone, Idaho,

U.S.A.). Whey protein isolate and MPI powders respectively contained 94.55 and 79.91 % (w/w) protein (N x 6.38) (Adler-Nissen 1988, European Council Regulation 1996)) as determined by nitrogen content determined by inductively coupled plasma spectroscopy. Hydrochloric acid (HCl) (37%, FCC, ACS, NF) was purchased from Mallinckrodt Baker (Paris, Ky., U.S.A.). Ethylenediaminetetraacetic acid, disodium salt dihydrate (EDTA), citric acid, citric acid trisodium salt dihydrate (sodium citrate), and sodium hydroxide (NaOH) (ACS pellets) were purchased from Fisher Scientific Inc. (Fair Lawn, N.J., U.S.A.). Sodium chloride (NaCl) was purchased from Sigma-Aldrich Corp. (St. Louis, Mo., U.S.A.). Nile Blue Sulfate A was purchased from Invitrogen Molecular Probes (Eugene, Ore., U.S.A.). Deionized water (>17 MΩ) was used for solution preparations.

2.2. Experimental design

To determine the effect of casein on whey protein isolate gels, 7% of the protein in whey protein isolate gels (18 % (w/w) total protein) was substituted with either casein micelles or dispersed casein at pH 6 and 5.5. In order to eliminate the variable of ionic strength, all gels were prepared at an equivalent ionic strength, except for one set of whey protein isolate gels, which served as a control. Throughout this chapter, treatments will be discussed using the following designations: Whey protein isolate gels (WP), with added NaCl (WP-NaCl), with casein micelles (WP-micelle), with dispersed casein (WP-dispersed).

2.2. Solution preparation

Whey protein isolate solution (25 % (w/w) protein) was prepared by dispersing WPI in deionized water by mixing for 4 hr using a magnetic stirrer. Solutions were held over night at 4 ± 1 °C to allow for complete hydration. Milk protein isolate solution (14 % (w/w) casein based on casein representing 80% of total protein) was prepared by mixing MPI with deionized water under vacuum in a high shear Stephan mixer (Columbus, Ohio, U.S.A.) for one minute at room temperature (21 ± 2 °C). The MPI solution was heated for one hour at 55 ± 1 °C in a waterbath to allow for hydration and stored overnight at 4 ± 1 °C. The MPI solution served as the casein micelle source.

Dispersed casein solution was prepared from MPI solution at 2 ± 1 °C. Granular EDTA was stirred by hand into MPI solution (at a 1:1 molar ratio of calcium:EDTA) and allowed to rest for 30 min. While stirring by hand, solution pH was decreased to 4.8 using 6 M HCl then raised to 5.3 using 6 M NaOH. It was assumed that casein micelles were dispersed since the quantity of EDTA added was greater than the critital concentration required for complete casein micelle dissociation (Pitkowski and others 2008). Dispersed casein solution was held at 4 ± 1°C for 24 h.

2.4. Gel preparation

The WPI solution pH was adjusted to pH 6 or 5.5 using 6 M HCl then combined with MPI or EDTA dispersed MPI solution to yield solutions containing 11 % (w/w) whey protein and 7 % (w/w) casein. The whey protein contributed by the MPI was included in the total whey protein concentration. Solutions were prepared at ~80 % of the final solution weight

and adjusted to pH 6 or 5.5 using 6 M NaOH and brought to final weight. Solution ionic strength was measured using a conductivity meter (Hanna Instruments, Woonsocket, R.I.) and brought to an equivalent level sodium chloride. Whey protein isolate solutions without NaCl addition served as a control. All solutions were degassed for one hour and poured into glass tubes (19 mm diameter x 180 mm height) that were stoppered on one end with a rubber plug and coated with food grade silicone mold release (Price Driscoll Corp., Waterford, CT, U.S.A.). Glass tubes were covered with aluminum foil to prevent evaporation and heated in a water bath at 80 ˚C for 30 min. Immediately after heating, gels were cooled in ice water and held for 24 h at 4 ± 1 °C. Three replications were prepared for each treatment.

2.6. Imaging

Gel microstructure was elucidated using confocal scanning laser microscopy. For images, 20 µL of Nile Blue A Sulfate (0.2 % (w/v) dissolved in deionized water) was placed on top of a 5 x 5 x 3 mm section of gel. After 10 min, the gel was inverted onto a glass bottom microwell dish (35 mm petri dish, 14 mm Micro well, Nr 1.5 cover glass (0.15 to 0.19 mm) (MatTek Corp., Mass, U.S.A.). All samples were capped with the microwell dish top to prevent moisture loss and imaged within 30 min using an inverted Leica TCS SP1 CSLM (Leica Inc., Bannockburn, IL, U.S.A.) with 40 x C-Apochromat water emersion objective (N.A = 1.1). Dye was excited and emission collected at 633 and 650-700 nm respectively to elucidate the protein fraction.

2.7. Water holding

Water holding capacity was determined by the method described by Kocher and Foegeding (1993). Briefly, cylindrical gels (1 cm height x 0.48 cm d_o) at room temperature were centrifuged at 159 x g for 10 min in a 1.5 mL centrifuge tube containing an inner tube with screened bottom. Water released during centrifugation was collected. Water holding capacity was expressed as the ratio of water released/original sample weight.

2.8. Large strain rheological testing

Torsional fracture. Torsional fracture was determined according to procedures given in Chapter 3.

Uniaxial compression. Recoverable energy and breakdown properties were determined under uniaxial compression. For all tests, gel cylinders (19 mm diameter) were cut to a length of 21.5 mm and compressed at room temperature (21 ± 2 ˚C) using an Instron universal testing instrument type 5565 equipped with a 5 kN load cell (Instron Engineering Corporation., Mass., U.S.A). Samples were compresses at a rate of 50 mm/min between plates lubricated with mineral oil had a diameter of 5 cm. This diameter was greater than the maximum diameter of samples after compression.

Percent recoverable energy. Samples were compressed to 20% of original height. The percent recoverable energy (% RE) was calculated from the area under the compression-decompression force-deformation curves according method of Nussinovitch and others (1990), using Eq. 4:

$$\% RE = \left(\frac{decompression\ area}{compression\ are} \right) x\, 100 \qquad (4)$$

Breakdown properties. Breakdown properties were evaluated using a post fracture normalized force-deformation curve as described by van den Berg and others (2008). Samples were compressed to 80% of the original sample height. The point of fracture was taken to be the peak force in the force-deformation curve. Normalized force was calculated as the peak force divided by the post fracture force and normalized deformation was calculated as the deformation at peak force divided by post fracture deformation.

2.8. Sensory analysis

Sensory texture of gels was determined by descriptive analysis using the Spectrum™ method (Meilgaard and others 1999, Drake and Civille 2003). The panel consisted of six members between the ages of 30 and 65 who had more than 250 hr of experience in texture evaluation. Panelists were presented with WP-dipsersed gels at pH 6 and WP gels at pH 6 and 5.5 for training and calibration purposes. Through discussion and training sessions, gel textural attributes were identified and 15 sensory terms for texture attributes were selected from previous texture lexicons for whey protein gels (Gwartney and others 2004, Çakır and others 2012). One additional term, tackiness was also added for evaluation. Definitions and evaluation techniques used for sensory terms are listed in Table 1. Sensory texture attributes were classified according to the non-oral and oral processing phases of first compression, first chew, mastication and residual (Table 1). Attribute intensity was rated using a 0 to 15 point product-specific scale for each term.

For analysis, panel members were given six pieces of cylindrical gel samples (15 mm height, 19 mm in diameter) at room temperature (21 ± 2 °C). Samples were cut 2 hr prior to evaluation, stored in lidded 60 mL souffle cups, and presented in randomized order with a three digit code for identification. One batch replicate was evaluated per session and each panelist evaluated gel treatments in duplicate. Panelists were provided with WP-dipsersed gels at pH 6 and WP gels at pH 6 and 5.5 for calibration during each session. During evaluation, panelists were instructed to expectorate gels and had a mandatory rest period of three minutes between sample evaluations. Panelists were provided with water and saltine crackers for palate cleansing between sample evaluations.

2.9. Statistical analysis

Principle component analysis (PCA) for averaged sensory scores relative to treatment was conducted using XLSTAT (Statistical software version 2006.3, Addinsoft, New York, NY).

3. Results and Discussion

3.1 Microstructure

Studies of microstructures formed in phase separated whey protein-polysaccharide gels by researchers from our group and other labs have identified several microstructures including homogeneous, protein continuous, bi-coninuous, particulate and coarse stranded (van den Berg and others 2007, Çakır and others 2011). The microstructures formed in each

treatment are shown in Table 2. The purple colored areas represent space occupied by protein and non-colored areas represent space void of proteins. Addition of salt and casein altered the whey protein isolate gel structure. A homogeneous microstructure was formed in the WP gel at pH 6 whereas the WP gel at pH 5.5 and WP-NaCl gel at pH 6 and 5.5 formed a particulate microstructures. The particulate microstructures appeared to be formed of clusters of protein aggregates. It is well known that whey protein gels form particulate microstructures under conditions of high ionic strength or at pH close to the isoelectric point of β-lactoglobulin (5.2) (Ako and others 2009). The microstructure transition from homogeneous to particulate reflects the increased clustering of protein particle aggregate as charges are screened by the presence of salt and as the net charge is reduced with decreased pH.

The WP-micelle gel at pH 6 also had a homogeneous microstructure. Kappa-casein, a known holdase chaperone (Guyomarc'h and others 2009), resides at the exterior of the casein micelle (McMahon and Oommen 2013). Holdase chaperone behavior is thought to involve hydrophobic interactions between the chaperone and target protein (Hartl and others 2011). The hydrophobic portion of κ-casein however would not be accessible to β-lactoglobulin as this portion of the protein is associated with the micelle and its hydrophilic portion is associated with the solvent (McMahon and Oomen 2013). This means that the change in microstructure was likely not due to holdase chaperone behavior but rather some other interaction. Another explanation for the change in microstructure could be that the casein micelle and denatured whey protein cooperatively formed a continuous network. When heated, denatured β-lactoglobulin interacts with κ-casein to form appendages at the

casein micelle surface (Mottar and others 1989). In considering that whey protein gel network formation stems from interactions between tetramers of aggregated denatured β-lactoglobulin, it plausible that the β-lactoglobulin appendages on κ-casein could interact with neighboring appendages to form a three dimensional network. This hypothesis is highly speculative however and further investigations should be conducted to probe the relationship of caseins and whey in the gel structure. When the pH was reduced to 5.5, the homogeneous WP-micelle microstructure shifted to particulate. Like the particulate microstructure of the WP gel at pH 5.5 and the WP-NaCl gels at pH 6 and 5.5, the WP-micelle microstructure was composed of clusters of protein aggregates. The protein aggregates, however, were slightly less dense in the WP-micelle gel and were slightly smaller. For this reason, this microstructure will be referred to as small-particle particulate. In milk, a reduction in pH causes calcium to be released from the micelle and casein micelles aggregate in the presence of calcium (Lucey and others 1996). Thus, the microstructural transition from homogeneous to small-particle particulate via pH reduction could be due to a three step gel formation process whereby 1) casein micelles aggregated in the presence of calcium then, 2) β-lactoglobulin appendages formed at the exterior of casein micelle aggregates which then 3) interacted with nearby appendages to form a three dimensional network.

A small particle-particulate microstructure was also formed in the WP-dispersed gel at pH 6 and 5.5. Relative to the WP-NaCl gel microstructures, a reduced particle size was likely a result of β-, α-, and κ-casein interaction with the whey proteins. In dispersed casein solutions such as caseinate β-, α-, and κ-caseins act as holdase chaperones that compete for

interaction with β-lactoglobulin leading to reduced aggregated protein particle (Guyomarc'h and others 2009).

3.2. Microstructure relations to mechanical properties

Substitution of whey protein with protein from casein micelles or dispersed casein clearly impacted the microscopic features of the gels. To understand how these changes in microstructure influenced whey protein isolate gel material and sensory properties, all treatments were evaluated for water holding capacity, pre- and post-fracture material properties by large strain rheology and sensory texture by quantitative descriptive analysis.

3.2.1. Pre-fracture deformation

3.2.1.1. Water holding and mechanical properties of gels

Water holding capacity (Figure 1) had a tendency to follow porosity of microstructure (van den Berg and others 2007). The homogeneous microstructure of the WP gel at pH 6 had the highest water holding capacity, followed by particulate microstructures. This is in line with the current theory that WHC is governed by porosity of microstructure where a greater degree of porosity leads to lower WHC (van den Berg 2007). Based on this theory, the homogeneous microstructure of the WP-micelle gel at pH 6 should have had a relatively high WHC. However, this system had a low WHC and therefore does not fit the current WHC-microstructure porosity theory. Structural elements below the microscopic length scale may play a role in the WP-micelle WHC.

3.2.1.2. Recoverable energy

Recoverable energy for each treatment is shown in Figure 2. At pH 6, the WP gel had the highest recoverable energy (46 %) while WP-NaCl, WP-micelle, and WP-dispersed gels had similar recoverable energy levels (~ 30 %). At pH 5.5, all treatments had low recoverable energy levels that ranged between 23 and 19 %. It is interesting to note, that for all treatments, recoverable energy was greater at pH 6 than 5.5.

Recoverably energy is used to indicate the loss of energy during deformation. During compression, energy was supplied to the material via normal force. This energy may dissipate throughout the material or be stored; energy dissipates through friction between material components or viscous flow (van Vliet and others 1991). Water holding is related to viscous flow and is highly correlated with recoverable energy in phase separated protein-polysaccharide gels (Çakır and others 2012). In the whey protein isolate gels, WHC was highly correlated ($r = 0.93$) with recoverable energy. Conversely, a poor correlation ($r = 0.59$) was found between WHC and recoverable energy in the whey protein-casein gels. This suggests that energy loss due to friction between material components played a more important role than viscous flow in the ability, or lack-there-of, of the whey protein-casein gels to store elastic energy.

No distinct pattern that associated microstructure with recoverable energy was found. The small-particle particulate microstructure of the WP-micelle gel at pH 5.5 was similar to that of the WP-dispersed gel at pH 6. Likewise, the particulate microstructure of the WP-NaCl gel at pH 5.5 was similar to that at pH 6, and the homogeneous microstructure of the WP gel at pH 6 was similar to that of the WP-micelle gel at pH 6. In all three cases however,

recoverable energy differences between treatments with similar microstructures was always higher at pH 6. This would suggest that pH had a greater influence on recoverable energy, and that structure at the nano-scale need to be probed for differences.

3.2.2 Fracture properties

Addition of salt and/or casein to whey protein impacted gel fracture properties at both pH (Figure 3). At pH 6, salt addition reduced the fracture stress from 120 kPa to 86 kPa. Casein addition further reduced fracture stress to 10 kPa and 16 kPa for the WP-micelle and WP-dispersed gels respectively. At pH 5.5, salt addition increased fracture stress from 70 kPa to 83 kPa. Similar to that at pH 6, casein addition reduced fracture stress to 28 kPa and 10 kPa for WP-micelle and WP-dispersed gels respectively. Fracture strain of WP gel at pH 6 (1.41) was reduced by the addition of salt and casein micelle to a nearly equivalent level (1.18 and 1.08 respectively), whereas dispersed casein addition increased fracture strain (1.86). At pH 5.5 whey protein gel fracture strain (1.36) was minimally altered by salt addition (1.42). Casein micelle and dispersed casein addition equivalently reduced fracture strain to 0.95.

Several studies have shown that changes in microstructure correlate with fracture properties for model phase separated protein-polysaccharide gels (van den Berg and others 2007, Çakır and others 2011, 2012). This study sought to establish similar microstructure-material property associations in model protein-protein gels. Among the protein gels of this study, no *universal* association between microstructure and fracture properties was found. Homogeneous microstructures were found in both the WP and WP-micelle gels at pH 6. In

the WP gel, moving from homogeneous to particulate microstructure lead to a reduction in fracture stress whereas in the WP-micelle gel moving from homogeneous to small-particle particulate increased fracture stress. This difference suggests that associations between microstructure and fracture properties are not universal and that changes at other length scales needs to be determined. In other words, fracture property-microstructure associations of whey protein gels are not the same as those for whey protein-casein gels. For this reason, fracture property-microstructure associations between the two pH levels of the WP, WP-dispersed, and WP-micelle systems will be discussed separately.

As stated previously, moving from the WP homogeneous microstructure to WP-NaCl particulate microstructure lead to a reduction in fracture stress and a minimal change in fracture strain. This change in fracture properties with change in microstructure is unlike that reported by other studies for whey protein gels at pH 7 (Mulvihill and Kinsella 1988, Kuhn and Foegeding 1991, Çakır and others 2011). In the WP-dispersed gel, a small-particle particulate microstructure was formed at both pH however reducing the pH form 6 to 5.5 caused a reduction in both fracture stress and fracture strain. In the WP-micelle gel, moving from a homogeneous to small-particle particulate microstructure caused an increase in fracture stress but a minimal change in fracture strain.

3.2.2.1. Breakdown properties

Breakdown properties describe the macroscopic failure of a material after fracturing at a maximum point of stress under an applied force. Other studies have successfully used normalized post fracture force-deformation data from compression testing to show

differences in breakdown patterns among treatments (van den Berg and others 2007, Çakır and others 2012). It has been argued that the slope of the post fracture curve is indicative of the crack propagation speed within a material (van der berg and others 2007). A steep slope represents a free running crack where as a slope closer to zero is indicative of a slower breakdown via multi-point fractures or yielding of the material. Representative post-fracture curves are presented in Figure 4-A and B. In addition, images of fractured gels after 80 % compression are presented in Figure 5.

During compression all gels maintained a cylindrical shape until fracture. At pH 6 (Figure 4-A), the WP gel had a steep decrease in normalized force after fracture, indicating a free running crack. Both casein micelle and salt addition reduced the post fracture curve steepness to a similar degree. The macroscopic failure of these gels however differed greatly. During compression, multiple small cracks developed at the surface of the WP-micelle gel whereas a few tensile cracks abruptly appeared for the WP-NaCl gel. Interestingly, the tensile cracks of the WP-NaCl gel were incomplete; the top and bottom portions of the gel cylinder did not fracture (see Figure 5). Consequently, the partially intact cylinders provided substantial resistance to compression leading to what falsely appeared as reduce crack speed propagation in the data. Addition of dispersed casein increased the steepness of the force-deformation curve relative to the WP gels. During compression, tensile fractures formed abruptly and large gel pieces slid away from each other upon further compression. Pieces of the WP-dispersed gel completely separated from each other whereas the WP gel cylinder remained partially intact (Figure 5). This incomplete fracture of the WP gel cylinder may explain the difference in post-fracture pattern whereby a partially intact

cylinder provided resistance to the applied normal force leading to a reduced slope relative to the whey-dispersed casein gel. At pH 5.5 (Figure 4B), the WP, WP-NaCl, and WP-micelle gels fractured in a manner similar to that described for WP-NaCl gel at pH 6.0 (Figure 5). This incomplete fracture lead to an inverted post-fracture pattern for the WP and WP-NaCl gels and what falsely appeared as reduced fracture pattern for the WP-micelle gel. In the WP-dispersed gel, multiple cracks appeared at the gel surface resulting in a slow post fracture pattern.

Elastically stored energy is used for crack propagation; a high degree of stored energy leads to a free-running crack (van Vliet and others 1991). As such, failure of materials with high recoverable energy tends to have steep post fracture force-deformation curves. The WP-dispersed gel at pH 6 had the steepest post fracture force-deformation slope yet it had a low recoverable energy (30 %). On the other hand, the WP-dispersed gel did have the highest fracture strain value (1.86) of all treatments. If we consider that part of the energy supplied to the gel during compression is cumulatively stored while part is dissipated, then at high strain levels a large amount of stored energy has been accumulated. The high amount of accumulated stored energy was then used for crack propagation at the point of fracture (van Vliet and others 1991) leading to the free-running crack observed. Overall, this observation suggests that in correlating crack propagation speed with recoverable energy, fracture stain should be taken into account.

In terms of microstructure, all gel types (homogeneous, particulate and small-particle particulate) exhibited abrupt tensile failure (vertical fracture). Also, both the WP-dispered small-particle particulate microstructure and the homogeneous microstructure of the WP-

micelle gel showed multiple points of fracture during compression leading to a slow post fracture speed. This difference between abrupt tensile failure and multipoint fracture could not be clearly distinguished from the normalized post fracture compression data. The data was convoluted by incomplete fracture (top and bottom of gel cylinders did not fracture) of several gels leading to what falsely appeared as a slow breakdown pattern or an inverted post fracture pattern.

Another way to evaluate the breakdown pattern of gels is to plot the torque vs. time data obtained during torsion testing. In this technique, the peak torque of the torque-time curve represents the time at which fracture occurred and the slope of the torque post fracture represents the breakdown pattern. Torque-time curves show distinct differences among treatments post fracture (Figure 6). Using this technique, the transition from a brittle-like failure to a more ductile failure is clearly elucidated.

Unlike compression, twisting samples (torsion test) allows for an abrupt decrease in force after fracture because the sample can separate into two pieces, breaking continuity with the testing apparatus. Also, the angle of the fracture plane indicates if the sample failed in shear or tension (Diehl and others 1979). Gels with particulate or small-particle particulate microstructure as well as the homogeneous WP gel exhibited abrupt tensile failure (fracture plane was 45 ° to the plane parallel to the gel cylinder diameter (Diehl and others 1979)) whereas shear failure (horizontal fracture) occurred in the small-particle particulate microstructure of the WP-dispersed gel at pH 5.5 and the homogeneous microstructure of the WP-micelle gel. These failure differences are represented clearly in the torque vs. time curves by a low slope post peak torque.

3.3. Descriptive sensory analysis of texture

Mean values for sensory texture attributes of all treatments are given in Table 3. Descriptive terms can be grouped according to how they are evaluated. First compression terms are tested in the hand by deforming the sample to a level that does not cause fracture. First chew terms are evaluated by deformation to fracture, and mastication terms are determined after a prescribed number of chews.

3.3.1. First compression

Springiness and deformability are sensory attributes that relate to textures perceived before fracture. Springiness reflects the degree of apparent elastic recovery after a large deformation. In whey protein gels, springiness has been related to continuity of strands within the gel structure. Other works have shown that particulate gels formed from large clusters of protein aggregate are less springy than particulate gels formed from small protein particles that are aligned (Langton and others 1996). Additionally, particulate gels in general are less springy than homogeneous gels due to the decreased protein network continuity of the structure (Çakır and others 2012). In this study, although the differences in springiness were minimal among homogeneous and particulate gels made from small or large clusters of protein aggregates, springiness tended to be greater in the small-particle particulate gels than in the large-particle particulate gels except for that of the WP-dispersed gel at pH 5.5, which had zero springiness suggesting that this structure had minimal ability to recover its original shape after deformation. Overall casein addition drastically reduced deformability of the gels causing the whey protein-casein gels to fracture easily.

3.3.2. First Chew

During the first chew of mastication, soft solid materials are fractured by a single compression between the molars. Firmness, fracturability, and moisture release were evaluated during this phase of the oral process. In the WP gels, shifting the homogeneous microstructure to particulate via pH reduction increased perceived firmness whereas shifting to this microstructure via salt addition did not change perceived firmness. Çakır and others (2012) also reported that salt induced microstructure shift did not alter perceived firmness. Although the WP-NaCl gels of this study had similar particulate microstructures, the gel at pH 6 was perceived as less firm than that at pH 5.5. This difference in perceived firmness could be related to structural features not evident at the confocal microscopic length scale. At fracture, shifting from a homogeneous microstructure to particulate increased the moisture release while decreasing fracturability, indicating that the particulate gels broke apart into fewer pieces while expressing the aqueous phase. High moisture release is a common phenomena of particulate whey protein gels that is highly correlated to water holding capacity (Chantrapornchai and McClements 2002, Gwartney and others 2004, Çakır and others 2012).

In the WP-micelle gels, shifting from homogeneous to small-particle particulate did not change perceived firmness, moisture release or fracturability. In the WP-dispersed gel, the small-particle particulate gel at pH 6 had increased perceived firmness relative to that at pH 5.5. For the other sensory terms, this drop in pH changed the texture to a gel that expressed more moisture but broke into fewer pieces when compressed to fracture.

3.3.3. Mastication

During oral processing of soft solid foods, bolus formation begins once the material has been fractured, which consists of continued particle size reduction via chewing and mixing with saliva. After 5 – 8 chews, samples were evaluated for their particle size, particle size distribution, cohesiveness of mass, adhesiveness, particle smoothness, chalkiness, moisture release and rate of break down. In essence, it is evaluating one stage of bolus formation. The homogeneous WP gel did not release any serum during mastication and broke down slowly into large, smooth, fairly uniform pieces that did not form a cohesive mass or substantially adhere to any oral surfaces. Contrarily, moisture was released from the particulate WP-NaCl gels as they were chewed and relative to the homogeneous gel broke down more quickly into smaller, rougher, chalky particles that were more or less homogeneous in size and had a low tendency to form a cohesive mass that had moderate adhesion to the oral surfaces. These striking differences between the homogeneous and particulate structure is in line with other reports for whey protein gels (Gwartney and others 2004). On the other hand, in the WP-micelle gel, shifting from homogeneous to small-particle particulate microstructure had a minimal impact on the masticatory texture attributes. These gels released a small amount of serum during mastication and broke down rapidly into small, relatively smooth but chalky, homogeneous particles that formed a cohesive mass that adhered moderately to the oral surfaces. In the WP-dispersed gel, both small-particulate particle gel microstructures had similar particle size, particle size distribution, rate of breakdown, and cohesiveness of mass. These gels broke down the most rapidly into very small, homogeneous particles that formed a cohesive mass. The transition in pH did however

correspond to differences in particle smoothness, chalkiness, moisture release and adhesiveness. The small-particle particulate gel at pH 6 released less serum during mastication, had smoother particles, was less chalky and did not adhere as much to the oral surfaces. It is interesting to note that in all treatments, gels at pH 5.5 were more adhesive that those at pH 6. This suggests that chemical factors could be involved in adhesion.

3.3.4. Residual

Once oral processing is complete, the bolus formed during mastication is swallowed leaving behind residual moisture and food particles in the oral cavity. In this study, panelists were instructed to expectorate the bolus formed then evaluate the oral cavity for residual moisture and particles coating the mouth. Replacing whey protein with casein decreased the range of number of chews required for adequate bolus formation. Residual particulate matter was greater for all gels at pH 5.5 than at pH 6 regardless of treatment. Residual moistures was low for all treatments.

3.3.5. Overall effect of treatments sensory properties

The main objective of this study was to determine how casein micelles and dispersed casein impact the sensory texture properties of whey protein gels. Using principle component analysis (Figure 7), several texture attributes were influenced by casein addition. Eighty six percent of the variability among treatments could be explained by several texture attributes, which can be seen in the correlation circle (Figure 8). Overall, the differentiating sensory attributes among treatments were adhesiveness, cohesiveness of mass, tackiness

firmness and deformability. Substitution of 7 % (w/w) whey protein for casein lead to decreased firmness and deformability and also increased adhesiveness, cohesiveness of mass and tackiness.

4. Conclusion

Gels prepared by combining casein and whey proteins have different microstructures, mechanical properties, and sensory texture than gels made of whey proteins alone. Changes in gel microstructure did not universally correspond with either changes in mechanical properties or sensory texture. Replacing the whey protein with casein drastically reduce gel strength but minimally altered recoverable energy. Recoverable energy was altered more by pH than protein composition. Instrumentally measured water holding capacity was decreased by casein addition. Breakdown patterns were shifted from brittle-like to ductile-like for dispersed casein at pH 5.5 or micellar casein at pH 6. Additionally, whey protein-casein gels broke down more rapidly into a less watery, more cohesive mass during mastication than did the whey protein gels without casein. Overall, it was demonstrated that the whey protein isolate gel mechanical and sensory properties can be altered using caseins as a texture modifier while maintaining a high total protein concentration. Future research should focus on gel structures at the nano-length scale and also underlying chemical changes in these systems that may be responsible for changes in mechanical and sensory properties.

5. References

Adler-Nissen J. 1986. Enzymic hydrolysis of food proteins. Adler-Nissen J, author. New York:Elsevier Applied Science Publishers. p 427.

Ako K, Nicolai T, Durand D, Brotons G. 2009. Micro-phase separation explains the abrupt structural change of denatured globular protein gels on varying the ionic strength or the pH. Soft matter 5(20):4033-41.

Bhattacharyya J, Das KP. 1999. Molecular chaperone-like properties of an unfolded protein, α_s-casein. J Biol Chem 274:15505–09.

Çakır E, Foegeding EA. 2011. Combining protein micro-phase separation and protein–polysaccharide segregative phase separation to produce gel structures. Food Hydrocolloid 25(6):1538-46.

Çakır E, Daubert CR, Drake MA, Vinyard CJ, Essick G, Foegeding EA. 2012. The effect of microstructure on the sensory perception and textural characteristics of whey protein/κ-carrageenan mixed gels. Food Hydrocolloid 26(1):33-43.

Chantrapornchai W, McClements DJ. 2002. Influence of NaCl on optical properties, large-strain rheology and water holding capacity of heat-induced whey protein isolate gels. Food Hydrocolloid 16(5):467-76.

de Jong S, van de Velde F. 2007. Charge density of polysaccharide controls microstructure and large deformation properties of mixed gels. Food Hydrocolloid 21(7):1172-87.

Diehl KC, Hamann DD, Whitfield JK. 1979. Structural failure in selected raw fruits and vegetables1. J Texture Stud 10(4):371-400.

Drake MA, Civille GV. 2003. Flavor lexicons. Comprehensive Rev Food Sci Food Safe 2(1):33-40.

European Regulation Commission. 1996. Laying down detailed rules of application for the public storage of skimmed-milk powder. Official J L 45:0005-23.

Guinee TP, Pudja PD, Reville WJ, Harrington D, Mulholland EO, Cotter M, Cogan TM. 1995. Composition, microstructure and maturation of semi-hard cheeses from high protein ultrafiltered milk retentates with different levels of denatured whey protein. Int Dairy J 5(6):543-68.

Guyomarc'h F, Nono M, Nicolai T, Durand D. 2009. Heat-induced aggregation of whey proteins in the presence of κ-casein or sodium caseinate. Food Hydrocolloid 23(4):1103-10.

Gwartney EA, Larick DK, Foegeding EA. 2004. Sensory texture and mechanical properties of stranded and particulate whey protein emulsion gels. J Food Sci 69(9):333-39.

Haque Z, Kristjansson MM, Kinsella JE. 1987. Interaction between. kappa.-casein and. beta.-lactoglobulin: possible mechanism. J Agr Food Chem 35(5):644-49.

Hartl FU, Bracher A, Hayer-Hartl M. 2011. Molecular chaperones in protein folding and proteostasis. Nature 475(7356):324-32.

Jang HD, Swaisgood HE. 1990. Disulfide bond formation between thermally denatured β-lactoglobulin and κ-casein in casein micelles. J Dairy Sci 73(4):900-04.

Kehoe JJ, Foegeding EA. 2011. Interaction between β-casein and whey proteins as a function of pH and salt concentration. J Agr FoodChem 59(1):349-55.

Kehoe JJ, Foegeding EA. 2014. The characteristics of heat-induced aggregates formed by mixtures of β-lactoglobulin and β-casein. Food Hydrocolloid 39:264-71.

Kocher PN, Foegeding EA. 1993. Microcentrifuge-based method for measuring water-holding of protein gels. J Food Sci 58(5):1040-46.

Kuhn PR, Foegeding EA. 1991. Factors influencing whey protein gel rheology: Dialysis and calcium chelation. J Food Sci 56(3):789-91.

Langton M, Aström A, Hermansson AM. 1996. Texture as a reflection of microstructure. Food Qua Prefer 7(3):185-91.

Lucey JA, Gorry C, O'Kennedy B, Kalab M, Tan-Kinita R, Fox PF. 1996. Effect of acidification and neutralization of milk on some physico-chemical properties of casein micelles. Int Dairy J 6(3):257-72.

McMahon DJ, Oommen BS. 2013. Casein micelle structure, functions, and interactions. In: McSweeney PLH, author. Advanced dairy chemistry, Volume 1A. Boston, Mass: Springer US. p. 185-209.

Meilgaard M, Civille GV, Carr BT. 1999. The spectrum descriptive analysis method. Sensory Eval Tech 4:189-253.

Mottar J, Bassier A, Joniau M, Baert J. 1989. Effect of heat-induced association of whey proteins and casein micelles on yogurt texture. J Dairy Sci 72(9):2247-56.

Mulvihill DM, Kinsella JE. 1988. Gelation of β-Lactoglobulin: Effects of sodium chloride and calcium chloride on the rheological and structural properties of gels. J Food Sci 53:231-36.

Nussinovitch A, Kaletunc G, Normand MD, Peleg M. 1990. Recoverable work versus asymptotic relaxation modulus in agar, carrageenan and gellan gels 1. J Texture Stud 21(4):427-38.

Page J. 2004. Whey and lactose: Natural milk products. In: Page J, Meyer D, Haines B, Lagrange V, Kenney A, editors. Reference manual for US whey and lactose products. Arlington, VA: US Dairy Export Council. p 11-14.

Pitkowski A, Nicolai T, Durand D. 2008. Scattering and turbidity study of the dissociation of casein by calcium chelation. Biomacromol 9:369-75.

Reddy IM, Kinsella JE. 1990. Interaction of beta.-lactoglobulin with kappa.-casein in micelles as assessed by chymosin hydrolysis: effect of temperature, heating time, beta.-lactoglobulin concentration, and pH. J Agr Food Chem 38(1):50-58.

van den Berg L, van Vliet T, van Der Linden E, van Boekel MAJS, van De Velde F. 2007. Breakdown properties and sensory perception of whey proteins/polysaccharide mixed gels as a function of microstructure. Food Hydrocolloid 21(5):961-76.

van den Berg L, Carolas AL, van Vliet T, van der Linden E, van Boekel MAJS, van de Velde F. 2008. Energy storage controls crumbly perception in whey proteins/polysaccharide mixed gels. Food hydrocolloid 22(7):1404-17.

van den Berg L, Rosenberg Y, van Boekel MAJS, Rosenberg M, van de Velde F. 2009. Microstructural features of composite whey protein/polysaccharide gels characterized at different length scales. Food hydrocolloid 23(5):1288-98.

van Vliet T, Luyten H, Walstra P. 1991. Fracture and yielding of gels. In: Dickinson E, editor. Food Polymers, Gels and Colloids, No. 82. Science Park, Cambridge: The Royal Society of Chemistry. p. 392-403.

Yong YH, Foegeding EA. 2008. Effects of caseins on thermal stability of bovine β-lactoglobulin. J Agr Food Chem 56 (21):10352-58.

Yong YH, Foegeding EA. 2009. Caseins: utilizing molecular chaperone properties to control protein aggregation in foods. J Agr Food Chem 58(2):685-93.

Table 1. Texture attributes, their definitions and evaluation protocols, used in sensory analysis

Sensory phase *evaluation protocol*	**Attribute**	**Definition**
Touch *Touch and release sample on cut surface*	Tackiness	Degree to which sample adheres to the fingers
First compression *Compress sample between the first finger and thumb*	Springiness	Degree to which sample returns to original shape after partial compression
	Deformability	Degree to which samples deforms before fracture
First bite *Compress the sample between molars until fracture*	Hardness	Force require to bite completely through sample
	Fracturability	Degree to which sample fractures into pieces on first bite
	Moisture release	Degree to which moisture is released on first bite
Mastication *Chew the sample 5-8 times*	Particle size	Size of fractured particles (small to large)
	Particle size distribution	Degree of particle size homogeneity
	Cohesiveness of mass	Degree to which the mass sticks together
	Adhesiveness	Degree to which the sample sticks to any oral surfaces
	Particle smoothness	Degree to which the mass or particles feel smooth
	Chalkiness	Degree to which fine chalk-like particles are perceived
	Moisture release	Degree to which moisture is released during mastication
	Rate of breakdown	Rate at which sample breaks down into smaller and smaller pieces (slow to fast)
	Number of chews	Number of chews required to prepare the sample for swallowing when chewed at a rate of 1 chew per second

Table 1. Continued

Sensory phase *evaluation protocol*	**Attribute**	**Definition**
Residual *Expectorate the sample and evaluate*	Particle mouthcoating	Amount of particles remaining in the mouth
	Moisture mouthcoating	Amount of moisture remaining in the mouth

Table 2. Confocal images of whey protein and mixed whey-casein gels

	WP	WP-NaCl	WP-micelle	WP-dispersed
pH 5.5	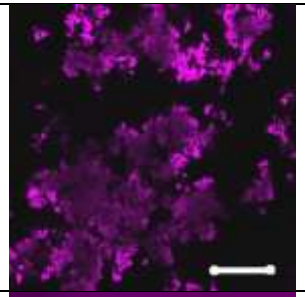	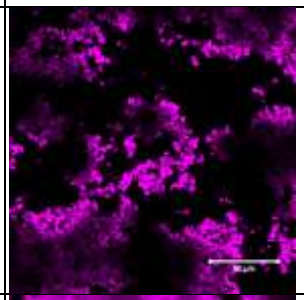	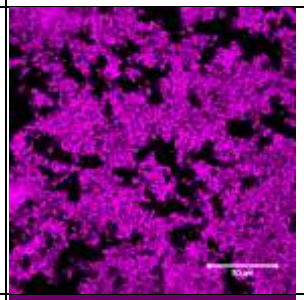	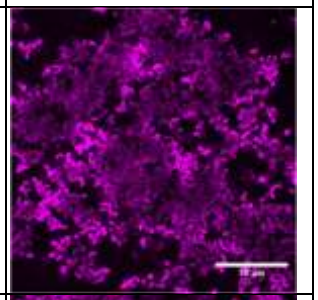
pH 6.0	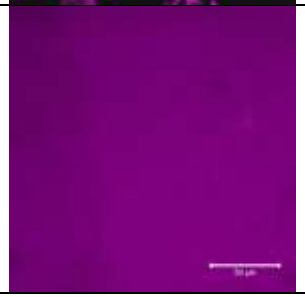	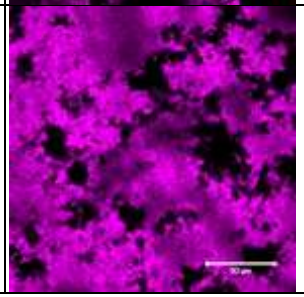	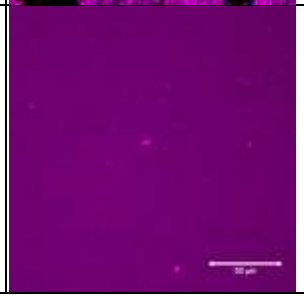	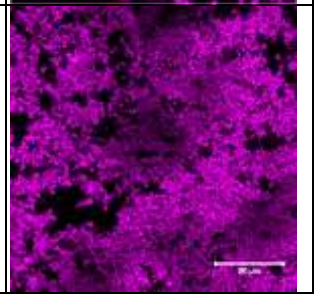

*Scale bar represents 50 μm.

Table 3. Sensory properties of whey protein gels with dispersed and micellar casein

Sensory attribute	Treatments							
	WP		WP-NaCl		WP-dispersed		WP-micelle	
pH	6	5.5	6	5.5	6	5.5	6	5.5
Tackiness	0.6	0.0	0.5	0.2	5.8	3.3	1.6	3.4
Springiness	15.0	13.6	14.8	13.9	14.3	0.0	14.5	14.4
Deformability	9.2	12.2	6.8	12.3	5.8	2.2	4.4	3.8
Firmness	8.8	12.4	8.5	14.1	3.3	2.3	2.8	2.8
Fracturability	10.0	2.3	7.4	3.0	2.6	0.4	2.6	2.8
Moisture release-first bite	0.0	7.9	2.8	8.3	1.7	2.8	1.5	1.8
Part size	8.3	4.0	7.9	5.4	2.9	1.8	3.9	3.7
Particle size distribution	8.2	10.3	7.7	10.3	12.2	13.9	11.3	12.1
Cohesiveness of mass	0.0	1.3	2.0	1.0	10.5	11.6	9.6	10.7
Adhesiveness	4.9	10.7	6.5	10.0	6.9	10.7	6.2	8.0
Particle smoothness	9.9	5.6	7.7	6.6	11.3	7.3	9.0	8.4
Chalkyiness	0.0	8.4	4.8	7.6	2.8	4.2	5.4	5.3
Moisture release-mastication	0.0	5.8	3.8	6.5	2.1	3.6	3.8	3.3
Rate of breakdown	4.8	10.2	7.8	10.6	13.5	13.8	11.8	12.3
Number of chews	41.0	28.3	32.7	36.2	19.7	12.8	20.5	18.3
Particle mouth coating	7.3	14.1	12.2	13.3	5.7	11.0	8.8	11.5
Moisture mouthcoating	3.8	2.7	3.7	2.6	3.5	4.4	4.0	3.8

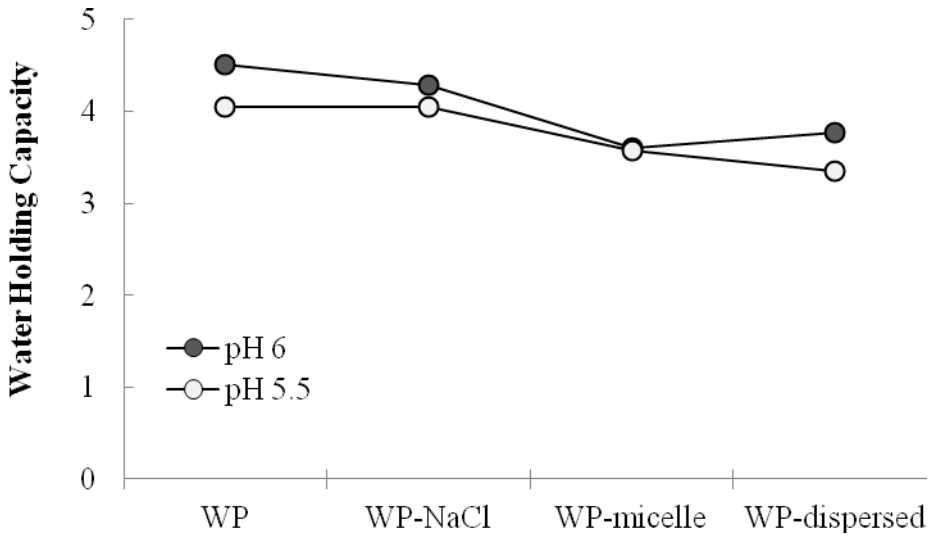

Figure 1. Water holding properties of whey protein (WP) gels with increased ionic strength (WP-NaCl), casein micelles (WP-micelle) and dispersed casein (WP-dispersed) at pH 6 (●) and 5.5 (○). Error bars represent standard deviation. Lines added are to guide the eye and do not represent continuous data.

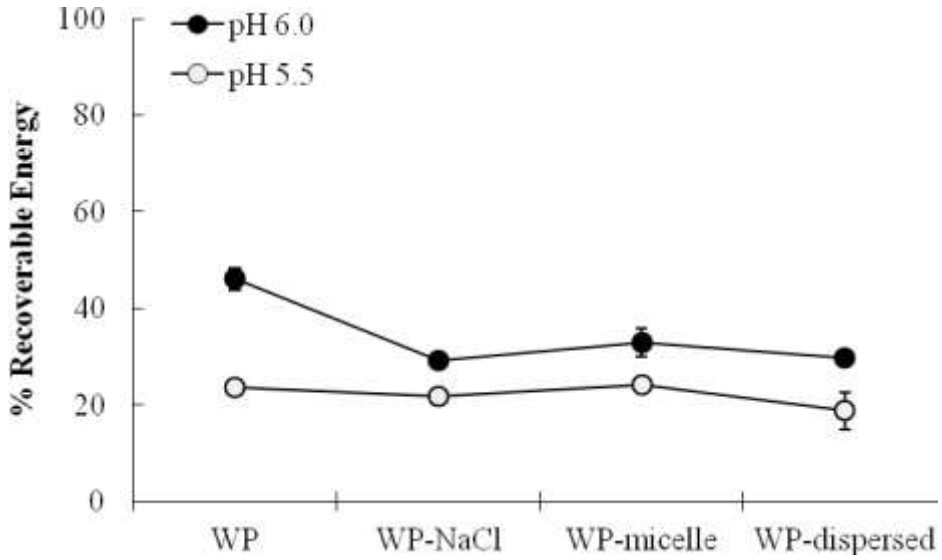

Figure 2. Percent recoverable energy of whey protein (WP) gels with increased ionic strength (WP-NaCl), casein micelles (WP-micelle) and dispersed casein (WP-dispersed) at pH 6 (●) and 5.5 (○). Error bars represent standard deviation. Lines added are to guide the eye and do not represent continuous data.

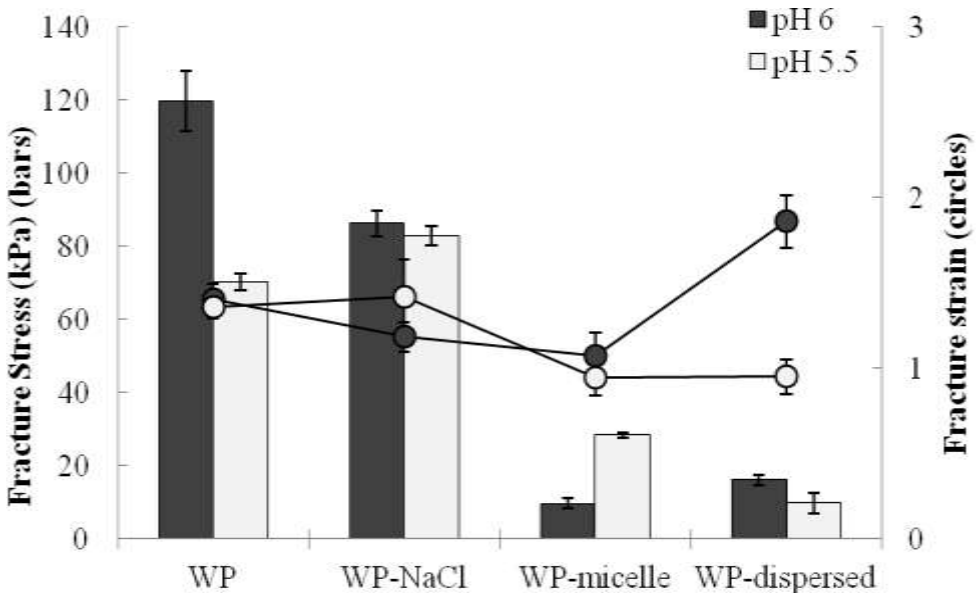

Figure 3. Fracture stress (bars) and fracture strain (circles) of whey protein (WP) gels with increased ionic strength (WP-NaCl), casein micelles (WP-micelle) and dispersed casein (WP-dispersed) at pH 6 (dark) and 5.5 (light). Error bars represent standard deviation. Lines added are to guide the eye and do not represent continuous data.

A.

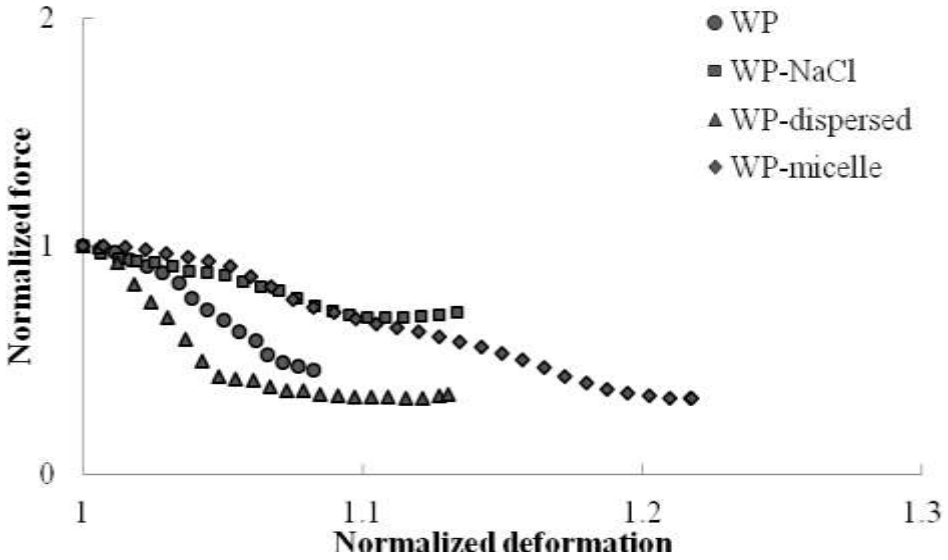

B.

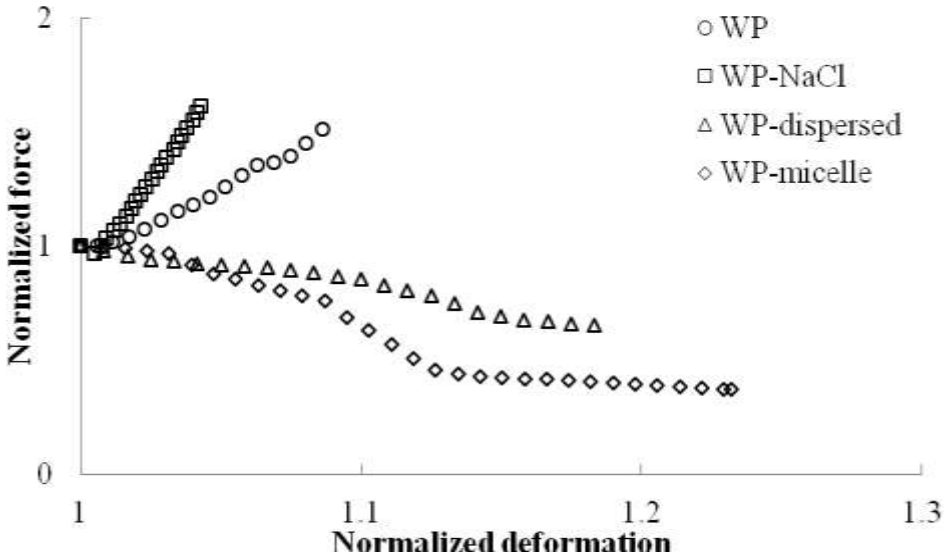

Figure 4. Normalized force and deformation after fracture of whey protein (WP) gels with increased ionic strength (WP-NaCl), casein micelles (WP-micelle) and dispersed casein (WP-dispersed) at A) pH 6.0 and B) 5.5.

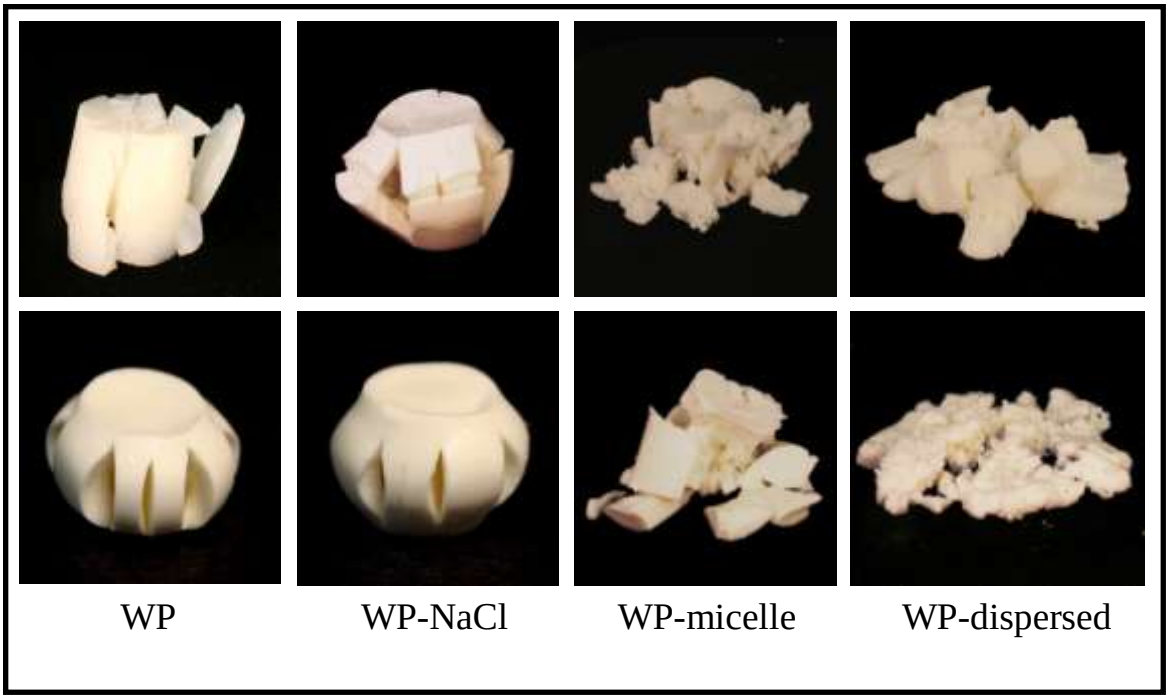

Figure 5. Images of whey protein (WP) gels with increased ionic strength (WP-NaCl), casein micelles (WP-micelle) and dispersed casein (WP-dispersed) at pH 6.0 (top row) and 5.5 (bottom row) after 80% compression.

A.

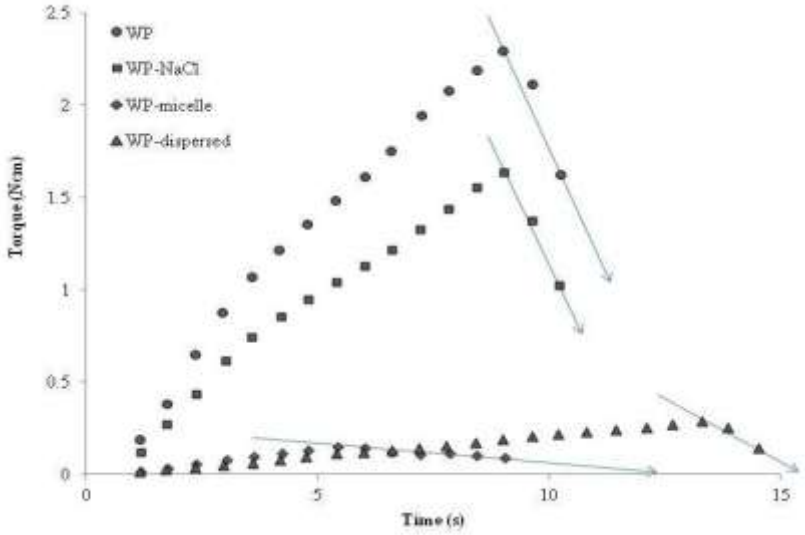

B.

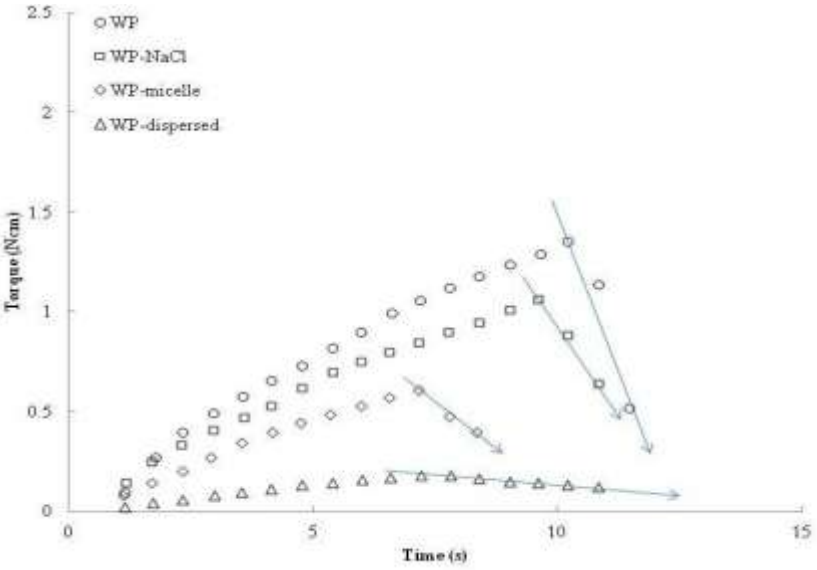

Figure 6. Torque vs time of whey protein (WP) gels with increased ionic strength (WP-NaCl), casein micelles (WP-micelle) and dispersed casein (WP-dispersed) at A) pH 6.0 and B) 5.5. Arrows have been added through the failure point to aid the eye.

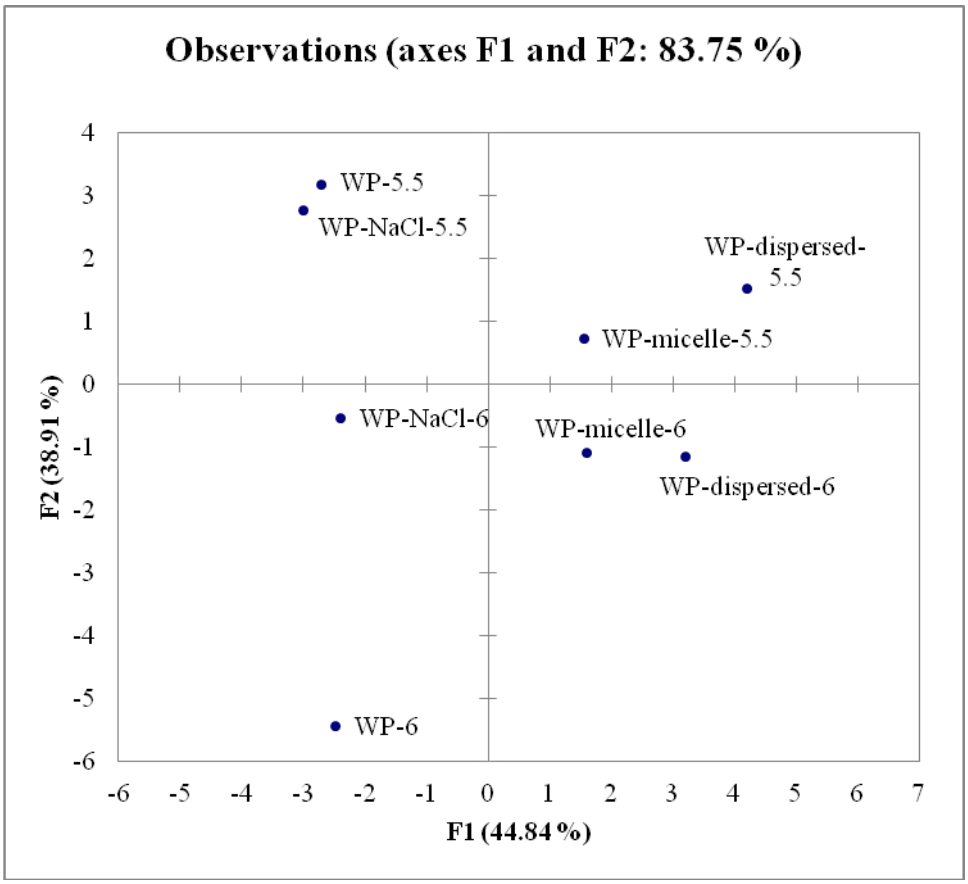

Figure 7. Principle component analysis of whey protein gels with added casein micelle and dispersed casein at pH 6 and 5.5.

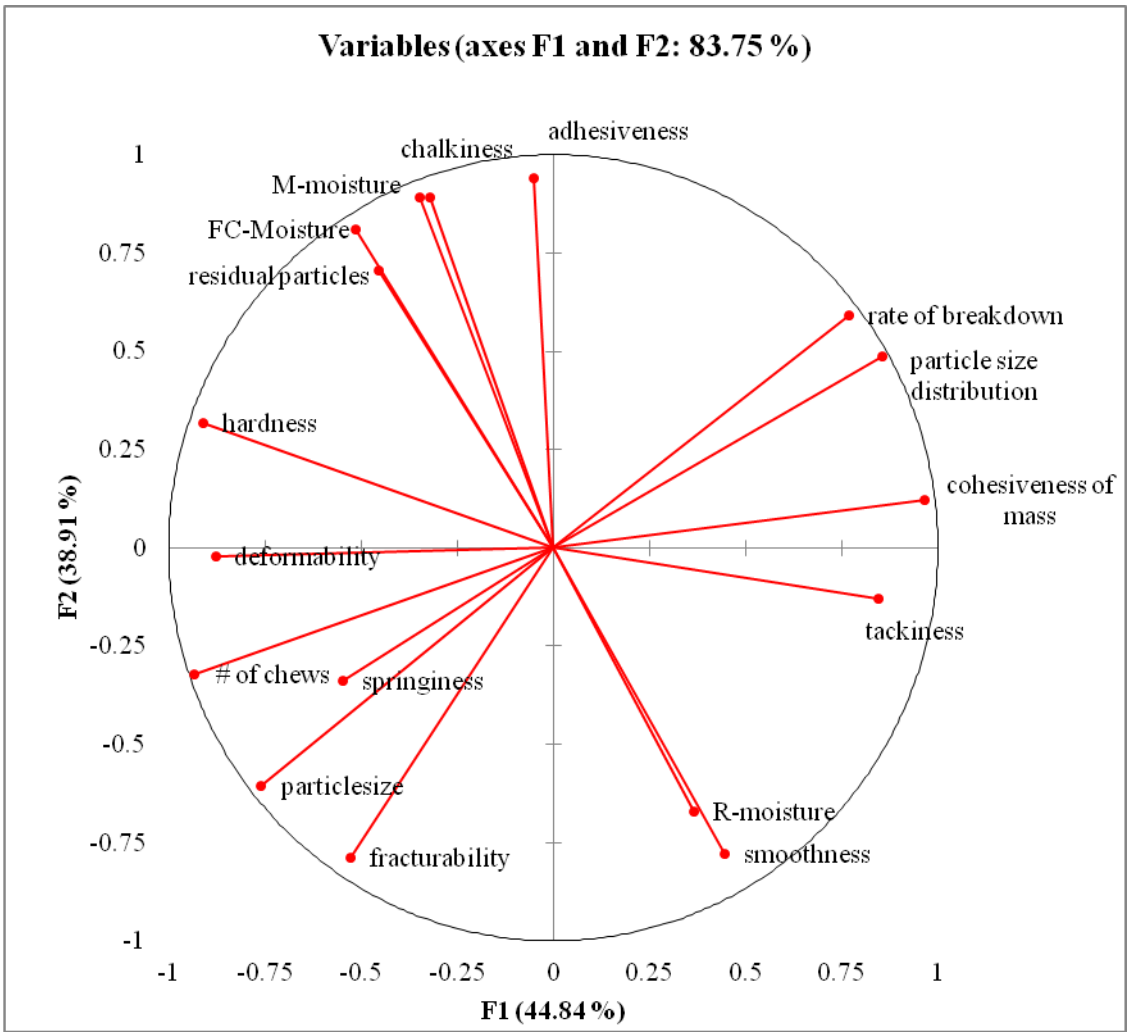

Figure 8. Correlation circle for sensory attributes of whey protein gels with casein micelle and dispersed casein addition at pH 6 and 5.5.

CHAPTER 5

Influence of dispersed casein and crystalline particles on whey protein gel properties

Abstract

Cheddar cheese is a popular food that has a high caloric density due, in part, to low water content. In chapter 4, gels formed from a mixture of dispersed casein and whey proteins were shown to have sensory texture attributes for cohesiveness of mass and chalkiness similar to Cheddar cheese but a somewhat faster breakdown pattern. Embedded particles within the matrix can give rise to void formation during deformation leading to pseudo-ductile failures that have slow breakdown patterns. The objectives of this research were to 1) develop a model whey protein-dispersed casein soft-solid gel with embedded particles and 2) to determine if the embedded particles could act as stress concentrators and slow the instrumental breakdown pattern of the gel.

Model gels with embedded particles were generated by combining whey protein solution with a dispersed casein solution prepared by calcium chelation using citrate with a molar ration of 0.7:1 citrate to calcium. The embedded particles had a starburst-like morphology with crystalline ordering and were predominately composed of citric acid (30 % (w/w)), calcium (22 % (w/w)), protein (5.5 % w/w), and fat (2.8 % (w/w)). Large strain post fracture analysis showed that the whey protein-dispersed casein gel had a slow breakdown. Crystalline particles did not influence the breakdown pattern; rather the breakdown patter was influenced by non-chelated calcium. Crystalline particles did however increase fracture stress and reduce fracture strain. Overall, the results demonstrate the feasibility of altering texture properties by combining whey and dispersed casein proteins at an 11:7 weight ratio of whey protein to casein and preparing that dispersed casein solution by adding citrate chelator at a 0.7:1 molar ratio citrate to calcium.

1. Introduction

The Center for Nutrition Policy and Promotion within the United States Department of Agriculture recommends that the daily intake of calories be spread throughout the day. Their Sample Meal Patterns suggest that the daily intake of foods be divided into three meals with snacking in between meals. The snacks recommended by the Center for Nutrition Policy and Promotion are those that are nutritious and low in fat and at least one snack should be a source of dairy protein. Ideally, snack foods would be satiating enough to sustain hunger between meals. Whey proteins provide short-term satiation whereas casein proteins provide long term satiation (Bendtsen and others 2013). Thus a suitable snack food would be one that combines the two dairy proteins in a low fat system to give both short and long term satiation.

Consumer preference of foods is governed by several factors including sensory texture perception (Cardello 1995). Sensory texture perception is a complex and dynamic process that involves neural response to stimuli perceived during the mastication of foods (Szczesniak 2002). Hutchings and Lillford (1988) have suggested that texture perception is influenced by the breakdown path of foods during mastication. This breakdown path is a culmination of the degree of food structure breakdown and its degree of lubrication that is experienced over time. Cheddar cheese is a popular food with slow instrumental breakdown pattern and low moisture release. However, the caloric density limits the use in snacking occasions. Given the popularity of Cheddar cheese texture, we sought to develop a no-fat, high protein, soft-solid gel with textural properties similar to Cheddar cheese. Furthermore,

the gel was based on a combination of casein and whey proteins so that both slow and fast absorbing proteins were present.

In chapter 4, we showed that gels formed from a mixture of casein and whey proteins have breakdown patterns that are different than whey protein gels. By combining whey protein with dispersed casein, a soft-solid gel was generated that released a low amount of moisture and broke down into a cohesive mass of smooth particles with little chalkiness during mastication. These sensory texture attributes are similar to those of Cheddar cheese (Gwatrney and others 2002, Carunchia Whetstine and others 2007). Instrumentally, the post-fracture breakdown pattern of full fat Cheddar cheese is slow (Patton 2013). On the other hand, the whey protein-dispersed casein gel had a rapid instrumental breakdown pattern. In order to mimic the instrumental breakdown properties of Cheddar cheese, it is desirable to reduce the breakdown speed of the whey protein-dispersed casein gel.

During compression of a perfectly homogeneous material, the stress experienced throughout the material is the same as the applied normal stress (Anderson 1995). The existence of a perfectly homogeneous material however is rare; materials typically contain imperfections, voids and inclusions. In this situation, the applied normal stress experienced throughout the material is amplified at the site of imperfections (Anderson 1995). The magnitude of amplification is dependent on the geometry of the imperfection where maximum stress occurs at the tip of the imperfection. Additionally, as the radius of tip curvature decreases, amplification of stress increases. This stress amplification is detrimental to material failure causing local failure of the material at the tip of the imperfection from which a micro-crack is formed (Anderson 1995). In composite biopolymer gels, the presence

of voids due to debonding of the filler-matrix interface leads to pseudo-ductile failure (Norton and Frith 2001). If we consider the micro-cracks formed at the particle tip to behave as voids, then one potential avenue to a slower breakdown pattern could be to introduce multiple sharp particles into the matrix that to generate numerous sites of void formation and thereby lead to a pseudo-ductile failure. However, it may be beneficial to textural properties by providing a multitude of internal cracks before complete failure.

In model phase-separated protein-polymer soft-solid gels, sensory texture and instrumental material breakdown have been related to gel failure mechanisms (van den Berg and others 2007). When multiple fracture events occur at various places throughout a coarse stranded structure, the instrumental breakdown speed is reduced (van den Berg and others 2008). If it is assumed that the same would hold true for a composite structure, then it is plausible that the multiple fracture points occurring at imperfection sites could also influence material breakdown patterns.

Sodium and calcium citrate crystals are commonly formed in processed cheese due to low solubility of either the emulsifying salt (sodium citrate) or the salt formed after calcium chelation (calcium citrate) (Guinee and others 2004). The sodium citrate crystal has a needle-like morphology that is slightly oblong in shape, is ~5 μm in length and has a sharply pointed tip that protrudes into the continuous protein phase (Rayan and others 1980). The tip of the needle-like crystal has a small radius of curvature. Formation of such a crystal in a protein gel matrix may act as a stress concentrator where cracks could initiate at multiple points throughout the continuous protein matrix and potentially influence the breakdown properties.

The objectives of this research were to 1) develop a model whey protein-dispersed casein soft solid gel with embedded stress concentrators and 2) to determine if the embedded particles could slow the instrumental breakdown pattern of the gel.

2. Materials and Methods

2.1. Materials

Whey protein isolate (WPI) was donated by Davisco Foods Inc. (Le Sueur, Minn, U.S.A.). Milk protein isolate (MPI) was donated by Idaho Milk Products (Jermone, Idaho, U.S.A.), Whey protein isolate and MPI powders respectively contained 94.55 and 79.91 % (w/w) protein (N x 6.38) as determined by nitrogen content determined by inductively coupled plasma spectroscopy. Hydrochloric acid (HCl) (37%, FCC, ACS, NF) was purchased from Mallinckrodt Baker (Paris, Ky., U.S.A.). Ethylenediaminetetraacetic acid, disodium salt dihydrate (EDTA), Citric acid, Citric acid trisodium salt dihydrate (sodium citrate), sodium hydroxide (NaOH) (ACS pellets) were purchased from Fisher Scientific Inc. (Fair Lawn, N.J., U.S.A.). Sigmacote® was purchased from Sigma-Aldrich Corp. (St. Louis, Mo., U.S.A.). Nile Blue was purchased from Invitrogen Molecular Probes (Eugene, Ore., U.S.A.). Deionized water (>17 MΩ) was used for solution preparations.

2.2. Solution preparation

Whey protein and milk protein isolate solutions were prepared according to procedures given in Chapter 4.

All dispersed casein solutions were prepared from MPI solution at 2 ± 1°C and under constant stirring from a mechanical overhead stirrer (model RZR 2021) with impeller attachment (Heidolph Instruments GmbH & Co., Elk Grove Village, Il., U.S.A.), For the citrate dispersed casein solution, MPI solution pH was decreased to 4.8 by slowing adding 3 M citric acid. Enough 1 M sodium citrate was added to give a 0.7:1 or 1:1 molar ration of citrate to calcium, which raised solution pH to ~5.0. Solution pH was further increased to 5.3 using 6 M NaOH. For the EDTA dispersed casein solution, granular EDTA as stirred into MPI solution and allowed to rest for 30 min. At this point, the solution viscosity was too high for the overhead stirrer to adequately mix the solution and therefore the solution was stirred manually. Solution pH was decreased to 4.8 using 6 M HCl then raised to 5.3 using 6 M NaOH. Dispersed casein solutions were held at 4 ± 1°C for 24 h.

2.3. Crystalline particle preparation

Crystalline particles were prepared from citrate dispersed casein solution. Citrate dispersed casein solution was diluted with deionized water to 10 % (w/w) casein and heated in a waterbath at 60 ± 1 °C for 30 min. Immediately after heating, solution was diluted with deionized water to facilitate particle precipitation. Supernatant was poured off and particles were washed with deionized water and allowed to settle. This process was repeated at least ten times over two days. Washed particles were stored at 4 ± 1 °C.

2.4. Gel preparation

2.4.1. Treatment gel preparation

The WPI solution pH was adjusted to pH 6.0 using 6 M HCl then combined with citrate dispersed solution (containing 0.7:1 molar ratio citrate to calcium) to yield solutions containing 11 % (w/w) whey protein and 0, 1, 3, 5, and 7 % (w/w) dispersed casein. The whey protein contributed by the MPI was included in the total whey protein concentration. Solutions were prepared at ~80 % of the final solution weight. Solution pH was adjusted to pH 6.0 using 6 M NaOH, brought to final weight and degassed for one hour. Degassed solutions were poured into glass tubes (19 mm diameter x 180 mm height) that were stoppered on one end with a rubber plug and coated with Sigmacote® siliconizing release agent. Glass tubes were covered with aluminum foil to prevent evaporation and heated in a water bath at 80 ˚C for 30 min. Immediately after heating, gels were cooled in ice water and held for 24 h at 4 ± 1 °C. Three replications were prepared for each treatment.

2.4.2. Control gel preparation

Control gels containing 11 % (w/w) whey protein and 7 % (w/w) citrate casein dispersed casein or EDTA dispersed casein were prepared similarly to the treatment gels described in section 2.4.1. Dispersed casein solutions had a 1:1 molar ratio of chelator to calcium. Crystalline particles (1.1 % (w/w)) were added to half of the whey protein-EDTA dispersed casein solution in place of water.

2.5. Composition analysis

Crystalline particles were evaluated for protein, fat, mineral, and citric acid content. Two samples per replicate were analyzed for moisture by the Forced Draft Oven method (AOAC International 977.11) whereby samples were dried in a 105 °C oven for 16 h. Two samples per replicate were analyzed for total fat was determined using the Mojonnier method (AOAC 991.20. 662). Three samples per replicate were analyzed for calcium, sodium, potassium, magnesium, phosphorous and nitrogen contents of particle were determined using inductively coupled plasma spectroscopy. Protein was determined from the nitrogen content (N x 6.38). Three samples per replicate were evaluated for citric acid using the method of Marier and Boulet (1958).

2.6. Imaging

Gel and crystalline particle microstructure was imaged using confocal scanning laser microscopy. For gel images, 20 µL of Nile Blue A Sulfate (0.2 % (w/v) dissolved in deionized water) was placed on top of a 5 x 5 x 3 mm section of gel. After 10 min, the gel was inverted onto a glass bottom microwell dish (35 mm petri dish, 14 mm Micro well, Nr 1.5 cover glass (0.15 to 0.19 mm) (MatTek Corp., MA, U.S.A.). For the particles, 100 µL of particles diluted in water was added to the microwell dish followed by 15 µL of Nile Blue Sulfate A. All samples were capped with the microwell dish top to prevent moisture loss and imaged within 30 minutes using an inverted Leica TCS SP1 CSLM (Leica Inc., Bannockburn, IL) with 10 X, Plan-Apochromat dry objective (N.A. = 0.45) (gel) and 40 X, C-Apochromat water imersion objective (N.A = 1.1) (particles). Dye was excited at 488 and

633 nm for the fat and protein phases respectively. Emissions were collected at 550-600 and 650-700 nm respectively. Differential interference contrast image of the crystalline particle was acquired simultaneously with the confocal image.

Crystalline particles were also imaged under polarized light using a Nikon Optiphot-2 microscope (Nikon Corporation, Tokyo, Japan) with 20 X objective.

2.7. Water holding

Water holding capacity was determined according to the procedure given in Chapter 4.

2.8. Large strain Rheology

Torsional fracture. Torsional fracture was determined according to procedures given in Chapter 3.

Recoverable energy and breakdown properties. Recoverable energy and breakdown properties were determined according to procedures given in Chapter 4.

3. Results

3.1. Imaging

Gel microstructure was elucidated using confocal laser scanning microscopy (Figure 1). Areas colored purple indicate the protein phase and areas with no color are void of protein. Microstructure of the whey protein gel with 0 and 1 % (w/w) citrate dispersed

casein were homogeneous. Gels with 3, 5 and 7 % (w/w) citrate dispersed casein show an increasing formation of starburst-like areas that were embedded in the homogeneous protein microstructure. Given that the starburst-like entity was embedded within the continuous protein matrix, it may be considered as type of filler particle. Filler particles can influence the material properties of filled gels depending on their phase volume, size and interaction with the matrix (Ross-Murphy 1983, van Vliet 1988, Langley and others 1989). As such, it was desirable to better understand the nature of this particle. When the citrate dispersed casein solution was heated without added whey protein, a starburst-like particle with similar morphology to that seen in the whey protein-citrate dispersed casein gel was formed and precipitated out of solution. Due to the morphological similarities, it was presumed that this precipitate and the starburst-like structure seen in the whey-citrate dispersed casein gels were one in the same.

The nature of the particle was explored using various microscopy techniques and chemical assays. The particle allowed light to pass the sample under polarized light microscopy indicating that part of its structure had crystalline ordering (Figure 2). Under differential interference contrast microscopy (DIC), the crystalline particle appeared to be formed of numerous needle-like entities that radiated outward (Figure 2). Three-dimensional DIC analysis (data not shown) showed that needles radiated outward from multiple central points. Under confocal scanning laser microscopy, both fat and protein were distributed throughout the particle (Figure 2). The presence of both fat and protein was confirmed by proximate analysis (Table 1). Based on the proximate analysis, mineral analysis and cirtic acid assay, it was concluded that the starburst-like particle was a type of protein-calcium

citrate complex. These particle will be referred to as crystalline particles throughout the remainder of this chapter.

3.2. Pre-fracture

3.2.1. Water holding and recoverable energy

During compression, energy is supplied to a material that may either dissipate or be stored elastically. According to the model by van Vliet and others (1991), energy can dissipate through a material via viscous flow or friction. Serum expressed from the gel under an applied force can be thought of as a form of viscous flow. Water holding represents the amount of serum expelled or held from a material after some external stress, in our case, centrifugation. The amount of serum held by the gels decreased as the concentration of citrate dispersed casein increased up to 3 % (w/w) then increased as the citrate dispersed casein concentration increased from 3 to 7 % (w/w) (Figure 3). Also, the ability of the gels to elastically store energy was reduced with increasing citrate dispersed casein concentration (Figure 3). Based on the theory of van Vliet and others (1991), the water holding and recoverable energy data collectively suggest that energy dissipated more through friction than viscous flow at high citrate dispersed casein levels. This corresponds with the presence of the crystalline particles.

3.3. Fracture properties

Fracture stress (Figure 4) increased then peaked with 3 % (w/w) citrate dispersed casein. Further increasing the citrate dispersed casein level reduced fracture stress. Fracture

strain was reduced with dispersed casein addition, which leveled off after 3 % (w/w) citrate dispersed casein. Adding citrate dispersed casein to the whey protein gel increased the complexity of the system by introducing several variables that could alter the material properties of the system. These variables include 1) increasing ionic strength through non-chelated calcium addition as determined by calculation and 2) the formation of a filler particle phase.

Fracture stress and strain of WPI gels are sensitive to changes in ionic strength. For example, in β-lactoglobulin gels, addition of 5 to 10 mM $CaCl_2$ increases gel strength while higher levels of added $CaCl_2$ (10 to 25 mM) reduce gel strength (Mulvihill and Kinsella 1988). Non-chelated calcium ions were likely present in the citrate dispersed casein solution due to the solution preparation technique used. During preparation, the pH was reduced to 4.8 then increased to 5.0 using citric acid and sodium citrate respectively. As such, citrate was added at a molar ratio of 0.7 to 1 citrate to calcium. Lucey and others (1996) found that calcium is released from the casein micelle as pH is reduced below pH 5.5 and remains in solution upon subsequent neutralization (as determined by calcium specific electrode). Assuming that the citrate sequesters calcium at a 1:1 molar ratio (Keowmaneechai and McClements 2002) it was calculated that roughly 70 % of the calcium was chelated. This means that ~ 30 % of the calcium was not chelated and could therefore increase the solution ionic strength. Based on these calculated assumptions, the amount of non-chelated calcium added to the gel systems was 0, 2, 6, 11, and 15 mM calcium for gels with 0, 1, 3, 5, and 7 % (w/w) citrate dispersed casein respectively. Based on the aforementioned observations of Mulvihill and Kinsella (1988), the changes in whey-citrate dispersed casein gel fracture

stress could be due to changes in presence of calcium ions alone, without a contribution from particles. This hypothesis will be addressed in subsequent sections.

The formation of crystalline particles could also have influenced the whey protein-citrate dispersed casein gel fracture properties. As described earlier, these filler particles had a starburst-like morphology where sharp needle-like entities protruded into the protein matrix. Spaces occupied by the filler particles may be considered as sites of imperfections within the material. In material science, it is generally accepted that applied normal stresses are amplified at imperfection sites and the magnitude of said amplification is dependent on the geometry of the imperfection where maximum stress occurs at the tip of the imperfection (Anderson 1995). As the radius of tip curvature decrease, amplification of stress increases causing a local failure of the material at the tip of the imperfection. The onset of filler particle appearance at 3 % (w/w) citrate dispersed casein addition (Figure 1) coincided with the minimum fracture strain (Figure 4), which leveled off at higher levels of added citrate dispersed casein. The treatment with 7 % (w/w) citrate dispersed casein had the highest amount of particles in the matrix and also the lowest fracture stress. Given the sharp geometry of the filler particle tips, it is plausible that they acted as stress concentrators causing the material to fail at reduced fracture stress and strain levels. This hypothesis will be addressed in subsequent sections.

Normalized post fracture force-deformation curves represent the breakdown speed after catastrophic failure due to compressive force. Negative slopes post-fracture show catastrophic breakdown and loss of resistance to compression. The greater the value of the negative slope, the more brittle-like the fracture. A distinct difference in gel breakdown

patterns emerged with increasing the citrate dispersed casein concentration. Gels with 0 to 3 % (w/w) citrate dispersed casein had a similar brittle-like fracture pattern that was different than the more ductile patters of gels with 5 and 7 % (w/w) citrate dispersed casein (Figure 5). The change in breakdown pattern coincided with both the presence of multiple particles in the gel matrix and the presence of non-chelated calcium in amounts greater than 10 mM as determined by calculation. The normalized post fracture force-deformation curve is intended to provide information on how a gel behaves once it has been fractured. To the best of our knowledge, the influence of calcium concentration on the breakdown properties of whey protein gels has not yet been systematically studied. However comparison of published data on sensory textures perceived during mastication of whey protein particulate gels formed by calcium or sodium addition show strikingly different sensory texture attribute intensities (Gwartney and othes 2004, Çakır and others). The rate of breakdown in terms of sensory perception is defined as the "rate at which the sample breaks into smaller and smaller particles (slow to fast)" after the sample has been chewed 5–8 times (Pascua and others 2013). Particle WPI gels (12 % protein, pH 7) prepared with 10 mM calcium have a fast rate of breakdown (socre of 11.7 on scale of 1-15) and required 15.2 chews for adequate bolus formation. On the other hand, particle WPI gels (13 % protein, pH 7) prepared with 250 mM NaCl required 22 chews for adequate bolus preparation and scored an 8.1 (on a scale of 1 – 15) for rate of breakdown. Comparatively, this suggests that calcium may influence the breakdown properties of whey protein gels.

The overall goal of this experiment was to develop a high protein gel that was self supporting, had a low moisture release, and had slow breakdown properties. The gel

containing 7 % (w/w) citrate dispersed casein exhibited these desired characteristics. It was unclear however what factors contributed to the slow breakdown properties. Both the presence of non-chelated calcium (as determined by calculations) and crystalline particles could have played a role in the breakdown properties of the gel. To establish the contributions of these factors, a series of control gels for the 7 % (w/w) citrate dispersed casein system were generated. To determine the effect of non-chelated calcium, a gel containing 11 % (w/w) whey protein and 7 % (w/w) citrate dispersed casein was prepared using a citrate dispersed casein solution that had a 1:1 molar ratio of citrate to calcium instead of a 0.7:1 molar ratio. Secondarily, to determine if the crystalline particles contributed to the gel breakdown properties, particles isolated from the citrate dispersed casein solution were incorporated into a similar whey protein-dispersed casein gel where the dispersed casein solution was prepared using EDTA. The EDTA chelator was added at a 1:1 molar ratio of EDTA to calcium and was chosen because 1) it does not have a propensity to form calcium crystals and 2) is thought to chelate calcium in a 1:1 molar ratio like citrate (Keowmaneechai and McClements 2002).

3.4. Control gel imaging and fracture properties

Control gels were imaged using confocal scanning laser microscopy (Figure 6). Purple colored areas represent protein and non-colored areas represent areas void of protein. Starbust-like particles appeared in both the citrate dispersed casein gel prepared from citrate dispersed solution with a 1:1 molar ratio of citrate to calcium and in the EDTA dispersed casein gel with added particles. No particles formed in the EDTA dispersed casein gel.

Increasing the molar ratio of chelator (citrate or EDTA) to calcium from 0.7:1 to 1:1 increased the whey protein-dispersed casein fracture stress and fracture strain (Figure 7). This suggests that non-chelated calcium did influence the fracture stress and strain. Incorporating the crystalline particles into the whey protein-EDTA dispersed casein gel increased fracture stress. This increase could be due to an increase in local protein concentration caused by the presence of the filler particle. Also, fracture strain was reduced when the particle was incorporated into the whey protein-EDTA dispersed casein gel. This reduction suggests that the particle may have acted as a local stress raiser.

All control gels broke down at a similar rate (Figure 8), which was faster than the gel prepared using citrate dispersed casein solution with 0.7:1 molar ration of citrate to calcium. This suggests that the filler particle did not influence the breakdown pattern; rather it was the non-chelated calcium that influenced the breakdown rate.

4. Conclusion

Model whey protein-dispersed casein soft-solid gels with embedded particles were generated by combining whey protein solutions with dispersed casein solutions, which were prepared by adding citrate to chelate the calcium in a molar ration of 0.7:1 citrate to calcium. The embedded particles had a starburst-like morphology with crystalline ordering and were predominately composed of citric acid (30 % (w/w)), calcium (22 % (w/w)), protein (5.5 % w/w), and fat (2.8 % (w/w)). The results suggest that the crystalline particles did not influence the breakdown pattern; rather it was the non-chelated calcium that influenced the breakdown pattern. The crystalline particles did however increase fracture stress and reduce

fracture strain. Overall, the results demonstrate the feasibility for development of a low fat, high protein (18 % (w/w)), high moisture retention gel structure with desirable breakdown properties.

References

Anderson TL. 1995. Fracture Mechanics:Fundamentals and Applications. 2nd edition. Boca Raton:CRC press. 688 pp.

Bendtsen LQ, Lorenzen JK, Bendsen NT, Rasmussen C, Astrup A. 2013. Effect of dairy proteins on appetite, energy expenditure, body weight, and composition: A review of the evidence from controlled clinical trials. Adv Nutr: Int Rev J 4(4):418-38.

Çakır E, Daubert CR, Drake MA, Vinyard CJ, Essick G, Foegeding EA. 2012. The effect of microstructure on the sensory perception and textural characteristics of whey protein/κ-carrageenan mixed gels. Food Hydrocolloid 26(1):33-43.

Cardello AV. 1994. Consumer expectations and their role in food acceptance. In: MacFie HJH, Thomson DMH, editors. Measurement of food preferences. Springer US, p. 253-97.

Carunchia Whetstine ME, Luck PJ, Drake MA, Foegeding EA, Gerard PD, Barbano DM. 2007. Characterization of flavor and texture development within large (291kg) blocks of Cheddar cheese. J Dairy Sci 90(7):3091-109.

Guinee TP, Carić M, Kalab M. 2004. Pasteurized processed cheese and substitute/imitation cheese products. In: Fox PF, editor. Cheese: chemistry, physics and microbiology, Vol 2. p. 349-94.

Gwartney EA, Larick DK, Foegeding EA. 2004. Sensory texture and mechanical properties of stranded and particulate whey protein emulsion gels. J Food Sci 69(9):333-39.

Hongsprabhas P, Barbut S. 1997. Protein and salt effects on Ca^{2+}-induced cold gelation of whey protein isolate. J Food Sci 62(2):382-85.

Hutchings JB, Lillford PJ. 1988. The perception of food texture: the philosophy of the breakdown path. J. Texture Stud. 19(2):103–15

Keowmaneechai E, McClements DJ. 2002. Influence of EDTA and citrate on physicochemical properties of whey protein-stabilized oil-in-water emulsions containing $CaCl_2$. J Agr Food Chem 50(24):7145-53.

Langley KR, Green M. 1989. Compression strength and fracture properties of model particulate food composites in relation to their microstructure and particle-matrix interaction. J Tex Stud 20(2):191-207.

Lucey JA, Gorry C, O'Kennedy B, Kalab M, Tan-Kinita R, Fox PF. 1996. Effect of acidification and neutralization of milk on some physico-chemical properties of casein micelles. Int Dairy J 6(3):257-72.

Marier JR, Boulet M. 1958. Direct determination of citric acid in milk with an improved pyridine-acetic anhydride method. J Dairy Sci 41(12):1683-92.

Mulvihill DM, Kinsella JE. 1988. Gelation of β-Lactoglobulin: Effects of sodium chloride and calcium chloride on the rheological and structural properties of gels. J Food Sci 53:231-36.

Norton IT, Frith WJ. 2001. Microstructure design in mixed biopolymer composites. Food Hydrocolloid 15(4):543-53.

Pascua Y, Koç H, Foegeding EA. 2013. Food structure: Roles of mechanical properties and oral processing in determining sensory texture of soft materials. Cur Opin Colloid Inter Sci 18(4):324-33.

Patton JQ. 2013. Development and Application of Whey Protein Particles for the Improvement of Low Fat Cheddar Cheese Texture. Thesis, North Carolina State University.

Rayan AA, Kalab M, Errlstrom CA. 1980. Microstructure and rheology of process cheese. Scanning Electron Microsc 3:635-43.

Ross-Murphy SB, Todd S. 1983. Ultimate tensile measurements of filled gelatin gels. Polymer 24(4):481-86.

Szczesniak AS. 2002. Texture is a sensory property. Food Qual Pref 13(4):215-25.

van den Berg L, van Vliet T, van der Linden E, van Boekel MAJS, van de Velde F. 2007. Breakdown properties and sensory perception of whey proteins/polysaccharide mixed gels as a function of microstructure. Food Hydrocolloid 21(5):961-76.

van den Berg L, van Vliet T, van der Linden E, van Boekel MAJS, van de Velde F. 2008. Physical properties giving the sensory perception of whey proteins/polysaccharide gels.Food Biophysics 3(2):198-206.

van Vliet T. 1988. Rheological properties of filled gels. Influence of filler matrix interaction. Colloid and Polymer Sci 266(6):518-24.

van Vliet TH, Luyten H, Walstra P. 1991. Fracture and yielding of gels. In: Dickinson E, editor. Food polymers, gels and colloids. Cambridge:Royal Society of Chemistry. p 392-403.

Table 1. Percent complex particle composition on a dry weight basis

Componet	**% (w/w)**
Protein	5.5 ± 0.03
Fat	2.8 ± 0.04
Ash	48 ± 0.48
Phosphorous	0.06 ± 0.03
Potassium	0.05 ± 0.02
Calcium	22 ± 1.1
Magnesium	0.00 ± 0.00
Sodium	0.13 ± 0.01
Carbohydrate by difference	44 ± 2.1
Citric acid	30 ± 1.8

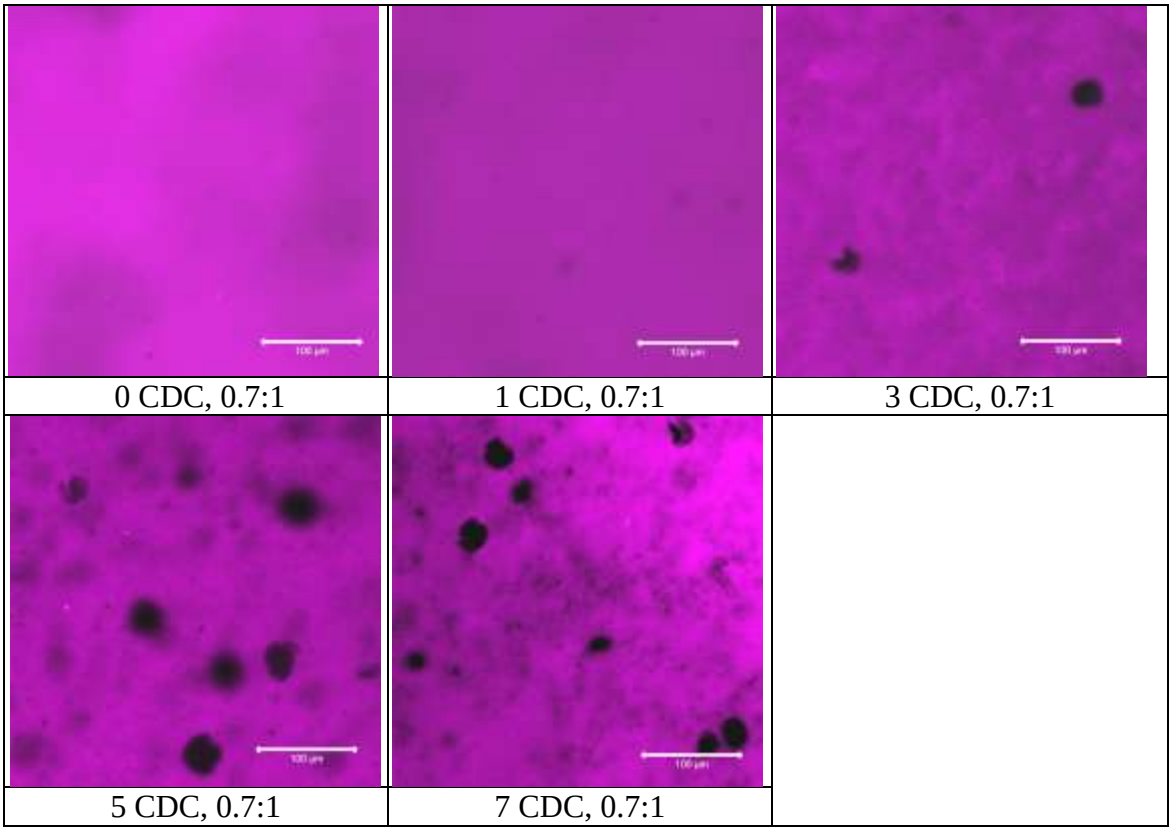

Figure 1. Confocal image of whey protein gels with 0, 1, 3, 5, and 7 % citrate dispersed casein (CDC). Citrate was present at 0.7:1 molar ratio of citrate to calcium. Scale bar represents 100 µm.

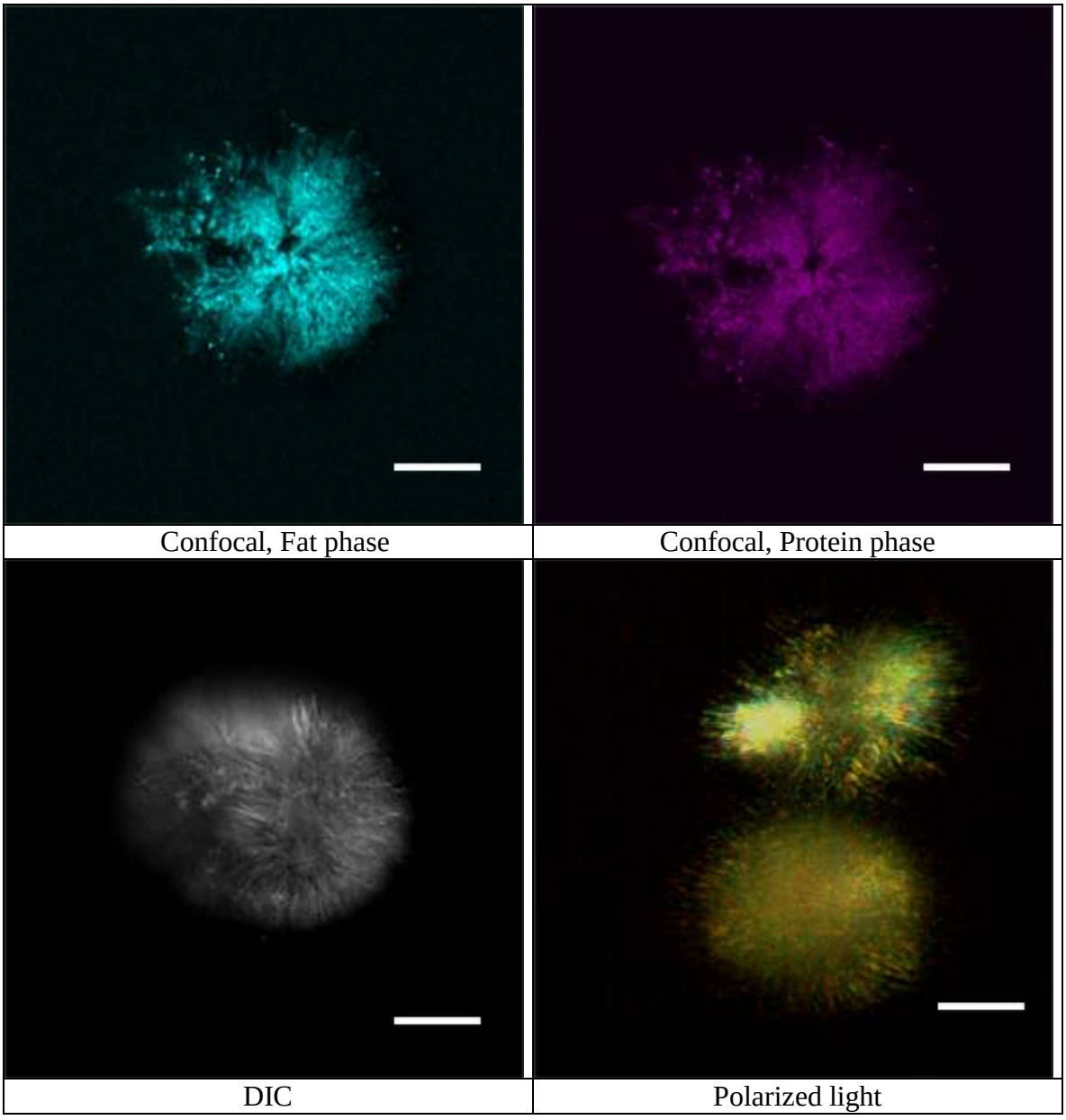

Figure 2. Confocal, DIC and polarized light images of crystalline particles. Size bar represents 20 μm.

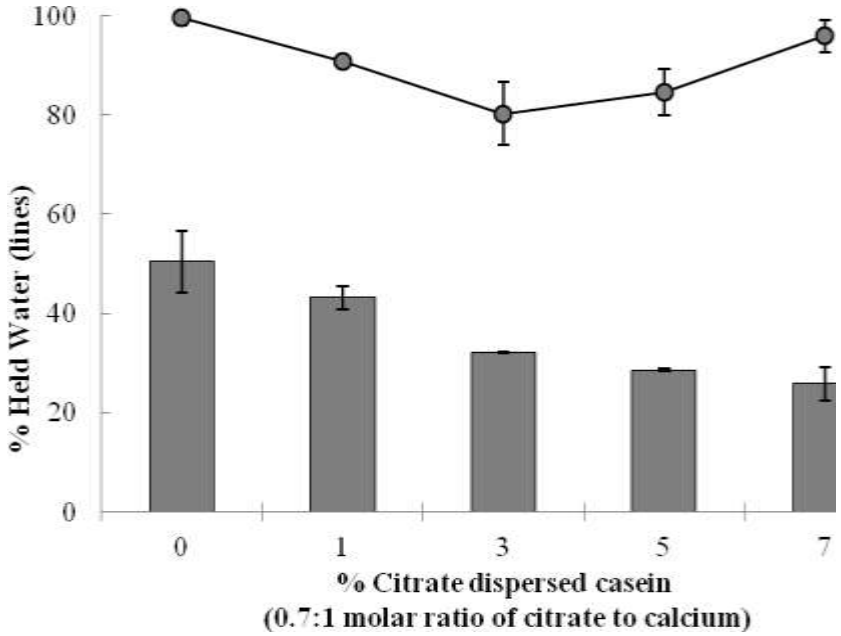

Figure 3. Percent recoverable energy (bars) and water held (circles) of whey protein gels with 0, 1, 3, 5, and 7 % citrate dispersed casein. Citrate was present at 0.7:1 molar ratio of citrate to calcium. Lines added are intended to aid the eye and do not represent continuous data. Error bars represent standard error.

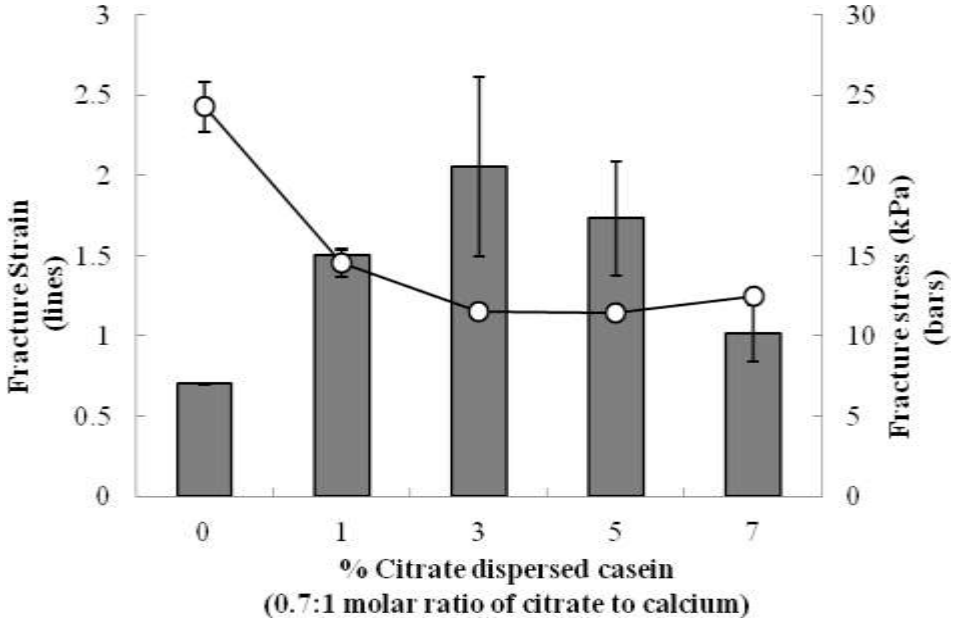

Figure 4. Fracture stress (bars) and strain (circles) of whey protein gels with 0, 1, 3, 5, and 7 % citrate dispersed casein. Citrate was present at 0.7:1 molar ratio of citrate to calcium. Lines added are intended to aid the eye and do not represent continuous data. Error bars represent standard error.

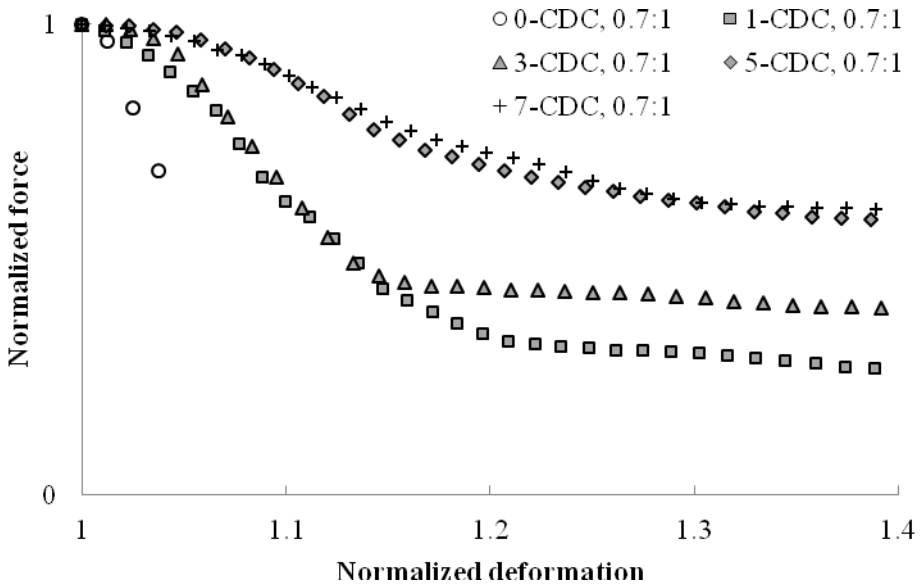

Figure 5. Representative normalized force versus deformation after fracture of whey protein gels with 0 (○), 1 (□), 3 (△), 5 (◇), and 7 % (w/w) (+) citrate dispersed casein. Citrate was present at 0.7:1 molar ratio of citrate to calcium.

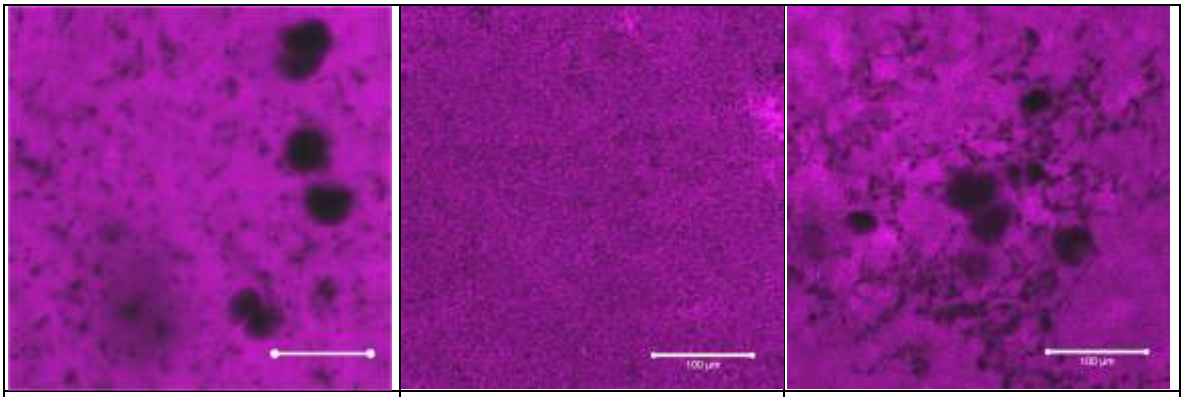

CDC, 1:1	EDC, 1:1	EDC, 1:1 + particles

Figure 6. Confocal image of whey protein gels with 7 % (w/w) citrate dispersed casein (CDC) with 1:1 molar ratio of citrate to calcium, EDTA dispersed casein (EDC) with 1:1 molar ratio of EDTA to calcium with and without added particles. Scale bar represents 100 µm.

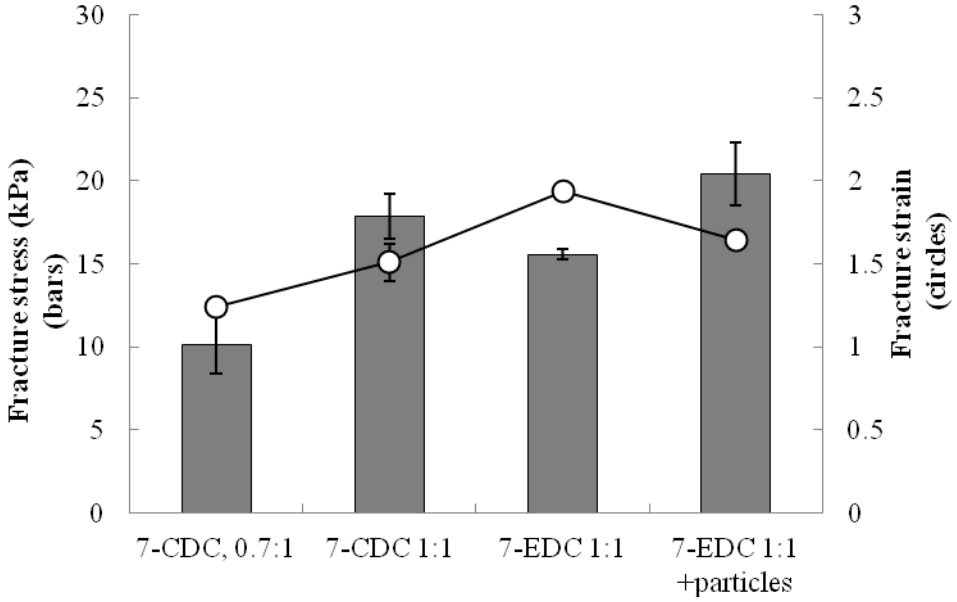

Figure 7. Fracture stress (bars) and strain (circles) of whey protein gels with 7% (w/w) casein from citrate dispersed casein with 0.7:1 molar ratio citrate to calcium, citrate dispersed casein with 1:1 molar ratio citrate to calcium, EDTA dispersed casein with 1:1 molar ratio EDTA to calcium, and EDTA dispersed casein with 1:1 molar ratio EDTA to calcium with added particles. Lines added are intended to aid the eye and do not represent continuous data. Error bars represent standard error.

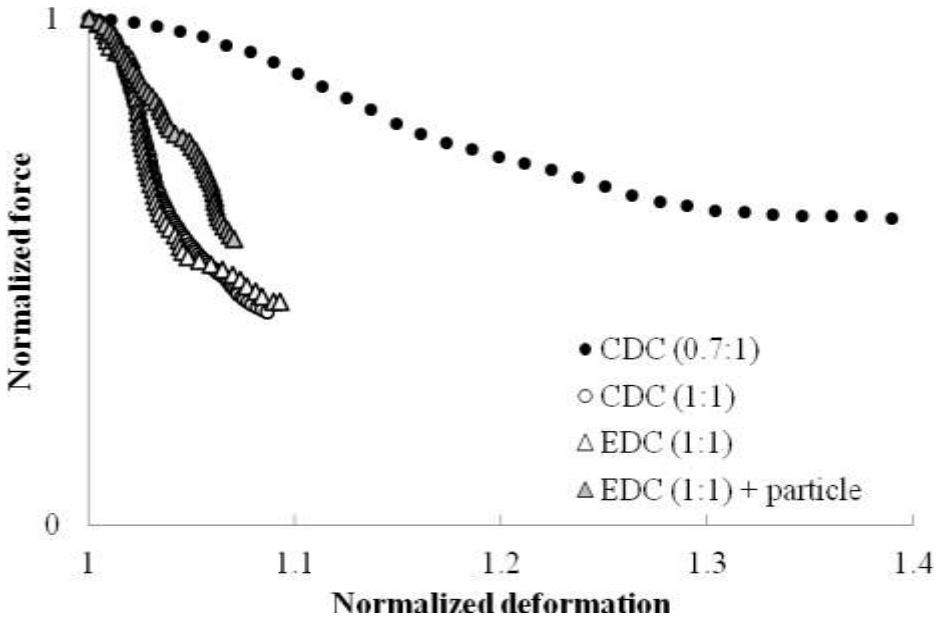

Figure 8. Representative normalized force versus deformation after fracture of control whey protein gels with 7 % CDC with 0.7:1 molar ratio citrate to calcium (●), 7 % CDC with 1:1 molar ratio citrate to calcium (○), 7 % EDC with 1:1 molar ratio EDTA to calcium (△), and 7 % EDC with 1:1 molar ratio EDTA to calcium with added particle (▲).